Separation and Purification Technology 284 (2022) 120286

Contents lists available at ScienceDirect

Separation and Purification Technology

journal homepage: www.elsevier.com/locate/seppur

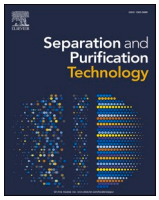

# Promising adsorptive materials derived from agricultural and industrial wastes for antibiotic removal: A comprehensive review

Diego M. Juela

*Department of Chemical Engineering, School of Chemical Sciences, University of Cuenca, Cuenca 010203, Ecuador*

ARTICLE INFO

*Keywords:*
Biosorbent
Adsorption
Residues
Porous materials
Photocatalysis
Emerging pollutants
Antibacterial removal

ABSTRACT

The development of novel materials and their application as adsorbents to improve water quality is one of the branches of materials science that has advanced significantly in the last decade. Due to the contamination of water resources with antibiotic residues, and the concern to contribute to the development of antibiotic resistance, scientists have tapped into agricultural and industrial wastes in order to transform them into new functional adsorbents that allow the adsorption of these pollutants. This review aims to summarize the different types of adsorptive materials that can be prepared using these residues and their application for removing antibiotics. From the reviewed literature, the adsorbents were classified as raw materials, surface-modified adsorbents, waste-based composites, carbon-based materials, and other adsorbents like zeolite, nano-hydroxyapatite, nano-cellulase, nano-silica, among others. Biochar and hydrochar are two of the most studied carbonaceous materials, with adsorption capacities ranging from 10 to 944 mg/g. Other leading adsorbents from the same family include mesoporous carbons, hierarchical and heteroatoms-doped porous carbons, and bio graphene, with surface area and adsorption performance over 1000 $m^2$/g and 500 mg/g, respectively. The most outstanding material prepared from waste was zeolite analcime, produced from electrolytic manganese residue, removing 1922 mg/g for roxithromycin. In addition, new methodologies or combined methods to produce these adsorbents, including new modifier agents (ionic liquids and deep eutectic solvents), templating, self-templating, doping techniques, and thermo-chemical approaches were reviewed for the first time. Furthermore, particular emphasis was given to photocatalyst-loaded adsorbents due to their synergistic effect of adsorption and degradation of antibiotics. Finally, novel methodologies to regenerate saturated adsorbents were discussed, such as UV radiation-assisted regeneration and ultrasound.

## 1. Introduction

In recent years, the presence of substances called emerging pollutants, including antibiotic residues, has been detected in aquatic environments. The incomplete removal of antibiotics by conventional wastewater treatment plants and the free discharge of domestic, hospital and pharmaceutical industry wastewaters loaded with these micropollutants into rivers, lakes, and other aquatic environments has favored their accumulation in the environment. The indiscriminate use of this medicine in humans and animals, together with their high persistence in the environment, make antibiotics a dangerous pollutant for the environment. Nowadays, traces of antibiotics have been detected not only in wastewaters, surface water, or groundwater but also in drinking water and food crops [1–4]. Consequently, aquatic animals and human beings are constantly exposed to these micropollutants, whether through the direct consumption of contaminated water or food grown with this water, which represents a significant threat to food safety and human health. Accordingly, their potential toxicity, teratogenicity, and

*Abbreviations:* GEM, gemifioxacin mesylate; MOX, moxifloxacin hydrochloride; AMX, Amoxicillin; ENR, Enrofloxacin; SDZ, Sulfadiazine; TMT, Trimethoprim; CEX, cephalexin; CTC, chlortetracycline; MET, metronidazole; SPF, sparfloxacin; TET, tetracycline; CIP, ciprofloxacin; LOM, Lomefloxacin; SAR, sarafloxacin; ENR, enrofloxacin; OFL, ofloxacin; OTC, oxytetracycline; LEV, levofloxacin; PEF, Pefloxacin mesylate dihydrate; RIF, rifampicin; DOX, doxycycline; TYL, tylosin; PEN-G, Penicillin G; NAP, naproxeno; ISO, isoniazid; NOR, norfloxacin; SAR, Sarafloxacin; SNM, Sulphanilamide; SAM, sulphacetamide; SMT, sulfamethazine; MRF, marbofloxacin; DNF, danofloxacin; SDM, sulfadimethoxine; SNM, sulfamonomethoxine; SM, sulfamerazine; TCL, triclosan; MER, meropenem; SCP, sulfachloropyridazine; SFT, sulfathiazole; CEF, cefixime; CAP, chloramphenicol; ETR, Erythromycin; PIP, piperacillin; TAZ, tazobactam; AMP, Ampicillin; MTX, mitoxantrone; STX, sulfamethoxamine; BLX, Balofloxacin; SPY, sulfapyridine; ROX, roxithromycin; AZM, azithromycin; ODX, oxolinic acid.

*E-mail address:* diego.juela@ucuenca.edu.ec.

https://doi.org/10.1016/j.seppur.2021.120286
Received 11 October 2021; Received in revised form 25 November 2021; Accepted 9 December 2021
Available online 14 December 2021

genotoxicity in aquatic organisms have attracted notable attention as a severe environmental apprehension. To date, a series of reviews have summarized the presence of trace amounts of antibiotics in aquatic environments, their occurrence, as well as their persistence, and their adverse impacts on human health and aquatic organisms [5–8]. Among these adverse effects, the emergence of bacteria resistant to antibiotics is of greatest concern to human health.

In the face of this environmental issue, there is an urgent need to remove antibiotics residues effectively from wastewaters to reduce their contact with the environment and humans. Several technologies have been successfully applied to remove these micropollutants. A general and systematic overview of these technologies is presented by Ahmed et al. [9] and Lu et al. [10]; among these, chemical, physical, biological, condition-based and combined strategies are summarized. The current status of antibiotics removal by advanced oxidation [11], biological [12,13], photocatalysis [14,15], membrane separation [16], and adsorption processes [17] have also been thoroughly reviewed. Adsorption is the most attractive technology among these technologies due to its low cost, easy design, simplicity, high efficiency, and easy scaling up. In addition, it is a method that has shown promising results for removing a wide variety of contaminants from aqueous media.

The essential factor in adsorption is the adsorptive materials since antibiotics are retained by physical or chemical forces in their active sites. Two critical aspects of an adsorbent are its adsorption rate and its adsorption capacity, which can be evaluated by equilibrium and kinetic studies in a batch system. A high rate of pollutant removal is essential from a practical viewpoint, as well as a short time to reach equilibrium since it entails that more volume of treated effluent can be treated in a short time. On the other hand, the adsorption capacity is determined by the properties of the adsorbent, mainly due to its porosity, specific surface area, and the presence of specific functional groups. The net surface charge, hydrophobicity/hydrophilicity ratio, pore distribution, reactivity, and dissociation constant are other fundamental properties. At present, a wide variety of bright synthetic adsorbents have been created for removing antibiotics from the aqueous medium; among these, layered double hydroxides [18], covalent-organic frameworks [19,20], metal–organic frameworks [14], hyper-cross-linked polymers [21], MXenes [22], and cyclodextrin polymers [23] have been extensively reviewed. Nevertheless, despite their remarkable adsorption performance, there are still technical limitations that inhibit their large-scale production, such as complicated synthesis procedures, use of toxic and expensive organic chemicals, high energy consumption, and unique and specific equipment [24,25]. Another sustainable approach to producing promising adsorbents is harnessing agricultural (AW) and industrial wastes (IW) derived from anthropogenic activities.

When AW and IW were initially seen as eco-friendly and renewable sources to create adsorbents, scientists began testing them to remove conventional pollutants. At first, AW and OW were applied in their natural or raw state, then chemical-modified adsorbents and waste-derived carbonaceous adsorbents appeared. Moreover, in recent years, the formation of waste-based composites and multi-functional materials derived from AW and IW have been prepared and used to remove antibiotics. Nonetheless, few review articles cover the whole scenario concerning the fabrication of these waste-derived adsorbents. Consequently, a review focusing on the different kinds of adsorbents obtained from AW and IW and their adsorption performance towards antibiotics is still needed. This review provides a comprehensive summary of the adsorption properties of different AW and IW-based adsorbents used for antibiotics removal; the review addressed from raw IW and AW to complex waste-derived adsorbents, examining issues such as advantages, drawbacks, and challenges. The study highlights the contribution of several advanced methods to create promising adsorbents using these residues. Additionally, critical factors of these adsorption materials such as specific surface area, total pore volume, average diameter pore, and adsorption capacity were presented and discussed. Offering an updated and focused review to summarize the adsorption performance of waste-derived adsorbents for antibiotic removal is of great importance for the future development of wastewaters' decontamination using green and sustainable adsorbents.

## 2. Agricultural and industrial waste as adsorbents

Agricultural and industrial wastes or industrial by-products have drawn attention to the adsorption field due to their eco-friendly approach and advantages such as easy access, high availability, and low cost compared to synthetic materials. These unorthodox materials are widely available in agro-industrial countries, and due to their high production, they have been analyzed as adsorptive materials within a circular economy approach. The structure of these materials has cavities and pores that allow the entrapment from small molecules, like metals, to complex molecules like dyes and antibiotics. Additionally, they have adequate adsorption capacity, feasibility to improve through chemical modification, and are susceptible to regeneration and degradability; these latter aspects lead to fewer problems in the final disposal after adsorption.

## 3. AW and IW in their raw state

Agricultural residues, food residues, and other industrial by-products in their raw state can be harnessed as low-cost adsorbents. On the whole, a simple pretreatment of crushing to increase their specific surface area, sieving, and washing to remove impurities is required before adsorption tests. Raw agricultural residues such as sugarcane bagasse, corn cob, rice husk have been employed to adsorb sulfamethoxazole (SMX) [26,27], ciprofloxacin (CIP) [28,29], and sulfadiazine (SDZ) [30]. Due to their content in cellulose, hemicellulose and lignin, functional groups like hydroxyl (−OH), alkyl ($-CH_3$, $-CH_2$), carbonyl (−COOH), and aromatic rings are present on the surface of these materials, and they are responsible for their adsorption properties [31]. Besides, some vegetable wastes have shown a fast adsorption rate toward several antibiotics, representing a practical benefit. For instance, Peñafiel et al. [29] employed raw sugarcane bagasse to remove CIP. This biosorbent removed 65% of CIP in the first 5 min and achieved an adsorption capacity of 16.6 mg/g at equilibrium. A similar effect was observed in the adsorption of SMX on corn cobs, removing 80% at equilibrium in the first 20 min [27]. The justification is due to the fact that organic residues are usually macroporous solids, where only the external diffusion controls the transfer mass mechanisms and the contribution of internal diffusion is low, thereby the equilibrium is reached in short operation time. Some physical properties of these agricultural waste along with their adsorption performance for several antibiotics are illustrated in Table 1. Specifically, the specific surface area determined by the Brunauer–Emmett–Teller method ($S_{BET}$), average pore diameter (Dp), pore volume (Vp), removal efficiency (%R), time to reach equilibrium ($t_e$), and maximum adsorption capacity at equilibrium ($q_{e\text{-}max}$) are summarized.

Alternatively, industrial by-products from different sectors, including fruits and vegetable peels, sludge, blast furnace slag, fly ash, palm oil ash, red mud, and others, have been reused as adsorbents. Besides, these reusing approaches decline the environmental impacts due to poor waste disposal (Table 1). Dube et al. [45] employed fly ash as an adsorbent to remove CIP and isoniazid (ISO), reaching equilibrium at around 30 min with a low adsorption uptake of 3.12 and 7.09 mg/g, respectively. Similar poor adsorption capacities were found with other industrial by-products such as olive pomace (16 mg/g for TET) [42], bauxite residue with 6.34 mg/g for CIP [46], iron ore waste with 14.16 m/g for norfloxacin (NOR) [43], and tamarind seeds with 9.17 mg/g for CIP [41]. However, some agricultural and industrial wastes also present adequate adsorption capacities (>100 mg/g), including spent coffee ground with 123.5 mg/g for tetracycline (TET) [49], wheat bran with 159 mg/g for CIP [39], ripe and unripe papaya peels with 215.09 and 213.99 for doxycycline (DOX) [36], and shrimp shell waste with 381.75

**Table 1**
Raw agricultural and industrial waste used as adsorbents for removing antibiotics.

| Adsorbent | Antibiotic[a] | $S_{BET}$ ($m^2/g$) | Vp ($cm^3/g$) | Dp (nm) | te (min) | % R | $q_{e\text{-}max}$ (mg/g) | Ref. |
|---|---|---|---|---|---|---|---|---|
| Sugarcane bagasse | CIP | 2.55 | 0.006 | 10.19 | 10 | 78 | 16.6 | [29] |
| Corn cob | SMX | 1.22 | – | – | 10 | 85 | 0.85 | [27,28] |
| | CIP | | | | 30 | 56 | 26.31 | |
| Rice husk | CIP | 0.78 | – | – | 30 | 60 | 5.55 | [28] |
| Rice husk | NOR | 0.902 | – | – | 40 | 78.2 | 20.12 | [32] |
| Coffee husk | NOR | 1.217 | – | – | 60 | 91.3 | 33.56 | [32] |
| Barley straw | NOR | 1.8 | – | – | – | <70 | 56 (E) | [33] |
| Groundnut shell powder | CIP | – | – | – | 15 | 79.6 | 8.07 | [34] |
| Palm bark | AMX | 124.36 | – | – | 80 | 98.1 | 35.92 | [35] |
| Ripe papaya peels | DOX | – | – | – | – | 87.9 | 215.09 | [36] |
| Unripe papaya peels | DOX | – | – | – | – | 87.5 | 213.99 | [36] |
| Maize straw | TYL | 1.32 | – | – | – | >50 | 0.497 | [37] |
| Maize cob | SMT | 2.984 | 0.0029 | 3.01 | 1440 | 80 | 0.362 | [38] |
| Maize husk | SMT | 2.587 | 0.0022 | 2.46 | 1440 | 80 | 0.308 | [38] |
| Maize straw | SMT | 2.768 | 0.0024 | 2.69 | 1440 | 80 | 0.334 | [38] |
| Wheat bran | CIP | – | – | – | 50 | 75 | 159.0 | [39] |
| Pomegranate peels | CIP | – | – | – | 120 | – | 1135.0 | [40] |
| Tamarind seeds | CIP | 279.55 | 0.092 | 2.82 | 50 | 45.08 | 9.17 | [41] |
| Olive pomace | TET | 0.324 | 0.002 | – | 30 | 75 | 16.0 (E) | [42] |
| Iron ore waste | NOR | 24.60 | – | – | 4320 | > 90 | 14.16 | [43] |
| Fly ash | NOR | 6.12 | 0.023 | 15.23 | 120 | 97.8 | 54.69 | [44] |
| Fly ash | CIP | 5.50 | – | – | 30 | 35 | 3.12 | [45] |
| | ISO | | | | 30 | 49 | 7.09 | |
| Bauxite residue | CIP | 38.91 | – | – | 720 | 75 | 6.34 (E) | [46] |
| Shrimp shell waste | TET | 8.90 | – | 4.47 | 900 | – | 381.75 | [47] |
| *Mytella Falcata* shells | RIF | – | – | – | 35 | 45.57 | < 5 | [48] |
| Spent coffee ground | TET | 419 | 0.23 | – | 20 | 97.2 | 123.46 | [49] |
| Pistachio nutshells | SAR | 4.24 | 0.0082 | – | 30 | 82.4 | 49.75 | [50] |
| *Aloe vera* leaves | SAR | 3.94 | 0.0112 | – | 30 | 29.15 | 3.50 (E) | [50] |
| Peel and seed of tomatoes | CIP | 2.594 | – | 3.16 | 240 | 96 | 0.76 (E) | [51] |
| Maple leaves | CIP | 1.058 | – | 5.26 | 240 | 98 | 0.75 (E) | [51] |
| Tangerine peel | CIP | 0.965 | — | 4.88 | 240 | 100 | 0.79 (E) | [51] |
| Eggshell | TYL | 1.059 | – | 6.70 | ~60 | 50 | 0.13 | [52] |
| Oakwood ash | TET | – | – | – | 15 | 80–10 | 0.059[c] | [53] |
| | OTC CTC | | | | | | 0.020[c] | |
| | | | | | | | 0.009[c] | |
| Pine bark | TET | – | – | – | 15 | 90–100 | 0.260[c] | [53] |
| | OTC CTC | | | | | | 243.22[c] | |
| | | | | | | | 0.060[c] | |
| Mussel shell | TET | – | – | – | 15 | 30–70 | 25.60[c] | [53] |
| | OTC | | | | | | 4.031[c] | |
| | CTC | | | | | | 165.45[c] | |
| Lemon and lime waste | SMX | – | – | – | 50 | 48.51 | 0.9 (E) | [54] |
| Peanut shell | SM | 2.01 | 0.011 | 18.73 | 720–1200 | 85 | 0.83 | [55] |
| | SMT | | | | | 63 | 0.18 | |
| | SFT | | | | | 60 | 0.20 | |
| | SMX | | | | | 40 | 0.27 | |
| Steel shaving waste | SMT TET | 2.718 | 0.0113 | 16.6 | 30–60 | 40.6 | 2.52 | [56] |
| | CAP | | | | | 67.8 | 1.72 | |
| | | | | | | 91.4 | 2.77 | |
| Rice husk ash | OFL | 32.6 | – | 6.5 | 200 | 93.4 | 8.478 | [57] |

[a] Removed antibiotics in adsorption tests.
[c] Expressed in mmol/g.

for TET [47]. Although, their long time to reach equilibrium was a negative aspect. Other physical properties of these wastes, like their specific surface area and pore volume, are also low compared to commercial adsorbents, usually less than 100 $m^2/g$ and 0.03 $cm^3/g$, respectively. Likewise, their average pore diameter is greater than 5 nm due to their high proportion of macro and mesoporous structure [31].

## 4. Approaches of surface modification

An enormous drawback of these materials is that most of them have poor adsorption efficiency and low selectivity towards antibiotics in question, which is usually less than 100 mg/g in their natural state, as shown in Table 1. Nonetheless, this limitation can be overcome by surface modification, in which specific functional groups are incorporated or eliminated to/from their surface, controlling in this degree the adsorption properties. Besides, the porosity and specific surface area are reinforced alongside the subsequent improvement of adsorption performance. Acid, alkaline, oxidizing, neutral, and organic agents can be typically employed to modify the functional groups of agricultural residues and by-products [58]. These adsorbents are summarized in Table 2.

The chemical modification influences the hydrophobic and lipophilic properties, the specific surface area and pore volume, surface charge properties, and the number of functional groups. In general, the acidic treatment induces a negative charge on the adsorbent's surface, increasing the content of oxygen-containing functional groups, such as carboxyl, carbonyl, quinone, hydroxyl, lactone and carboxylic anhydride. This last effect has also been observed with the use of oxidizing agents [59]. By contrast, the alkali modification provides a positive charge on the surface that optimizes the removal of negatively loaded species and increases the relative content of hydroxyl groups and surface area [58]. Hence, the type of modification must be done according to the

**Table 2**
Modified agricultural and industrial waste used as adsorbents for removing antibiotics.

| Adsorbent | Treatment | Antibiotic | $S_{BET}$ ($m^2$/g) | Vp ($cm^3$/g) | Dp (nm) | $t_e$ (min) | % R | $q_{e\text{-}max}$ (mg/g)[a] | Ref. |
|---|---|---|---|---|---|---|---|---|---|
| Garlic peels | $HNO_3$ | ENR | – | – | – | 10 | >60 | 29.8 | [79] |
| Carbon black waste | $H_2SO_4$ | TET | 375 | – | 6.63 | 100 | 80 | 205(E) | [80] |
| | | AMX | | | | 75 | 91 | 65 (E) | |
| Carbon black waste | $H_2SO_4$ | CIP | 409 | 0.96 | 1.7 | 150 | 90–99 | 13 (E) | [81] |
| | | SMX | | | | 450 | | 10 (E) | |
| Wheat straw ashes | HCl | TCL | – | – | – | 30 | 85–100 | 16.6 | [82] |
| Tamarind seeds | HCl | CIP | 471.98 | 0.0171 | 2.68 | 80 | 73.0 | 125.0 | [83] |
| Fly ash | HCl | NOR | 18.37 | 0.040 | 8.77 | 240 | 92.6 | 129.79 | [44] |
| Fly ash | NaOH | NOR | 31.27 | 0.077 | 9.76 | 240 | 96.7 | 189.40 | [44] |
| Grapefruit peel | NaOH | CIP | – | – | – | 120 | 96.4 | 2.54[b] | [84] |
| Tamarind seeds | NaOH | CIP | 432.80 | 0.0135 | 2.86 | 50 | 63.44 | 120.34 | [41] |
| Rice straw fiber | NaOH | CIP | 9.62 | – | 3.63 | 35 | 37 | 93.5 | [60] |
| Maize straw | MnOx | TYL | 10.55 | – | – | 450 | >50 | 13.31 | [37] |
| Maize straw | $FeMnO_x$ | TYL | 8.36 | – | – | 600 | >50 | 12.92 | [37] |
| Sawdust | $FeCl_3$ | TET | – | – | – | 120 | 98.40 | 5.41 | [85] |
| *Calotropis gigantea* fiber | $NaClO_2$ | ENR | – | – | – | 50 | 65–89 | 62.93 | [86] |
| | | CIP | | | | 25 | | 49.51 | |
| | | NOR | | | | 25 | | 68.95 | |
| Wheat substrate | $H_2SO_4$ and KOH | ENR | 11.0 | – | – | 1200 | 100 | 48.36 | [87] |
| Termite feces | $H_2SO_4$ and heating | NOR | 81.3 | – | – | 60 | 98 | 104.4 | [88] |
| Waste tire rubber | $H_2SO_4$ and boiling | TET | – | – | – | 100 | 90 | 303 | [89] |
| Watermelon seeds | $H_2SO_4$ and heating | SMX | – | – | – | 30 | 100 | 109.25 | [90] |
| | | SMT | | | | 30 | 97 | 97.80 | |
| Sawdust | $H_2SO_4$ and heating | SMX | – | – | – | 300 | 98 | 371.74 | [64] |
| | | TET | | | | 175 | 100 | 337.84 | |
| Spent Coffee | $H_2SO_4$ and heating | SMX | – | – | – | 175 | >50 | 256 | [65,91] |
| | | TET | | | | 50 | 100 | 462 | |
| Peanut shell | $H_2SO_4$ and heating | TET | 3.7 | – | – | 180 | 85 | 303 | [68] |
| Pinecones | $H_2SO_4$ and heating | TET | 4.55 | – | – | ~75 | 100 | 357.14 | [69] |
| Tea waste | $H_2SO_4$ and heating | SMX | – | – | – | 240 | 100 | 258.87 | [70,92] |
| | | TET | | | | 175 | 95 | 416.66 | |
| Oat hulls | $H_3PO_4$ and microwave | CIP | 460.83 | 0.246 | 2.13 | 1800 | 80 | 83 | [63] |
| Barley straw | $H_3PO_4$ and microwave | LEV | 1314 | – | – | 2880 | 100 | 408 | [33,67] |
| | | NOR | | | | 4320 | 100 | 398 | |
| Maize cob | NaOH and cellulase | SMT | 3.515 | 0.031 | 22.10 | 1440 | 80 | 2.92 | [38] |
| Maize husk | NaOH and cellulase | SMT | 3.145 | 0.028 | 17.365 | 1440 | 80 | 3.16 | [38] |
| Maize straw | NaOH and cellulase | SMT | 3.324 | 0.029 | 19.56 | 1440 | 80 | 3.01 | [38] |
| Sausage tree waste | Ionic liquid | PEN-G | 2.29 | 0.0078 | – | 40 | ~70 | 73.57 | [72] |
| Rice husk ash | Choline chloride-based DES | OFL | 23.12 | 0.03 | 6.5 | 400 | 77 | 35.77 | [66] |
| *Calotropis gigantea* fiber | Poly(m-phenylenediamine) | CIP | – | – | – | 10 | >70 | 203.7 | [77] |
| *Calotropis gigantea* fiber | Polydopamine | CIP | – | – | – | 50 | >80 | 268.9 | [78] |
| | | NOR | | | | 25 | | 105.8 | |
| *Calotropis gigantea* fiber | Polypyrrole | ENR | – | – | – | 180 | >40 | 78.27 | [75] |
| | | CIP | | | | 180 | >55 | 76.61 | |
| | | NOR | | | | 180 | >75 | 68.90 | |
| Construction and demolition waste | APTES | CIP | – | – | – | 100 | 71 | 124.5 | [76] |
| Steel shaving waste | Plasma treatment | SMT | 4.562 | 0.016 | 13.6 | 30–60 | 48.9 | 2.70 | [56] |
| | | TET | | | | | 68.4 | 2.16 | |
| | | CAP | | | | | 95.5 | 2.92 | |

APTES: 3-aminopropyltriethoxysilane, DES: deep eutectic solvent.
[a] Expressed by the Langmuir isotherm; otherwise, it is specified as experimental (E).
[b] Expressed in mmol/g.

target antibiotic to be eliminated. For instance, Huang et al. [60] modified rice straw fiber with NaOH, which exposed the majority of cellulose and eventually improved the specific surface area and adsorption capacity, reaching 93.5 mg/g of CIP at equilibrium at approximately 35 min. Similarly, Chen et al. [44] used fly ash, a by-product of coal combustion, modified with HCl and NaOH in order to enhance its affinity towards NOR. It was observed that the alkali treatment was more beneficial, improving the alkaline functional groups and $S_{BET}$ by 353% and 411%, due to the reaction of $SiO_2$ on fly ash with NaOH. Subsequently, the alkali-modified fly ash adsorbed NOR effectively, the adsorption capacity increased by 350%, passing from 54 to 189 mg/g. Yin et al. [37] improved the adsorption efficacy for TYL by modifying maize straw with iron and manganese oxides, which triggered a larger surface area than raw biosorbent (8.36 > 1.32 $m^2$/g), prompting an considerable rise in adsorption of tylosin (TYL). This study also indicated that manganese and iron oxides exhibited a synergistic capacity that is greater than individual $MnO_x$.

Additionally, other chemical modifications, including esterification, etherification, and surfactant, have been adopted to develop functional materials using agricultural and by-product waste. Esterification and etherification methods aim to create esters and ethers by reacting hydroxyl groups on lignocellulosic structures with specific reagents [58]. Fan et al. [61] applied the esterification reaction to banyan aerial roots with $HNO_3$, which successfully introduced new carboxyl groups on the fibeŕs surface that improved the adsorption capacity for CIP, passing from 42.56 to 86.58 mg/g. Etherification modification usually introduces amino groups into the surface via the reaction of epichlorohydrin with lignocellulose in the presence of N,N-dimethylformamide. On the contrary, surfactant modification favorably enhances lignocellulosic materials' pore and hydrophobic properties by using cationic or anionic surfactants [58,62]. To the best of our knowledge, no studies have used either etherification or surfactant modification on lignocellulosic waste and applied them to remove antibiotics. However, in either case, both esterification, etherification, and surfactant modifications

decline the specific surface area owing to blockage and narrowing of pores after the treatment [58], but with a simultaneous increase in the functional groups involved in the adsorption of organic pollutants, which translates into a better adsorption performance.

Besides, a combination of different treatment methods can be applied to improve even further the properties of biomass-based adsorbents. For instance, Movasaghi et al. [63] applied a treatment with $H_3PO_4$ and microwave to raw oat hulls. The combined treatment produced a substantial weight loss of the precursor due to the decomposition and conversion of hemicellulose, lignin and cellulose; this drove fragmentation and formation of a porous structure (Fig. 1a and 1b), increasing its surface area remarkably. Additionally, the acid treatment created acidic functional groups such as carboxyl, which enhanced the adsorption capacity by around 400% for CIP. Similar results were reported by Yan and Niu [33,67] with barley straw treated with $H_3PO_4$ and microwave to remove levofloxacin (LEV) and norfloxacin (NOR). Analogously, Zhang et al. [38] modified raw maize cob (MC), maize husk (MH), and maize straw (MS) using cellulase and NaOH, and applied them to adsorb sulfamethazine (SMT). The modified MC had the highest adsorption performance (531.78 mg/kg) owing to the hydroxyl and aromatic structures presented on the modified surface that interacted with SMT via hydrogen bonds and π-π EDA interaction. Similarly, Islam et al. [68,69] and Ahsan et al. [64,65,70] conducted a myriad of modification tests on lignocellulosic wastes (pine cone, tea waste, coffee waste, and sawdust) using a thermochemical method (sulfuric acid reflux at temperatures below 100 °C). After the sulfonation process, samples showed

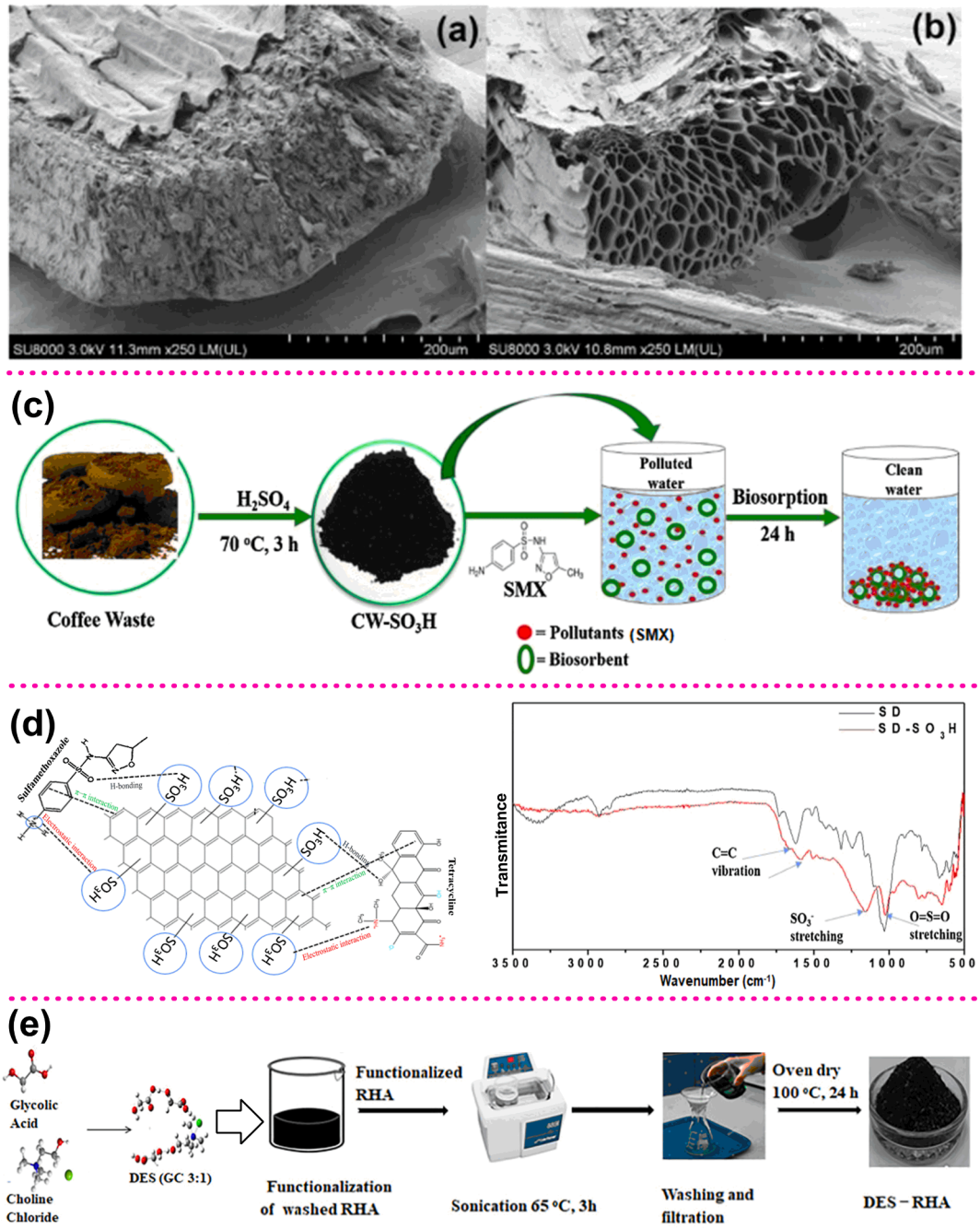


**Fig. 1.** (a and b) SEM images of oat hulls before and after the treatment with $H_3PO_4$ and microwave. Reproduced with permission of [63]. Copyright 2021 Elsevier B. V. (c and d) Preparation of sulfonated coffee waste, FTIR spectrum, and possible interactions with SMX and TET with sulfonated coffee waste. Reproduced with permission of [64,65]. Copyright 2021 Elsevier B.V. (e) Preparation of RHA modified with DEs. Reproduced with permission of [66]. Copyright 2021 Elsevier B.V.

the presence of sulfonate groups such as $SO^{3-}$ and O═S═O, and despite that the treatment did not increase the surface area, the samples showed a remarkable improvement in the adsorption capacity (250–500 mg/g) for antibiotics like tetracycline (TET) and SMX due to the sulfonic groups ($SO_3$-H). These new functional groups formed electrostatic attractions, π-π interactions, and hydrogen bonds with antibiotics (Fig. 1d). These studies corroborate that apart from the surface area, the functional groups on the surface are also an essential factor in the adsorption process.

The ordinary acid and alkali solutions used as modifier agents usually are toxic and highly volatile in large volumes. In recent years, researchers have intensified the lookup of new and greener solvents, and ionic liquids and deep eutectic solvents are presented as promising alternatives. Ionic liquids (ILs) are made up of an organic cation and an inorganic or organic anion, unlike traditional solvents that are composed of molecules. Therefore, ILs show the properties of salts [71]. Besides, due to the strong electrostatic force among ions, ILs present low volatility and high viscosity; other desirable properties such as biodegradability can be adjusted by changing the type of cation and/or anion. In the adsorption field, ILs containing hydroxyl and carboxyl groups are seen as potential modifiers since —OH and —COOH functional groups can be introduced on the adsorbent's surface. In this context, Lawal and Moodley [72] used a cationic IL (1-methyl, 3-decahexzyl imidazolium) at room temperature to modify waste from sausage trees; the treated adsorbent exhibited a better removal efficiency for penicillin G (PEN-G), passing from 5.51 to 73.57 mg/g. FTIR and XRD spectrums showed the removal of hemicellulose and decomposition of cellulose by the addition of IL. The presence of methylene groups was also detected; similar findings were reported in peanut shells modified with the same IL to remove other organic pollutants [71,73]. On the other hand, deep eutectic solvents (DEs) are an "improved version" of ILs, with greener credentials, easier to prepare, more biodegradable and inexpensive than ILs, but with similar properties and applications [74]. Recently, Kaur et al. [66] prepared a type of DEs using glycolic acid and choline chloride and employed it to functionalize risk husk ash (RHA) by sonication at 65 °C for 3 h (Fig. 1e). According to characterization analyses, the prepared adsorbent diminished $S_{BET}$ from 32.6 to 23.12 $m^2/g$ since DEs molecules were embedded inside the pores of RHA; the FTIR analysis, however, showed a prominent new peak due to the presence of —COOH group of glycolic acid on the surface of RHA, which eventually improved the removal of ofloxacin (OFL) from 50 to 77% with the formation of hydrogen bonds. Even though ILs and DEs are potential replacements for typical modification agents owing to their eco-friendly approach, to date, there are a limited number of published reports on the adsorption of antibiotics using ILs and DEs-modified agricultural and industrial waste.

Finally, in this section, it is necessary to highlight the grafting process. In this modification, a monomer is polymerized along with the structure of AW or IW; in other words, AW and IW materials are used as templates for the polymerization of a given monomer. Generally, the grafted adsorbent improves its surface functionality by introducing new favorable adsorption sites, which ensures the easy removal of antibiotics from the solution [58]. Based on this, Cao et al. [77] reported the polymerization of m-phenylenediamine (mPD) via the conventional chemical oxidative method by using *Calotropis gigantea* fiber (CGF) as a natural bio-template. A poly-mPD layer was formed along the fiber surface, declining the hydrophobicity and providing N-rich functional groups; however, the experimental adsorption capacity for CIP decreased as the dose of mPD increased due to the aggregation of polymeric particles and the formation of water clusters at the hydrophilic sites. A similar aggregation phenomenon was observed with the polymerization of pyrrole on the surface of the same fiber [75], where CGF was first treated with $NaClO_2$ to remove the attached wax (Fig. 2a). The authors reported adsorption capacities of 78.27 mg/g for

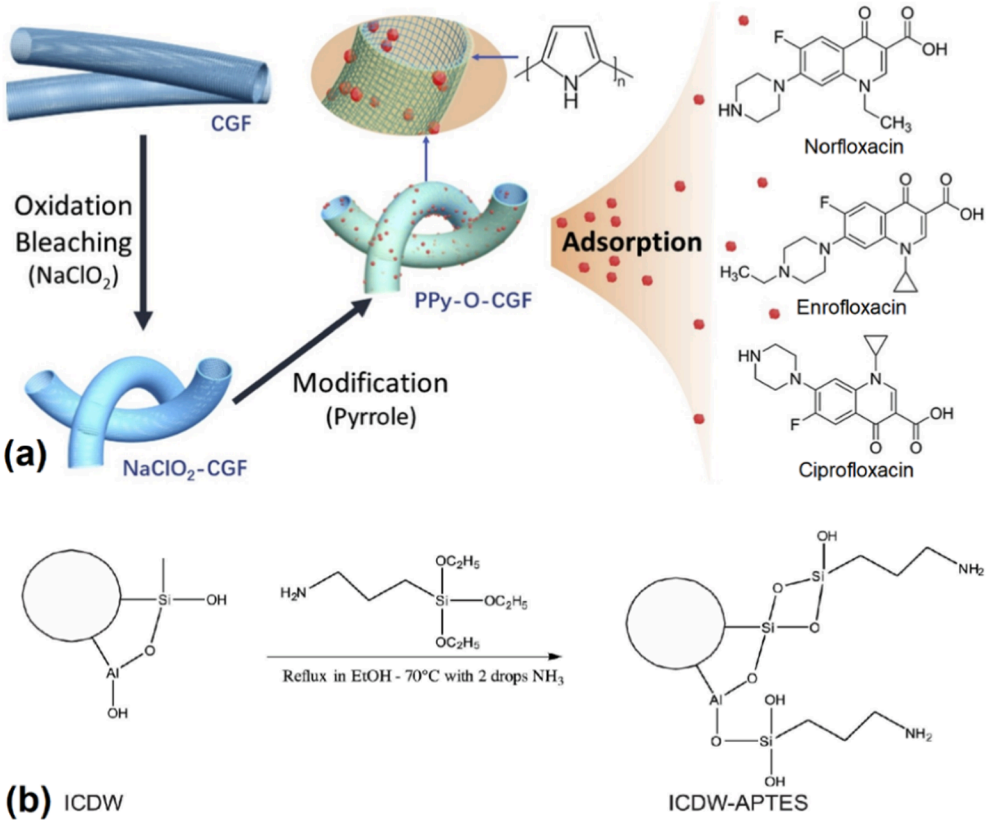


**Fig. 2.** (a) Preparation of polypyrrole functionalized *Calotropis gigantea* fiber and adsorption of ENR, CIP, and NOR. Reproduced with permission of [75]. Copyright 2021 Elsevier B.V. (b) Preparation of ICDW-APTES from ICDW using alkaline catalysis. Reproduced with permission of [76]. Copyright 2021 Elsevier B.V.

enrofloxacin (ENR), 76.61 mg/g for CIP and 68.90 mg/g for NOR with CGF coated with polypyrrole, 77.3 mg/g for CIP with CGF coated with poly(m-phenylenediamine), and 136.43 mg/g for CIP and 88.43 mg/g for NOR with CGF grafted with polydopamine [75,77,78]. Likewise, construction and demolition wastes were grafted with APTES (3-aminopropyltriethoxysilane). The oxygen groups of silicates and aluminates from this waste reacted with the silanol group from APTES, yielding a very stable amino-functionalized adsorbent. The grafted material was applied in CIP adsorption, showing a maximum adsorption capacity of 124.5 mg/g at 25 °C [76].

## 5. Agricultural and industrial waste-based composites

Another strategy to create functional adsorbents with better adsorption performance towards target pollutants is the formation of waste-based composites. In general, a composite is made up of a matrix (dominant phase) and functional species, which maintain their own identity while contributing beneficial properties to the entire system. In recent years, waste-based composites have received tremendous interest since new functionalities can be introduced, creating a synergetic effect between two different materials, hence improving the adsorption performance and selectivity. For the composite materials presented in this review, the traditional nomenclature was adopted, described as A/B composite in which A is the functional species and B is the matrix. When agricultural and industrial wastes act as the matrix, functional species such as nanoparticles, nanowires, and nanofibers can be loaded into the material in order to give these residues the nanomaterials' properties and suppress their downsides.

For the most part, nanoparticles (NPs) are super-adsorbents due to their excellent surface properties, small size, as well as high activity. However, the easy aggregation of NPs limited its performance and diminished the adsorption capacity and reactivity. To solve such drawbacks, various materials, including lignocellulosic structures, have been used as supporters for NPs producing composites or hybrid adsorbents, which have shown improvements in the adsorption efficiency towards antibiotics. In particular, two methods have been extensively applied to create NPs/waste composites: the blending and in-situ growth methods. In the blending technique, NPs and the residue are mixed by mechanical stirring or sonification with a suitable dispersant, and then the solvent is separated by filtration to leave the composite material [93,94]; namely, Mohammed & Kareem [94] prepared a ZnO/Pistachio shell composite using this procedure (Fig. 3a). By contrast, in-situ growth method, the matrix is immersed in the solution containing NPs precursors and stirred under an $N_2$ atmosphere. Then, the aqueous alkaline solution is added to form the NPs, with subsequent washing [95,96]. Fig. 3b depicts the procedure followed by Aydin et al. [95] to synthesize $Fe_3O_4$ NPs/red mud composite using this methodology. Some waste-based composites prepared using these methodologies are detailed in Table 3.

Nanoscale zero-valent iron particles (nZVIs) are another effective nanomaterial to remove organic pollutants. A comprehensive review of the application of nZVIs and their composites in the removal of organic compounds was performed by Lie and colleagues [97]. An additional upside of nZVIs is that the removal of antibiotics occurs by adsorption and degradation when they are supported on agricultural waste [96,98]. Shao and colleagues synthesized wheat straw supported with nZVIs particles via in-situ growth methodology; SEM images indicated that nZVI particles were successfully supported on the straw, where the biomass inhibited the agglomeration of nZVI nanoparticles (Fig. 4b). The experimental results showed that, compared with nZVI and wheat straw, nZVI/wheat straw composite possessed higher removal efficiency with a maximum removal capacity of 363.63 mg/g for CIP at 25 °C. The enhancement was justified by the synergistic effect of adsorption and redox processes caused by $Fe^0$ in the composite [96]. A similar synergistic effect of adsorption and photocatalysis has been observed with other photocatalytic materials such as carbon nitride (g-$C_3N_4$) [99].

Furthermore, although some industrial wastes in powdered form show high adsorption efficiency for antibiotics, their form limits practical application due to the difficult recovery in batch systems and the high-pressure drop in continuous systems. Hence, researchers have focused on the encapsulation and magnetization of these waste materials in order to create composites that can be easily and selectively separated from aquatic environments, thereby facilitating their large-scale application. For the encapsulation approach, particles of AWs and IWs are confined in polymeric matrices in order to form granules or beads. Based on this, Mitra et al. [80] dispersed powdered leached carbon black waste (LCBW) in a matrix of carboxymethyl cellulose (CMC) to elaborate a composite in the form of beads (Fig. 4c). The approximate size of the CMC/LCBW spherical bead was 3 mm, yet its adsorption efficiency for SMX decreased by around 25% compared to powdered carbon black waste. The same effect was observed with LCBW/chitosan composite beads, where the adsorption capacity for TET was 181 and 39 mg/g with LCBW and LCBW-based composite, respectively [80]. The reduction was attributed to the decline in adsorption

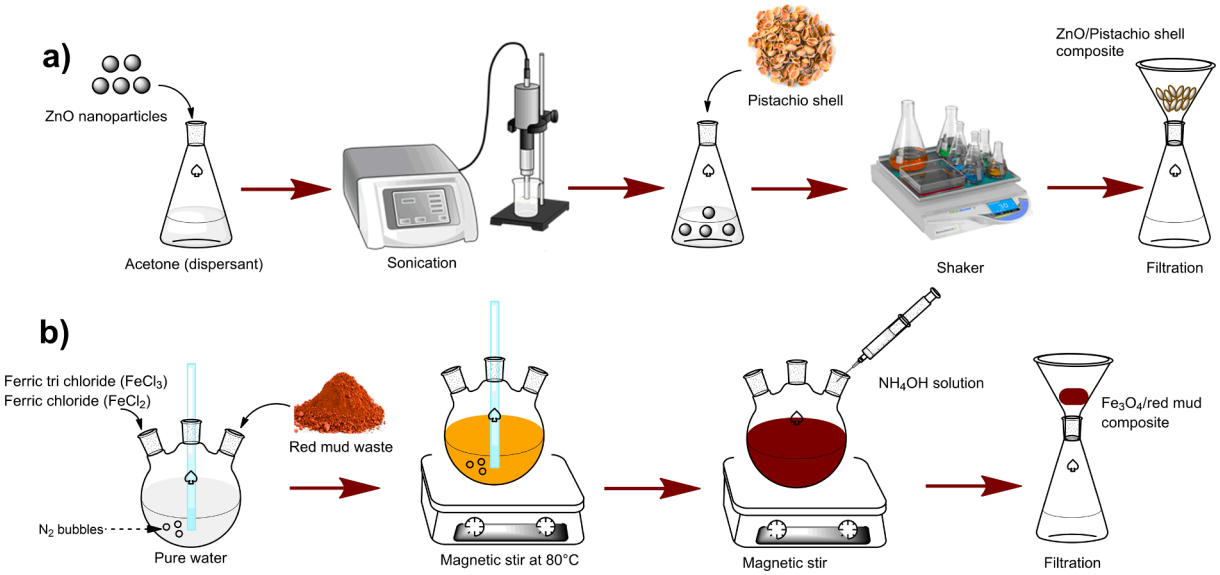


**Fig. 3.** Solution blending method (a) and in-situ growth of NPs (b) for the synthesis of NPs/waste composites.

**Table 3**
Composites derived from agricultural and industrial residues for removing antibiotics.

| Composite | Antibiotic | $S_{BET}$ ($m^2$/g) | Dp (nm) | te (min) | % R | $q_{e\text{-}max}$ (mg/g)[a] | Ref. |
|---|---|---|---|---|---|---|---|
| nZVI NPs/Blast furnace slag | OTC | – | – | ~30 | 95 | ~ 400 (E) | [100] |
| nZVI NPs/wheat straw | CTC | – | – | 30 | 100 | 1280.80 (E) | [98] |
| $Fe_3O_4$ NPs/red mud composite | CIP | 83.2 | – | 180 | 83 | 169.49 | [95] |
| ZnO NPs/pistachio shell composite | TET | – | – | 90 | 82.6 | 95.06 | [94] |
| ZnO NPs/pistachio shell composite | TET | 4.24 | – | 30 | 75 | 92.45 | [93] |
| | AMX | | | 60 | 75 | 98.72 | |
| | CIP | | | 30 | 90 | 132.24 | |
| Terbium/$HNO_3$-modified garlic peels | ENR | – | – | 20 | >80 | 580 | [79] |
| Europium/$HNO_3$-modified garlic peels | ENR | – | – | 20 | >80 | 421 | [79] |
| Tb-Eu/$HNO_3$-modified garlic peels | ENR | – | – | 20 | ~97 | 769 | [79] |
| ZnS:Mn/Maize straw | TYL | – | – | 720 | 80 | 3.45 | [101] |
| MnOx/maize straw | TYL | 10.55 | – | 300 | – | 13.3 | [37] |
| Mg@Fe-LDHs/Rice husk | MER | 32.3 | – | 50 | 92 | 93.46 | [102] |
| LCBW/chitosan beads | TET | 375 | 3.63 | 1400 | 92 | 39 (E) | [80] |
| | AMX | | | 1400 | 62 | 12 (E) | |
| LCBW/CMC beads | SMX | – | – | 600 | 50 | – | [81] |
| Bacteria/peanut shells composite | SMX | – | – | 5–10 | 100 | – | [103] |
| | SMT | | | | 90 | | |
| | STX | | | | 80 | | |

NPs: nanoparticles, LDHs: layered double hydroxides, LCBW: leached carbon black waste, CMC: carboxymethyl cellulose.
[a] Expressed by the Langmuir isotherm; otherwise, it is specified as experimental (E).

sites of LCBW owing to its encapsulation within the polymeric matrix and the increase in the mass transfer resistance (and longer path) of intraparticle diffusion [80,81]. On the other hand, magnetic modification is also adopted in the development of functional adsorbents. Generally, magnetic nanoparticles (NPs) such as magnetite, maghemite, some ferrites, and metallic iron are loaded on the surface of the residue; the prepared material not only exhibits a response to an external magnetic field, but it in some cases also increases the adsorption efficiency. In this context, Aydin et al. [95] coated red mud with $Fe_3O_4$ NPs by the co-precipitation method and applied it for CIP removal. The synthesized $Fe_3O_4$/red mud composite had an adsorption uptake of 169.49 mg/g and a saturation magnetization of 12.1 emu/g that was enough to separate the particles by an external magnet. The study also demonstrated that the agglomeration and iron leaching of $Fe_3O_4$ NPs are overcome by combining these two materials.

## 6. Carbonaceous materials derived from AW and IW

Agricultural and industrial wastes can also be used as precursors to produce carbon-rich adsorbents. These carbonaceous materials (CMs), including biochar and hydrochar, have gained significant attention in recent years; compared to the commercial activated carbon, these materials are usually produced under lower temperature conditions and in an oxygen-limited environment, which represents an economic advantage. Besides, CMs can be obtained from various organic feedstocks, including waste biomass, municipal waste, agricultural and livestock waste, food production, and industrial residues. Fig. 5a and 5b depict the primary carbonaceous materials covered in this review alongside their adsorption capacity.

### 6.1. Biochar

Although biochar (BC) was originally used for agricultural purposes, nowadays, this carbonized material is largely used in various fields, including adsorption. In liquid-phase adsorption, BC has shown excellent adsorption properties for heavy metals, dyes, and other inorganic compounds. In general, pristine biochar is produced when a given feedstock is exposed to a thermochemical process called pyrolysis at temperatures up to 700 °C in an atmosphere with or without oxygen [104]. Depending on the precursor and pyrolysis conditions, such as temperature, time, carrier gas, and heating rate, different physicochemical properties can be obtained. An exhaustive review of the effect of these parameters has been reviewed by Krasucka et al. [105] and Janu et al. [106]. In relation to antibiotic adsorption, comprehensive reviews of the adsorption performance of pristine BCs, as well as modifications, can also be found in several reviews papers [104,107,108]. Since this topic has been thoroughly summarized in several papers, this review will only provide a brief overview, which focuses on recent developments and examples of particular interest to the readers; therefore, only BCs with outstanding adsorption capacities ($q_{e\text{-}max} \geq 100$ mg/g) were collected and detailed in Table 4. Additionally, several modifications and new approaches to create superior carbon-based adsorbents are discussed.

Most pristine biochar shows limited antibiotics adsorption capacities ($q_e < 100$ mg/g) mainly due to their poorly developed pores and limited surface areas [105]. For instance, biochar produced from wheat straw with 1.03 mg/g for SMX [109], from food scraps with 8.23 mg/g for TET [110], from soapsuds seeds with 33.44 mg/g for CIP [111], from palm oil fiber with 57.47 mg/g for cephalexin (CEX) [112], from pine bark with 58.47 mg/g for TET [113], from sewage sludge with 53.19 mg/g for amoxicillin (AMX), 24.57 mg/g for SMX, and 98 mg/g for TET, to name a few. This is in part due to the lack of affinity between the antibiotic and the adsorbent, which is influenced by aromaticity, polarity, and the absence/presence of required/not required functional groups on the BC. Hence, the adsorption properties of BCs need to be further improved. For this, the classical strategy is to activate BC physically or chemically; although the physical and chemical activations produce highly porous carbons with high adsorption performance towards antibiotics ($q_e > 400$ mg/g) [114–116], yet these are old and energy-intensive methods and thus are not covered in this review. Instead, novel and newly developed methods were comprehensively reviewed. As discussed above, modification aims to change the surface's chemistry and physical properties, giving specific functional groups for specific sorbates and increasing $S_{BET}$ and $V_p$. Some new physical modification methods include ball milling, microwave modification or microwave pyrolysis, and ultrasonic modification. Besides, like raw agricultural and industrial waste, the same chemical modification can be used to tailor the BC's surface. Table 4 summarizes the adsorption performance of several modified BCs for the adsorption of antibiotics.

#### 6.1.1. Physical modification methods

In general, physical modification methods change the porous structure of the biochar, thereby increasing $S_{BET}$, $V_p$, and the proportion of micro and mesopores; however, these methods can also expose new surface functional groups [105]. Ball milling aims to grind BC and reduce its particles to nanometer size, whereby the specific surface area,

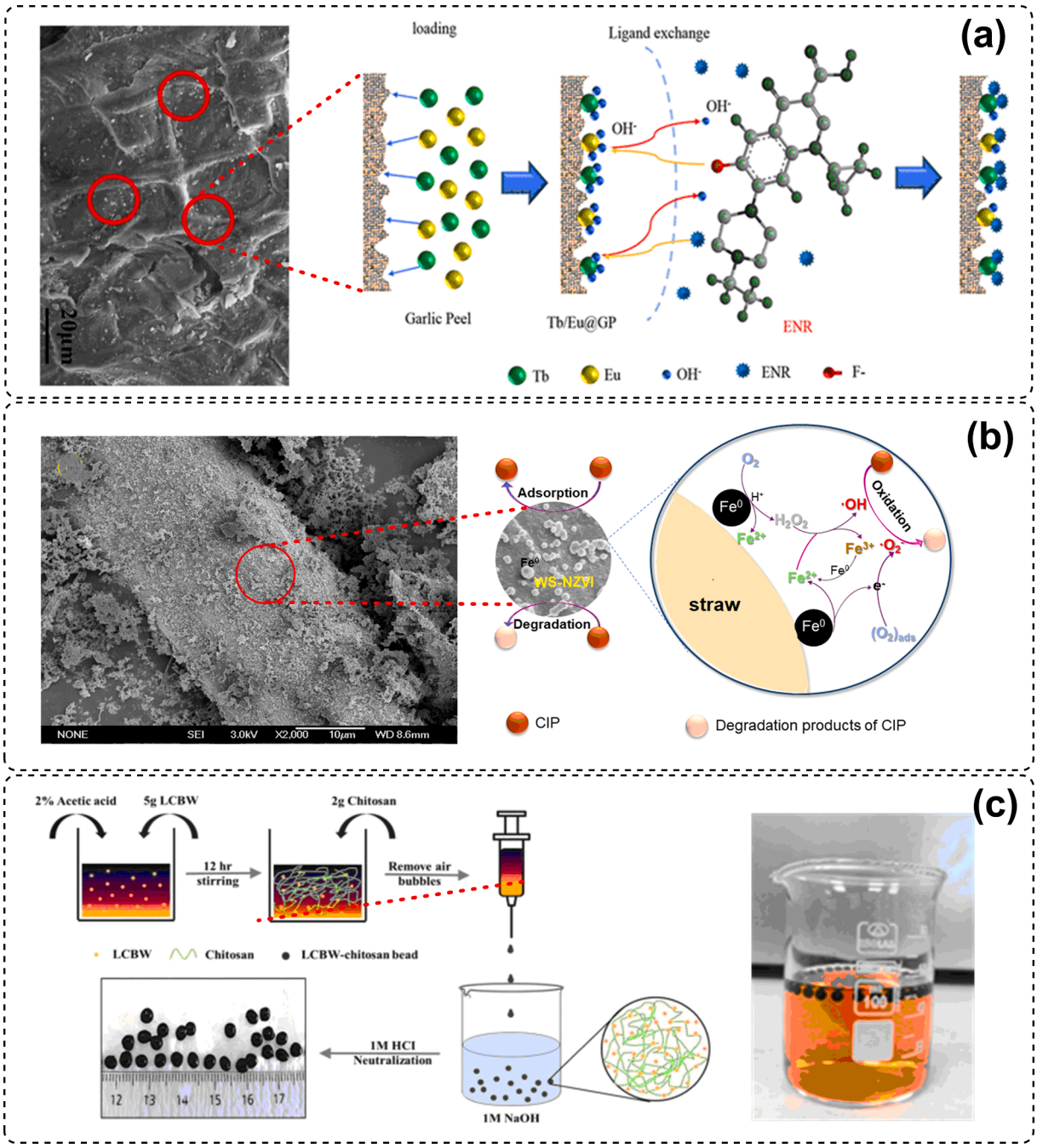


**Fig. 4.** (a) SEM micrographs of Tb-GP/$HNO_3$ modified garlic peels and adsorption mechanism of ENR. Reprinted with permission from [79]. Copyright 2021 American Chemical Society. (b) SEM of nZVI/wheat straw composite and synergistic effect of adsorption and redox processes in CIP removal. Reproduced with permission [96]. Copyright 2021 Elsevier B.V. (c) Preparation of composite beads from a hydrogel of chitosan and LCBW. Reproduced with permission [80,81]. Copyright 2021 Elsevier B.V.

surface functional groups, and pore structure enhance significantly. For instance, Huang et al. [117] showed that ball milling greatly enhanced the specific surface area (from 9.8 to 309 $m^2/g$) and the oxygen-containing functional groups, which boosted the ability of biochar to sorb SMX and sulfapyridine (SPY) through the formation of hydrogen bonds. Likewise, when the grinding process is carried out using a solvent (wet milling), new functional groups are created on the surface of biochar [107]. An overview of the efficiency of ball-milled biochars and their composites for the removal of emerging contaminants was written by Amusat et a. [118]. Microwave pyrolysis involves using microwave radiation as a heating source for biomass pyrolysis, which reduces energy consumption and shortens reaction times. Ram et al. [119] prepared BC from waste cotton seeds using a microwave-assisted synthesis for the adsorption of AMX; it was found that the microwave energy enlarged the specific area and pore volume of biochar, which enhanced the adsorption of AMX. Finally, during the ultrasonic method, the cavitation effect of ultrasound irradiation creates a uniform biochar suspension, exfoliating and breaking apart the regular shape of graphitic oxide layers of biochar, cleaning smooth surfaces, and increasing the porosity and permeability of biochar's carbonaceous structure [120]. Consequently, the biochar's structure is boosted with a combination of micro and mesoporous surfaces. Currently, although ball milling, ultrasonic and microwave-assisted methods are green modification and synthesis techniques, few experiments have been performed on the

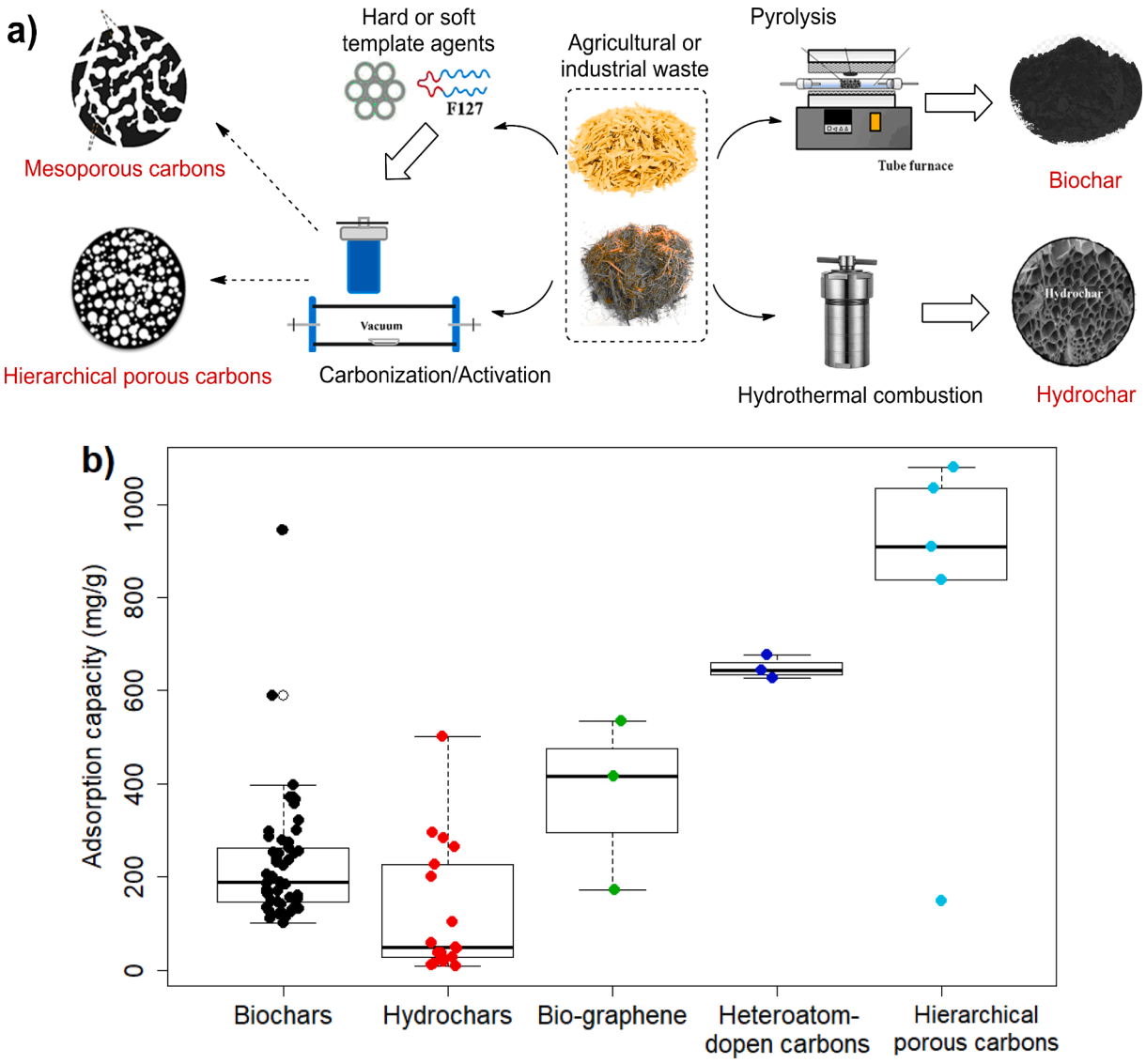


**Fig. 5.** (a) Schematic for synthesizing biochar, hydrochar, mesoporous carbons, and hierarchical porous carbons. (b) Adsorption capacities for the carbon-based adsorbents; data were taken from Table 4.

adsorption of antibiotics using these pre-synthesis and post-synthesis treatments.

### 6.1.2. *Chemical modification methods*

Most of the chemical modifications aim to increase or create new functional groups on the surface of biochar and not enhance the physical properties like specific surface area. In fact, in some of these chemical treatments, the specific surface area and pore volume decreased due to the destruction of the porous structure [107]: some studies are summarized in Table 4. Some functionalization treatments for biochar are oxidation, sulfuration, and nitrogenation. Oxidative modification aims to increase the number of oxygen-containing functional groups on the biochaŕs surface by using hydrogen peroxide ($H_2O_2$) or nitric acid ($HNO_3$) at temperatures under 100 °C. For example, Geng et al. [121] synthesized $HNO_3$-modified biochar from walnut shells at 60, 80, and 100 °C with 12 h constant stirring. It was observed that after $HNO_3$ - modification, a large number of functional groups including O—H, C═C, C═O, N═O, O═C—O and C—O on the surface were substantial, and the intensity of these peaks gradually increased along with the temperature; the maximum adsorption capacity was 160.97 and 215.94 mg/g at 25 °C for sulfamethazine (SMT) and sulfachloropyridazine (SCP), respectively. The same effect was observed in the biochar obtained from sugarcane bagasse and modified with 30% hydrogen peroxide [122]. In sulfurization, sulfur-containing groups such as sulfonic acid and sulfhydryl can be introduced on the surface of BCs following the same procedure explained for raw agricultural and industrial wastes. Another sulfur-containing compound to functionalize BCs recently studied is xanthate [123]; they formed the xanthate-functionalized BC by reacting the hydroxyl groups of the biochar with $CS_2$ in an alkaline medium. The adsorption performance of the prepared material for TET was higher than other materials, including commercial activated carbon. Finally, nitrogen modification introduces N into BC, which is commonly accomplished with ammonia and acid nitric [105]. Other innovative modification agents recently studied to functionalize biomass-based biochars include deep eutectic solvents [124,125], as well as anionic and cationic surfactants [126]. Finally, although the chemical activation agents are not discussed in this review, it is worth noting that new reagents have been explored in recent years, such as ammonium polyphosphate [116], potassium tartrate [127], boric acid [128], and ammonium chloride [129].

**Table 4**
Pristine and modified carbonaceous materials, carbon-based composites, and advanced carbonaceous materials derived from agricultural and industrial waste for antibiotic removal.

| Adsorbent | Precursor | Technique used | Antibiotic | $S_{BET}$ ($m^2$/g) | Vp ($cm^3$/g) | Dp (nm) | te (min) | %R | $q_{e\_max}$ (mg/g)[a] | Reference |
|---|---|---|---|---|---|---|---|---|---|---|
| BC | Olive stones | Pyrolysis (400 °C/5h/air) | AMX | 476 | – | – | 150 | ~95 | 1.33 × $10^7$ | [178] |
| BC | *Alfalfa Medicago* sativa L. | Pyrolysis (500 °C/0.5 h/$N_2$) | TET | 31.1 | – | – | 3000 | >80 | 372.3 | [179] |
| BC | Spent bleaching earth | Pyrolysis (300 °C/2h/air) | TET | 39.7 | 0.106 | 10.71 | 175 | 100 | 297.9 | [180] |
| BC | Used tea leaves | Pyrolysis (540 °C/0.5 h/$N_2$) | CIP | 8.06 | 0.012 | 4.44 | 720 | 50 | 238.1 | [181] |
| BC | Rice straw | Pyrolysis (700 °C/2h/$N_2$) | DOX | 20.55 | 0.019 | 6.42 | 120 | 80 | 170.4 | [182] |
| BC | Pinewood sawdust | Pyrolysis (500 °C/1h/air) | TET<br>SDZ | 738.00 | 0.344 | – | 2880 | 50–70 | 163.0<br>261.0 | [183] |
| BC | Coconut shells | Pyrolysis (450 °C/1h/$N_2$) and ultrasonic treatment. | LEV<br>TET | 1452.00 | – | – | 150<br>150 | 99.6<br>78.23 | 397.7<br>320.9 | [184] |
| Honeycomb tubular-like BC | Fargesia leaves residues | Pyrolysis (800 °C/6h/$N_2$) with $ZnCl_2$. | TET | 461.00 | 0.122 | 3.06 | 90 | 90 | 123.6 (E) | [185] |
| $K_2SO_3$-modified BC | Wing husk waste | Extraction and pyrolysis (700 °C/2.2 h/$N_2$) | TET | 2008.00 | 1.175 | 3.169 | 275 | >80 | 944.3 | [186] |
| $ZnCl_2$-modfied BC | Chinese herbs | Pyrolysis (500 °C/1.5 h/$N_2$) and modification | CTC<br>TET<br>OTC | 1556.00 | 0.870 | 3.46 | 80<br>100<br>125 | 90–100 | 200.0<br>188.7<br>129.9 | [187] |
| $H_3PO_4$-modified BC | Rice straw | Pyrolysis (700 °C/2h/$N_2$) and acid modification | TET | 372.21 | 0.230 | – | 12,000 | >80 | 167.5 | [188] |
| $H_3PO_4$-modified BC | Swine manure | Pyrolysis (700 °C/2h/$N_2$) and acid modification | TET | 314.04 | 0.250 | – | 12,000 | >80 | 160.3 | [188] |
| HCl-modified BC | Pharmaceutical sludge | Pyrolysis (600 °C/1h/$N_2$) and acid modification | TET | 319.80 | 0.537 | 3.823 | 200 | ~85 | 183.5 | [189] |
| KOH-modified BC | Coconut husk | Microwave-assisted method at 540 W/10 h and alkali modification | CIP<br>TET | – | – | – | 30<br>30 | 50–80 | 232.0<br>232.0 | [190] |
| NaOH and HCl-modified BC | Sewage sludge | Pyrolysis (800 °C/2h/$N_2$) and alkali/basic modification | TET | 102.38 | 0.146 | 3.88 | 1800 | 86 | 224.0 | [191] |
| Sodalye and $HNO_3$-modified BC | Sewage sludge | Pyrolysis (800 °C/2h/$N_2$) and modification | TET | 202.52 | 0.256 | 3.86 | 1600 | 86 | 187.3 | [192] |
| DES-modified BC | *Vitex doniana* residues | Pyrolysis (300 °C/6h/air) and DES modification | CIP | 12.54 | 0.190 | – | 400 | 70 | 140.3 | [125] |
| Co/Gd-loaded BC | Camellia oleifera shells | Impregnation and pyrolysis (879 °C/5h/$N_2$) | TET | 370.37 | 0.199 | 2.15 | 360 | 100 | 119.1 | [193] |
| Fe/N loaded BC | Rice straw | Impregnation and pyrolysis (700 °C/2h) | TET | 606.62 | 0.335 | 2.21 | 50 | >90 | 156.0 | [194] |
| Fe-loaded BC | Sewage sludge | Pyrolysis (600 °C/2h/$N_2$), impregnation, and pyrolysis. | TET<br>AMX | 38.08 | 0.018 | 1.19 | 1440 | – | 123.35<br>109.89 | [195] |
| Fe-loaded BC | Bermudagrass | Impregnation and pyrolysis (800 °C/2h/$N_2$) | SMX | 1013.40 | – | – | 1500 | 80 | 252.81 | [196] |
| Fe/Zn-loaded BC | Municipal sludge | Pyrolysis (600 °C/2h/$N_2$) and impregnation (hydrothermal method) | TET | 176.00 | 0.404 | 9.12 | 1500 | 91.2 | 145.0 | [197] |
| $MnO_x$-loaded BC | Peanut shell | Impregnation and pyrolysis (500 °C/2h/$N_2$) | DOX | 50.61 | 0.155 | 12.24 | 1440 | ~78 | 171.36 | [198] |
| Mn/Fe loaded BC | Vinasse waste | Impregnation (co-precipitation) and Pyrolysis (800 °C/1h/$N_2$) | PEF<br>CIP | 94.94 | 0.127 | 1.63 | 1500 | >80 | 256<br>357 | [131] |
| Mn/Fe loaded BC | Vinasse waste | Impregnation and Pyrolysis (800 °C/1h/$N_2$) | LEV | 93.40 | – | – | 3000 | 83 | 278 | [199] |
| Fe/Zn loaded BC | Sawdust | Impregnation and Pyrolysis (600 °C/2h/$N_2$) | TET | – | – | – | 3000 | 94.1 | 102 | [200] |
| $Fe_3O_4$/BC composite | Sugarcane bagasse | Impregnation and pyrolysis (800 °C/2h/$N_2$) | SMX | 605.59 | 0.310 | 1.73 | 100 | >97 | 205 | [135] |
| $Ga_2S_3$/sulfur-BC composite | Sugarcane bagasse | Impregnation and high-temperature sulfurization | CIP | 681.67 | 0.221 | 1.41 | 45 | – | 367.45 | [201] |
| $MnO_2$/BC composite | Chinese herbal residues | Pyrolysis (500 °C/2h/$N_2$) and impregnation (co-precipitacion) | TET | 31.74 | 0.063 | 7.97 | 3000 | ~80 | 131.49 | [202] |
| g-$MoS_2$/BC composite | Rice straw | Pyrolysis (500 °C/2h/$N_2$) and impregnation (hydrothermal method) | TET | 176.80 | 0.084 | 3.51 | 1100 | >85 | 249.38 | [203] |
| $NiFe_2O_4$ NPs/BC composite | Vinasse waste | Impregnation (co-precipitation) and pyrolysis (700 °C/1h/$N_2$) | LEV | – | – | – | 1200 | ~90 | 251 | [134] |
| TiO2 NPs/BC composite | Spent coffee grounds | Pyrolysis (500 °C/1h), and impregnation (hydrothermal method) | BLX | 50.54 | 0.048 | 2.44 | 30 | ~65 | 196.73 | [204] |
| CoO NPs/BC composite | Spent coffee ground | Impregnation and pyrolysis (700 °C/2h/Ar) | TET | 741.10 | – | – | 1440 | 85 | 370.37 | [205] |

(*continued on next page*)

**Table 4** (*continued*)

| Adsorbent | Precursor | Technique used | Antibiotic | $S_{BET}$ ($m^2$/g) | Vp ($cm^3$/g) | Dp (nm) | te (min) | %R | $q_{e\_max}$ (mg/g)[a] | Reference |
|---|---|---|---|---|---|---|---|---|---|---|
| Nano-HCP/BC composite | Wood residues | Impregnation and Pyrolysis (700 °C/6h) | TYL<br>SMX | 566.06 | – | 3.83 | 4320 | 60–85 | 135.13<br>588.24 | [206] |
| Nano-HCP/BC composite | Wood residues | Impregnation and Pyrolysis (700 °C/6h) | TYL<br>SMX | 509.38 | 0.397 | 3.42 | 4320<br>1440 | – | 112.55<br>149.25 | [207] |
| Montmorillonite/BC composite | Municipal solid waste | Pyrolysis (450 °C/4h) and impregnation | CIP | 6.51 | – | – | 900 | >60 | 120 (H) | [208] |
| Bentonite/BC composite | Municipal solid waste | Pyrolysis (450 °C/0.5 h) and impregnation | CIP | – | – | – | 600 | 80 | 286.6 (H) | [209] |
| $F_3O_4$/BC composite | Furfural residue | Impregnation (co-precipitation) and Pyrolysis (500 °C/1h/$N_2$) | NOR | 463.00 | 0.524 | 4.527 | 240 | 40.4 | 299.57 | [210] |
| γ -$F_2O_3$/BC composite | Cornhusk | Pyrolysis (300 °C/1h/$N_2$) and impregnation. | LEV<br>TET | 94.10 | – | – | 1440 | >70 | 273.7<br>149.1 | [211] |
| $FeMnO_3$/BC composite | Pine sawdust | Impregnation and pyrolysis (500 °C/2h/$N_2$) | TET | 666.33 | 0.220 | 2.43 | 200 | >80 | 126.43 | [133] |
| Chitosan/Fe/S/BC composite | Waste sludge | Pyrolysis (500 °C/2h/$N_2$) and impregnation. | TET | 20.18 | 0.050 | 9.36 | 900 | >80 | 183.01 | [136] |
| ZnO/$Fe_3O_4$/BC composite | Camphor leaves residues | Pyrolysis (650 °C/2h/$N_2$) and impregnation | CIP | 915.00 | 0.552 | – | 200 | >75 | 236.9 | [114] |
| La/$F_3O_4$/BC composite | Sugarcane bagasse | Pyrolysis (600 °C/2h/$N_2$) and impregnation (co-precipitation) | TET | – | – | – | 1440 | >50 | 122.5 | [212] |
| Chitosan/BC beads | Grapefruit peel | Pyrolysis (450 °C/15 min) and pH-precipitation method | CIP | – | – | – | 600 | – | 153 | [213] |
| Heteroatom-doped BC | Spent tea leaves | Pre-oxidation and pyrolysis (500 °C/1h/$N_2$) | CTC | 503.00 | 0.250 | 4.07 | 30 | 97.4 | 627 | [214] |
| HC | Olive oil wastes | HTC at 240 °C for 6 h | TCL | 7.62 | 0.051 | 26.9 | 120 | 98 | 13.8 (E) | [140] |
| HC | Spent coffee grounds | HTC at 160 °C for 10 h | SDZ<br>SMX | 0.93 | 0.0043 | 18.35 | 3000<br>1200 | – | 295.1<br>740.6 | [139] |
| HC | Rice husk | HTC at 200 °C for 20 h | NOR | 2.88 | – | – | 3000 | – | 9.68 | [141] |
| HC | Corn stalk | HTC at 200 °C for 2 h | NOR | 7.34 | – | – | 4500 | – | 9.96 | [141] |
| HC | Tea waste | HTC at 200 °C for 10 h | TET | 5.21 | 0.015 | 11.36 | 200 | – | 18.27 | [115] |
| Fe-loaded HC | Sewage sludge | HTC at 180 °C for 3 h and impregnation. | DOX<br>TET | 82.78 | – | 1.43 | 3000 | 100<br>95 | 201.45<br>226.09 | [215] |
| $H_2SO_4$- modified HC | Cotton straw | HTC at 200 °C for 6 h and acid modification | TET<br>NOR | 3.24 | 0.015 | 32.4 | 1500<br>250 | –<br>– | 37.82<br>58.18 | [142] |
| KOH- modified HC | Cotton straw | HTC at 200 °C for 6 h and alkali modification | TET<br>NOR | 6.50 | 0.042 | 22.5 | 750<br>750 | –<br>– | 46.59<br>28.68 | [142] |
| $KMnO_4$- modified HC | Cotton straw | HTC at 200 °C for 6 h and acid modification | TET<br>NOR | 137.79 | 0.217 | 6.7 | 500<br>500 | –<br>– | 104.38<br>37.01 | [142] |
| NaOH- modified HC | Sugarcane bagasse | HTC at 200 °C for 24 h and alkali modification | TET | 27.55 | 0.134 | 19.50 | 1440 | – | 26.60 (E) | [143] |
| $TiO_2$ NSs/HC composite | Wheat straw waste | HTC at 453 K for 6 h and sol–gel method. | TET | 66.00 | 0.160 | 9.4 | 250 | 93 | 49.26 | [145] |
| MgSi/HC composite | Pine sawdust | Co-precipitation and HTC at 180 °C for 12 h. | TET | 107.70 | 0.489 | 11.1 | 720 | 99 | 264 | [146] |
| $Fe_3O_4$/GO/HC composite | Citrus peel | Impregnation and HTC | CIP<br>SPF | 1556.00 | 1.000 | 2.56 | 4200<br>1800 | –<br>– | 283.44<br>502.37 | [216] |
| HPC | Bovine bone | Self-templating method at 400 °C for 2 h with $N_2$ | SMT<br>CAP | 3231.80 | 1.976 | 2.45 | 200<br>300 | –<br>– | 1035<br>1079 | [159] |
| HPC | Straw waste | Self-templating (950 °C/2 h/$N_2$) with $KHCO_3$ | CIP | 1297.00 | – | – | 5 | 99.53 | 909.09 | [158] |
| SiOC/HPC composite | Rice husk | Soft-templating (1000 °C/2 h/$N_2$) with silicone resin | CIP | 766.61 | 0.840 | 4.35 | 10 | 100 | 148 | [217] |
| Amine-modified bio graphene | wheat straw | Thermo-chemical reduction at 790 °C/2h | MET | 389.00 | 0.273 | 2.8 | 30 | 100 | 416.7 | [169] |
| Amine- functionalized bio graphene | corn stover | Thermo-chemical reduction at 800 °C/2h | CIP | 493.54 | – | – | 60 | 99.9 | 172.6 | [173] |
| Magnetic bio graphene | Banana pee | Thermo-chemical reduction at 900 °C/2h | ETR | 1905.50 | 1.190 | 1.29 | 15 | 90 | 534 | [172] |

BC: biochar, HC: hydrochar, HPC: Hierarchical porous carbon, NSs: nanosheets, NPs: nanocomposites, DES: deep eutectic solvent, GO: graphene oxide, HCP: hydroxyapatite.

[a] Expressed by the Langmuir isotherm; otherwise, it is specified as experimental (E) or Hill isotherm (H).

### 6.1.3. *Biochar-based composites*

BCs are a suitable matrix for synthesizing composites, especially for the growth of nanoparticles in their cavity. This not only reduces the agglomeration of nanoparticles through interactions with functional groups of biochar, but also improves the dispersion of BCs in aqueous media [108]. Table 4 lists some significant studies on the formation of composites using BCs as the matrix. For instance, Ni-Co-S nanoparticles were deposited on the surface of BC (Ni-Co-S/BC composite), where the maximum adsorption capacity was displayed as 962.21 mg/g for TET and 744.70 mg/g for CIP, with the formation of hydrogen bonding, π-π interactions, and metal coordination [130]. In another study, Xiang et al. [131] prepared an innovative biochar magnetic composite (Mn-Fe/BC) by co-precipitation of Fe and Mn on vinasse wastes, with subsequent pyrolysis under controlled conditions. The prepared adsorbent had a surface area of 94.943 $m^2$/g and a maximum adsorption capacity higher than 150 mg/g for CIP and pefloxacin (PEF). Similar reports

revealed that manganese ferrite and their derivative composites displayed high adsorption performance for various antibiotics due to their relatively stable structure with strongly saturation magnetization [132,133,134].

The use of magnetic nanoparticles for the recovery of BC has been the primary approach in BC-based composites. Based on that, Chakhtouna et al. [132] successfully immobilized $CoFe_2O_4$ nanoparticles on the external biochar surface and applied this composite for the removal of AMX. It was observed that $CoFe_2O_4$ NPs had outstanding thermochemical stability and high saturation magnetization, which facilitated its recovery via the application of an external magnetic field; the $S_{BET}$ also increased from 25.6 to 190.5 $m^2/g$ after the impregnation with $CoFe_2O_4$ NPs, and the maximum adsorption capacity was 136.83 mg/g at 70 mg/L of AMX. Usually, NPs are impregnated on biomass prior to the pyrolysis process (pre-calcination modification), or these can be deposited on the biochar as a post-calcination modification (Fig. 6a and b). Finally, biochar-based composites with multiple functional species have been synthesized recently. For instance, Liu and colleagues modified biochar with chitosan and Fe/S using a post-calcination methodology (Fig. 6c). The multicomponent composite had better adsorption efficiency in contrast to the pristine biochar (183.01 > 51.78 mg/g), where electrostatic attraction, π-π stacking, pore filling, silicate bonding, chelating, and hydrogen bonding were the main adsorption mechanisms for TC removal [136].

### 6.2. Hydrochar

Although the production of BCs requires less energy than commercial activated carbons, it still demands high reaction temperatures and energy consumption. An alternative to pyrolysis is hydrothermal carbonization (HTC), whereby a solid char, referred to as hydrochar (HC), can be directly synthesized at lower temperatures (150–350 °C) from biomass with high moisture content (>50%) [137]. Hence, HTC eliminates the need for pre-drying of organic waste. Compared to the traditional pyrolysis process, HTC uses water as a reaction medium instead of $N_2$ or other inert gas, and although HTC is performed under lower temperature than conventional pyrolysis, more reaction time is needed to obtain HC (between 4 and 10 h). Like the pyrolysis process, in the HTC process, several factors affect the physicochemical properties of hydrochar, including the biomass' moisture content, feedstock, biomass-to-water ratio, temperature, and time. The influence of these aspects has not been thoroughly reviewed yet. In general, high biomass-to-water ratios lead to a decreased yield of hydrochar, with high O/C and H/C and low $S_{BET}$ and $V_P$. Subsequently, the adsorption performance is poor [138]. In the same sense, $S_{BET}$, the pore volume, and their adsorption performance towards antibiotics typically increase with reaction time and HTC temperature [139].

The adsorption capacity of some pristine hydrochars derived from organic wastes is 13.8 mg/g for TCL from olive oil wastes [140], 740.6 μg/g for SMX from spent coffee grounds [139], 9.68 mg/g for NOR from rice husk[141], 9.96 mg/g for NOR from corn stalk [141], and 18.27 mg/g for TET from tea waste [115]; these values are lower than pristine

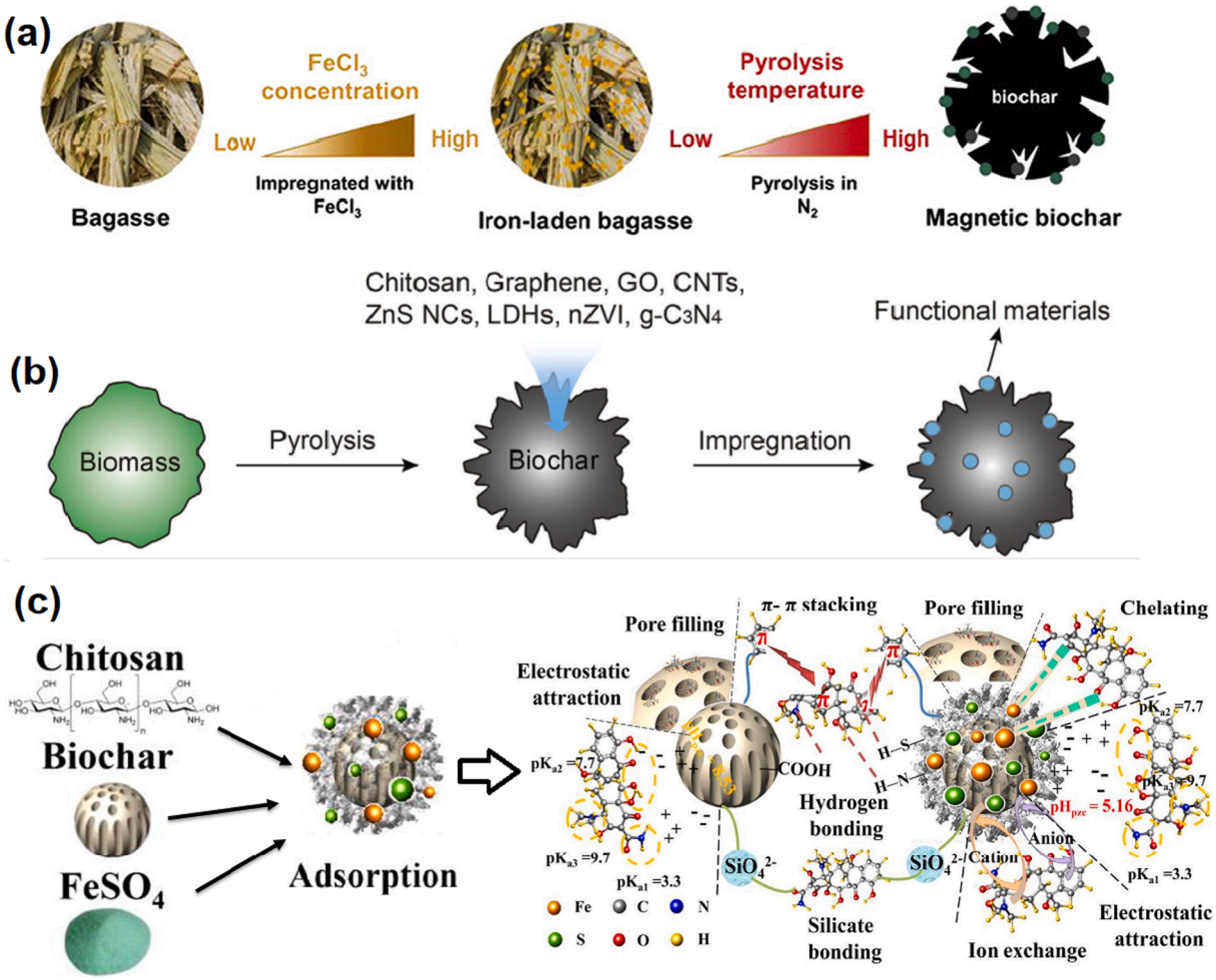


**Fig. 6.** (a and b) Pre-calcination and post-calcination modification treatments to produce biochar-based composites. Reproduced with permission from [135]. Copyright 2021 Elsevier B.V. (c) Multicomponent composites for antibiotic adsorption. Reproduced with permission from [136]. Copyright 2021 Elsevier B.V.

biochars. Similar to BC, the physiochemical properties of hydrochar can be adjusted via physical modification, chemical modification, and integrating other functional species (hydrochar-based composites). Some studies with chemical modifications include the use of $H_2SO_4$, KOH, $KMnO_4$ [142], and NaOH [143]. Regarding physical modifications, Li et al. [144] recently deployed an ultrasonic-assistant fore-modified method to produce self-functionalized hydrochar with enhanced adsorbability towards antibiotics using corncobs as the precursor. The produced hydrochar had an ultrahigh surface area of 2368 $m^2/g$, and the adsorption capacity was between 420–482, 360–411, and 410–416 mg/g for AMX, TET, and LEV, respectively. It was observed that the ultrasonic-assistance fore-modified treatment increased the microporous structure, and subsequently, the surface area raised by around 210%. On the other hand, $TiO_2$ nanosheet-impregnated HC [145] and magnesium silicate-functionalized HC [146] are some hydrochar-based composites synthesized to remove antibiotics. Finally, it is worth noting that HCs can also undergo classical chemical and physical activation in order to improve their porous structure and functional groups, forming activated hydrochars [147].

Even though the production of HCs requires less energy and their yield is superior to BCs, their physicochemical properties and adsorption performance are poor compared to biochar. This is partly due to the pyrolysis process produces a higher degree of carbonization, and hence more aromatic structures on the BCs, which is usually reflected in the higher carbon content in BCs [115,139]. Zhang and colleagues found that biochar derived from spent coffee has higher hydrophobicity, aromaticity and lower polarity than hydrochar obtained from the same feedstock; this discrepancy brought about the adsorption capacity for SDZ and SMX was higher for the biochar, despite their identical surface area to hydrochar [139].

### 6.3. Advanced carbon-based adsorbents

Biochar and hydrochar obtained by the conventional carbonization process possess a structure dominated by micropores, with a percentage of micropore volume that ranges from 12.1 to 58.0% [148]. Nonetheless, a wide distribution of macropores and mesopores is also conducive for the diffusion of antibiotics and for swifter mass transfer rates. Hence, researchers have focused on looking for new approaches and additional treatments in order to produce engineered biochar, which holds a well-tailored pore dimension, preferable surface area, and wide structural heterogeneity of pores. The advanced carbon-based adsorbents include mesoporous carbons, hierarchical porous carbons, and heteroatoms-doped porous carbons. Their adsorption properties are summarized in Table 4.

#### 6.3.1. Mesoporous carbon

A method recently studied to control the pore size of carbon materials is the template methodology. Mesoporous carbon materials prepared by this method possess larger specific surface area and pore volume, higher porosity, and more ordered pore size distribution than biochar obtained by direct high-temperature pyrolysis [149]. On the whole, in the templating method, a carbon precursor and a template material are mixed together, carbonized, and then the template is removed, leaving a porous structure. Depending on the type of template agent, this method is classified into hard-template (inorganic material as templating agent) and soft-template method (organic compound, frequently polymers as template). However, the latest method is more convenient due to its simplicity, low cost, good repeatability, and it does not require the additional step to remove the templates since these are entirely decomposed during carbonization [150]. In relation to the carbon precursor, phenolic resins, sucrose, and lignin are commonly used [149], and biomass has recently been applied directly as a carbon source to prepare mesoporous carbons via this method. Zheng et al. [151] implemented a soft-template-assisted hydrothermal route to produce a mesoporous hydrochar using biomass batatas and F127 (polyethylene-polypropylene glycol) as carbon source precursor and soft-template agent, respectively. The prepared hydrochar exhibited excellent textural properties, $S_{BET}$ and $V_P$ were up to 16 times higher than biochar prepared by conventional pyrolysis, which was attributed to the well-developed pore structures. Consequently, this mesoporous hydrochar showed outstanding adsorption capability for TCT (238.7 mg/g at 35 °C). Sugarcane bagasse [150], soluble starch [152], and palm kernel shell [153] are other biomass used as carbon precursors to produce mesoporous carbons using this methodology.

#### 6.3.2. Hierarchical porous carbons

An additional approach for enhancing the adsorption capacity of these carbonous materials is to modify their structure, passing from single natural structures to artificially assembled multi-structured adsorbents with a significant increase of specific surface area. An excellent example of these engineering-based adsorbents is the hierarchical porous carbons (HPCs), which possess abundant macro, meso, and micropores compared to conventional activated carbon with only a micropore-dominant structure [154]. With this wide pore distribution, a more accessible surface area, shorter diffusion distance, and higher mass transfer rate are obtained [155]. The nanoporous geometry of HPCs played a critical role in the adsorption of antibiotics. Trimodal and bimodal pores benefit the intraparticle mass transfer, the accessibility of adsorption sites, and the adsorption affinity; thereby, HPCs possess superior adsorption performances, unlike the monomodal mesoporous and microporous carbons with similar surface areas [154]. HPCs usually are produced using the same template methodology used to synthesize mesoporous carbons, but instead use single, dual, or multiple nano-structured hierarchical templates that can tailor the pore structure of HPCs. Similar to mesoporous carbons, HPCs are synthesized from expensive and unnatural carbon sources that limit their large-scale fabrication and practical use. However, recently many studies have reported the preparation of HPCs employing natural biomass as a carbon source. For instance, Zhang et al. [156] reported HPC preparation with ultrahigh surface area using sodium carboxymethyl cellulose (CMC), a non-toxic and renewable material derived from natural cellulose, as carbon precursor via a combination of templating and activation methods. CMC was mixed with HNTS (halloysite nanotubes as hard template) and carbonized at 500 °C for 2 h with $N_2$ flow, then HNTs was removed with hydrofluoric acid, whereas the carbonaceous material was activated with KOH at 850 °C for 1 h with $N_2$ flow; the prepared HPC had $S_{BET}$ and $q_{max}$ for CAP of 2347.7 $m^2/g$ and 838.94 mg/g, respectively. This study illustrated that the templating/activation combination efficiently constructs carbonous materials with well-defined microporous and meso-/macroporous architectures.

Additionally, it should be noted that some biomass contains natural templates ($SiO_2$ in rice husk, $CaCO_3$ in soft pitch, among others) which could act as self-templates to produce HPCs during the activation process; this process usually involves simultaneous carbonization/activation (similar to the preparation of activated carbon), and it is best known as a self-templating method. For instance, yeast, an abundant, environmental-friendly, and renewable biomass source, was successfully converted into three-dimensional interconnected hierarchical porous carbon via template-free carbonization and alkaline-activation method [157]. Likewise, Wang et al. [158] converted straw waste into HPC with abundant macro, meso, and micropores using $KHCO_3$ as an activation reagent. It was found that the synthesis was similar to the "leaving" process, where $KHCO_3$ was decomposed during the activation generating large amounts of gas that would sweep the carbon skeleton, facilitating the formation of three-dimensional structures. The prepared HPC also exhibits notably large specific areas (1297 $m^2/g$); the removal efficiency for CIP reached nearly 100% only after 5 min with an adsorption capacity of 909.09 mg/g. Other biomass-based HPCs obtained by the self-templating method were produced from bovine bone [159], banana peels [160], rice husk [161], sugarcane bagasse, fish scales, and pomelo peel [155].

#### 6.3.3. Heteroatoms-doped porous carbons

A new advance in the development of highly effective carbon materials is the modification by hetero-atom doping. By introducing heteroatoms (N, O, P, and B) in the carbon framework, its properties like electrical conductivity, chemical stability, and electron donor properties can be significantly fostered. Further, heteroatom doping provides more active sites to the carbon material, facilitating the adsorption of pollutants [162]. N-doped porous carbon (NPC) is the most studied material within this group, which is typically obtained through the carbonization and activation of carbonaceous precursors mixed with nitrogen-containing compounds (like urea, ammonia, melamine, cyanamide, and hydrazine). Another cleaner strategy to produce NPCs is the carbonization of nitrogen-rich biomass such as shrimp shells, alfalfa, soybean residue and sorghum stalks, in which the addition of nitrogen-containing compounds is not necessary. For instance, Qin et al. [163] converted shrimp shells into N-doped hierarchically porous carbon via the carbonization and alkali activation process at distinct temperatures. It was found that increasing activation temperature and the material ratio was beneficial to improve the porosity, pore volume and BET surface area. The best physical properties were obtained at the KOH/C weight ratio of 2.0 and 800 °C of activation (3171 $m^2/g$ of $S_{BET}$; 1.934 $cm^3/g$ of $V_P$), and the maximum adsorption capacity was 643.5 and 676.1 mg/g for SMZ and CAP at 25 °C. Other heteroatoms-doped porous carbons prepared from agricultural or industrial waste include O-doped HPC from silkworm cocoon with $S_{BET}$ of 3134 $m^2/g$ [164], N/S dual-doped HPC from chicken feathers with $S_{BET}$ of 1383.5 $m^2/g$ [165], B/P dual-doped porous carbon from bean shells with $S_{BET}$ of 2471 $m^2/g$ [166], O/N/S triad-doped HPC from lotus leaves with $S_{BET}$ of 3601 $m^2/g$ [167], and N/P dual-doped porous carbon from tobacco stalk [168].

#### 6.3.4. Bio graphene

Curiously, graphene, a carbon-based material, can also be produced from biomass or agricultural residues through a thermochemical process. In general, biomass-derived ash is used as a starting material, followed by a thermo-chemical reduction process mixing the biomass ash with a reducing agent (frequently KOH), with subsequent filtration, drying, and crashing. Finally, the material is activated at temperatures between 600 and 900 °C in an electric furnace under a nitrogen gas [169–171]. When starting from agricultural or industrial waste, a previous combustion process is required. In this context, Bahmei et al. [172] prepared porous magnetic graphene from banana peel residue to remove erythromycin (ETR). In the first stage, a carbonaceous material was obtained combusting banana peel at 600 °C for 1 h under argon gas. Then, the carbonized sample was mixed with KOH (1:5 ratio of KOH/ash). Finally, after drying and crashing, it was activated at 900 °C under argon gas for 2 h. The obtained green graphene was functionalized with $Fe_3O_4$ nanoparticles; it was found that the magnetic nanosheet had an outstanding surface area (1905.5 $m^2/g$) and high adsorption capacity (534 mg/g). Similarly, Ghadiri et al. [173] prepared a bio-graphene from corn stover, which was functionalized with an amine to improve the affinity towards the elimination of CIP; the prepared bio-graphene had a specific surface area of 493.54 $m^2/g$ and a maximum adsorption capacity of 172.6 mg/g provided by the Langmuir isotherm. Following the same above methodology, graphene derived from wheat straw [169–171], rice straw and rice husk [174,175], *Populus Caspica* pruning wastes [176], and fruit residues [177] have been synthesized. Nonetheless, only a few studies evaluated their adsorption properties with antibiotics.

## 7. Other adsorbents derived from waste

In addition to the aforementioned adsorbents, other potential materials can be synthesized using industrial and agricultural wastes as precursors via different methods. At present, organic waste in some countries is combusted directly to generate bioenergy, and an inorganic residue called ash is left. Biomass ash is not only another waste but also an environmental hazard, the disposal of which requires an economic inversion. Nonetheless, biomass ash is also a residue rich in silica and other oxides that can be a resource with tremendous potential that needs to be explored and utilized in order to increase its added value. One strategy to use this waste is the usage as precursors to synthesize zeolites [218]. Since the ash derived from organic waste comprises mainly silicon, aluminum, and iron in the form of oxides, this makes this residue a good substrate for producing synthetic zeolites, which can be applied as adsorbents to remove antibiotics. In this context, Zide and colleagues prepared several zeolites through calcination and hydrothermal processes from alkali-fused coal fly ash (Fig. 7f); the removal efficiency by the synthesized zeolites for CIP was significantly higher in acetic acid (92–94%) compared to HCl (27–61%) at pH 3 [219]. Another zeolite produced by the hydrothermal process is the zeolite analcime from carbothermal reduction electrolytic manganese residue, which was used to adsorb roxithromycin (ROX) and azithromycin (AZM) [220]. Alternatively, Alie et al. [221] synthesized NaY zeolite using wheat straw ash as a precursor; the ash was crystallized by the sol–gel method with subsequent calcination at 500 °C for 3 h. This methodology prepared a zeolite with high purity (composition of 66.05% $SiO_2$, 25.35% $Al_2O_3$, and 7.92% $Na_2O$), and its maximum uptakes of TET were 201.77, 218.51, and 230.69 mg/g at 30 °C, 40 °C, and 50 °C, respectively, according to the Langmuir isotherm.

Biomass-derived ash is composed chiefly of $Al_2O_3$ and $SiO_2$. However, when other unusual compounds like CaO and unburned carbon are presented in the ash or from other waste, different materials can be obtained apart from zeolite, which forms composite materials. For instance, Khanday and Hameed [222] reused oil palm ash (containing 5.5% unburned carbon) and steel slag (with CaO exceeding 15 %) to convert them into a hybrid material composed of zeolite (Z), hydroxyapatite (HAP), and activated carbon (Z/HAP/AC composite). Increasing the activated oil palm ash ratio during synthesis resulted in increased surface area of Z/HAP/AC composite due to an increase in the carbon component (from 388.15 $m^2/g$ to 732. 27 $m^2/g$), and the maximum monolayer adsorption capacity for TET was 186.09 mg/g at 30 °C. Furthermore, hydroxyapatite [$Ca_{10}(PO_4)_6(OH)_2$] is commonly manufactured from waste with high content of calcium along with a phosphate-based compound like $H_3PO_4$. Nonetheless, phosphate can also be obtained from other waste. To illustrate, Faisal et al. [223] produced nano-hydroxyapatite by extracting the calcium from cement kiln dust and the phosphate from sewage sludge. The HAP nanoparticles were deposited on a filter cake remaining after extraction to produce HAP-coated filter cake, which was applied to remove TET, obtaining a removal efficiency of over 90% and a maximum adsorption capacity of 43.5 mg/g.

Water treatment sludge has also been seen as a conducive source to produce other adsorbents, and so avoid the high disposal cost. Sludge is a waste that contains Fe, Si, and Al compounds. In general, Fe-containing compounds in sludge like ferrihydrite, hematite and andradite are converted into magnetite, maghemite, and jacobsite using reductants (e.g., glycol, ascorbic acid, pyrite and methane). However, magnetic adsorbents can also be produced without the addition of reductants. Qu et al. [225] converted ferrihydrite from sludge to maghemite and hematite via a one-step hydrothermal method using NaOH solutions; even though a low conversion of ferrihydrite was obtained (18.9%), the adsorbent had a good magnetic response and suitable adsorption capacity (362.3 mg/g for TET). Recently, a new advance to improve the adsorption efficiency of these materials was presented by Hu and colleagues, where erdite-bearing particles have been synthesized from ferrihydrite through the hydrothermal method using only $Na_2S{\cdot}9H_2O$; the resulting product was used to adsorb TET and oxytetracycline (OTC) with outstanding adsorption performances (>500 mg/g) [226,227]. Further, it was observed that in contrast to other adsorbents, in erdite particles, their spontaneous hydrolysis to generate Fe oxyhydroxide with adequate hydroxyl groups to link OTC and TET is the prime mechanism to remove antibiotics. Likewise, Chen et al. [224]

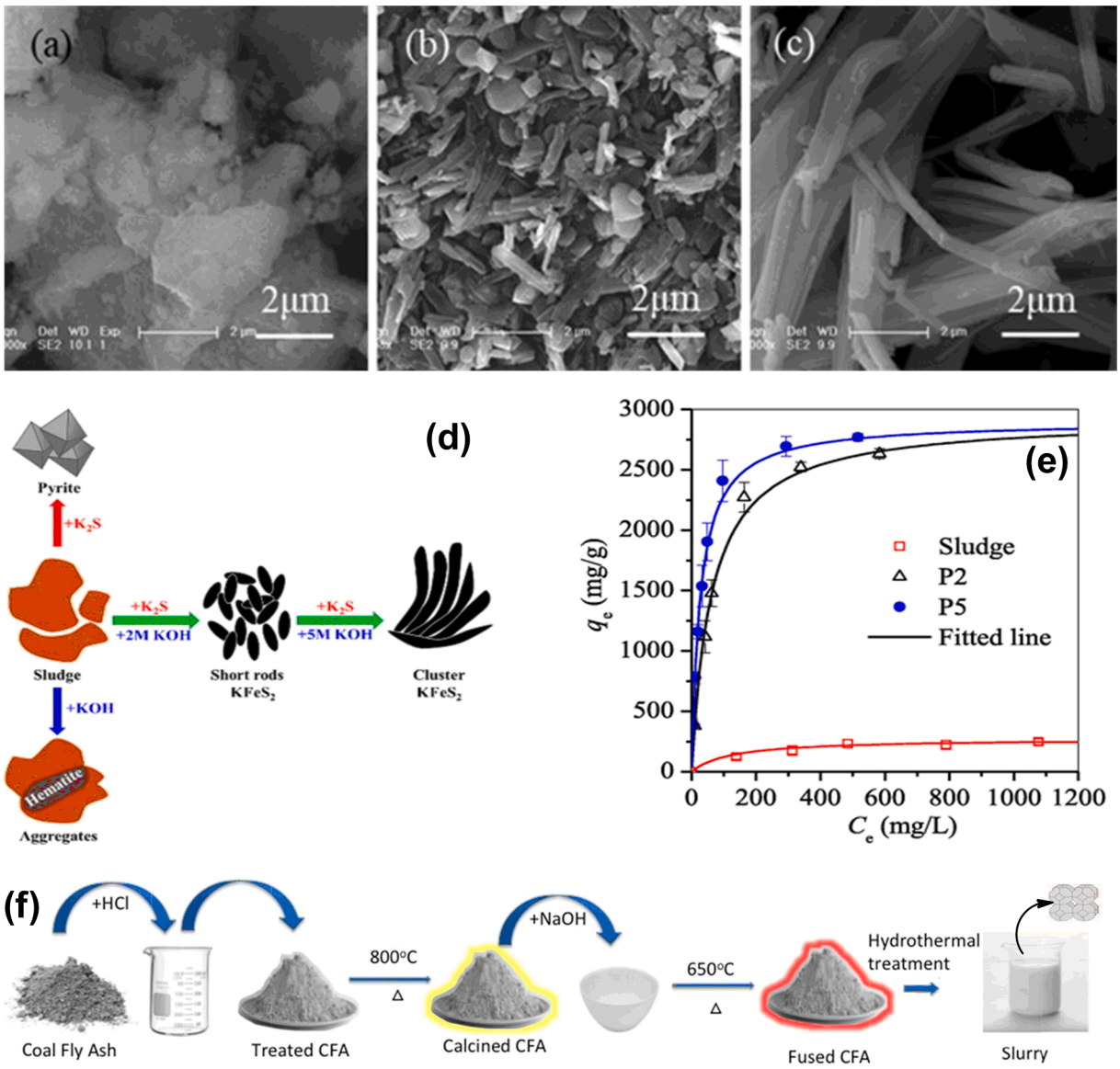


**Fig. 7.** (a) Scanning electron microscopy images of raw sludge and $KFeS_2$ prepared with (b) 2 and (c) 5 M KOH; (d) Conversion of sludge to $KFeS_2$ in the $K_2S$/KOH-bearing solution, (e) and adsorption isotherms of DOX on raw sludge, P2 and P5 (with 2 and 5 M KOH, respectively. Reproduced with permission from [224]. Copyright 2021 Elsevier B.V. (f) Preparation of zeolites through calcination and hydrothermal process from alkali-fused coal fly ash. Reproduced with permission from [219]. Copyright 2021 Elsevier B.V.

converted a Fe-rich sludge to $KFeS_2$ clusters using KOH and $K_2S$ by a one-step hydrothermal route. During the process, FeOOH from the sludge became a mixture of hematite and $KFeS_2$, which grew with the KOH concentration passing from short rods (at 2 M) to clusters (at 5 M), as can be seen in Fig. 7a-7d. The $KFeS_2$ short rods and clusters were employed to remove DOX, showing a remarkable maximum adsorption capacity of 2811.18 and 2933.6 mg/g at 120 min, respectively (Fig. 7e). Nevertheless, a considerable drawback was that $KFeS_2$- and erdite-bearing adsorbents could not be feasibly reused since their removal efficiency dropped under 30% in their first regeneration [224,226]. Analogously, Si/Al compounds in sludge, specially boehmite and quartz, can be dissolved in $Si(OH)_5^-$ and $Al(OH)_4^-$ with the addition of alkali solutions and recrystallized under hydrothermal conditions to form high-purity materials such as cancrinite and sodalite [228,229], which have shown desirable adsorption capacity of TET (>488 mg/). Additionally, in the synthesis of cancrinite and sodalite, the phase transformation from ferrihydrite to maghemite and hematite occurred in parallel, giving magnetic properties to these adsorbents [230].

Other adsorptive materials for antibiotics removal produced from waste include keratin particles from waste feathers via a thermal alkali hydrolysis process [231], nanocellulose from lignocellulosic residues via extraction methods [232], nanosilica from rice husk via the hydrothermal method [233], $Fe_3O_4$ and nZVI nanoparticles from fruit peels and leaf waste via plant-mediated synthesis [234,235], hydrogel using chitosan extracted from shrimp shells [236], among others. These adsorptive materials are detailed in Table 5.

## 8. Adsorbents with a synergistic effect of adsorption and degradation

A novel scheme that has won considerable attention in the last years is the combination of two or more removal techniques. In particular, increasing attention has been paid to the adsorption-photocatalytic degradation combined technique. Photocatalytic oxidation, by itself, is a promising method to enhance the treatment efficiency of antibiotics via their degradation into low-toxicity organic small molecules [251].

**Table 5**
Other adsorbents derived from agricultural and industrial waste for the removal of antibiotics.

| Waste | Method | Adsorbent | Antibiotic | $S_{BET}$ ($m^2$/g) | Vp ($cm^3$/g) | $t_e$ (min) | % R | $q_{e\text{-}max}$ (mg/g)[a] | Ref. |
|---|---|---|---|---|---|---|---|---|---|
| Peels of lemon | Plant-mediated synthesis | $Fe_3O_4$ NPs | AMP | 137.4 | 0.29 | 120 | 80 | 10.08 | [237] |
| | | | TET | | | | 100 | 11.45 | |
| | | | TMT | | | | 22 | 11.93 | |
| | | | TAZ | | | | 79 | 8.59 | |
| | | | PIP | | | | 100 | 16.08 | |
| | | | ETR | | | | 100 | 13.64 | |
| Peels of black grapes | Plant-mediated synthesis | $Fe_3O_4$ NPs | AMP | 112.3 | 0.37 | 120 | 75 | 17.12 | [237] |
| | | | TET | | | | 100 | 19.48 | |
| | | | TAZ | | | | 52.7 | 4.38 | |
| | | | PIP | | | | 70.6 | 4.62 | |
| | | | ETR | | | | 51.8 | 5.79 | |
| | | | SMX | | | | 12.2 | 25.64 | |
| Peels of cucumber | Plant-mediated synthesis | $Fe_3O_4$ NPs | AMP | 90.5 | 0.28 | 120 | 85 | 16.16 | [237] |
| | | | TET | | | | 100 | 12.64 | |
| | | | TAZ | | | | 90 | 12.99 | |
| | | | PIP | | | | 95 | 14.86 | |
| | | | ETR | | | | 100 | 17.12 | |
| | | | SMX | | | | 35 | 10.67 | |
| *Excoecaria cochinchinensis* leaves | Plant-mediated synthesis | $Fe_3O_4$ NPs | RIF | 111.8 | 9.06 | 30 | 100 | 84.8 | [234] |
| Green tea waste | Plant-mediated synthesis | Mn NPs | MTX | – | – | 30 | 97 | 163.93 | [238] |
| Nettle leaf waste | Plant-mediated synthesis | nZVI NPs | CEX | – | – | 30 | ~100 | 1667 | [239] |
| Thyme leaf waste | Plant-mediated synthesis | nZVI NPs | CEX | – | – | 60 | ~100 | 1428 | [239] |
| *Moringa stenopetala* seeds | Protein extraction and electrospinning | Protein/PVA nanofibers | SNM | 2402.62 | 2.04 | 30 | 86.1 | 333 | [240] |
| | | | CIP | | | 30 | 94.9 | 500 | |
| | | | DNF | | | 30 | 95.0 | 1000 | |
| | | | OTC | | | 30 | 95.2 | 333 | |
| | | | SM | | | 30 | 96.0 | 125 | |
| | | | SMM | | | 30 | 94.796.8 | 250 | |
| | | | TYL | | | 30 | 96.2 | 500 | |
| | | | SDM | | | 30 | | 333 | |
| Waste hot-pot oil | Calcination at 300 °C | Attapulgite/carbon composite | TET | – | – | 125 | 90 | 256.5 (E) | [241] |
| Orange peel | Microwave-assisted extraction | $Fe_3O_4$/Pectine composite | SMX | – | – | 1440 | – | 120 | [242] |
| Electrolytic manganese residue | Hydrothermal method | Zeolite analcime | ROX | 138.4 | 0.108 | 400 | >80 | 1921.74 | [220] |
| | | | AZM | | | 400 | | 490.19 | |
| Wheat straw ash | Sol-gel method | NaY zeolite | DOX | 657.44 | 0.341 | 600 | – | 269.75 | [243] |
| Cotton waste | Oxidation mediated by TEMPO | Nanocellulose | CIP | – | – | 240 | 9 | 42 | [232] |
| | | | AMX | | | 60 | 80 | 551 | |
| *Cyprus rotundas* grass | NaOH and $H_2O_2$ treatment, and acid hydrolysis | Nanocellulose | CIP | – | – | 180 | 89 | 227.27 | [244] |
| *Pennisetum sinese* Roxb | Acid hydrolysis | Magnetic cellulose adsorbent | TET | 56.50 | 0.143 | 8400 | ~80 | 44.86 | [245] |
| Rice husk | Hydrothermal method and pre-adsorption | PDADMAC-modified nanosilica | AMX | 160.5 | – | 180 | 92.3 | 7.50(E) | [246,247] |
| | | | CEF | | | 120 | 93.5 | 10.4(E) | |
| Rice husk | Hydrothermal method and pre-adsorption | PMAPTAC -modified nanosilica | CEF | – | – | 25 | 90 | 10.9 | [233] |
| Moringa seeds and rice husk | Hydrothermal, solid–liquid extraction, and pre-adsorption | Protein-modified nanosilica | CIP | – | – | 25 | 89.8 | 85 (E) | [248] |
| Rice straw | Hydrothermal, solid–liquid extraction, and impregnation | $Fe_3O_4$/nanosilica composite | PEN-G | – | – | 350 | 50 | 164.7 | [249] |
| Shrimp shells and rice husk | Deproteinization, demineralization, and carbonization | Hydrogel | CIP | 52.08 | 0.135 | 300 | 97.4 | 106.04 | [236] |
| | | | ENR | | | 600 | 90.2 | 100.43 | |
| Alum sludge and low-grade charcoal | Pelletization and thermal treatment | Thermally-treated pellets | SMX | 167.2 | 0.037 | 240 | 70 | ~1.5 (E) | [250] |
| | | | SFT | | | 480 | 95 | ~2.0 (E) | |

Polyvinyl alcohol (PVA); 2,2,6,6-tetramethylpiperidine-1-oxyl (TEMPO); polyelectrolyte polydiallyldimethylammonium chloride (PDADMAC); poly(3-methacryloylamino propyl-trimethylammonium chloride) (PMAPTAC).

[a] Expressed by the Langmuir isotherm; otherwise, it is specified as experimental (E).

Nonetheless, photocatalytic particles usually agglomerate easily and are unsuitable for removing organic pollutants at low concentration levels [252]. In this sense, these waste-derived materials can be used as a carrier for photocatalysts, facilitating the conduction of electrons and the uniform dispersion of catalyst particles and, in turn, accelerating the degradation since the antibiotic is concentrated in the solid phase [60,251]. Therefore, combining adsorbents with photocatalysts in the form of composites can be an effective alternative to treat effluents loaded with antibiotics (Fig. 8a). Besides, photocatalyst-loaded adsorbents can not only improve antibiotic removal, but also assist in the regeneration of saturated adsorbents, avoiding secondary pollution [253]. According to many studies, the enhancement is due to the fact that a photocatalyst generates $h^+$ and $e^-$ under light, which react with $H_2O$ and dissolve $O_2$ to yield $^{\bullet}OH^-$ and $O_2^-$; these free radicals have powerful oxidization to photodegrade effectively antibiotics (Fig. 8b).

In this context, some photocatalysts, such as TiO2, g-$C_3N_4$, $Bi_2WO_6$, $WO_3$, ZnO, are loaded on the surface of adsorbents, and removal tests are performed under darkness, visible, or UV light. For example, Huang et al. [60] coated a $TiO_2$ hydrogel layer on the surface of alkali-modified rice straw for the CIP removal; their study demonstrated that removal

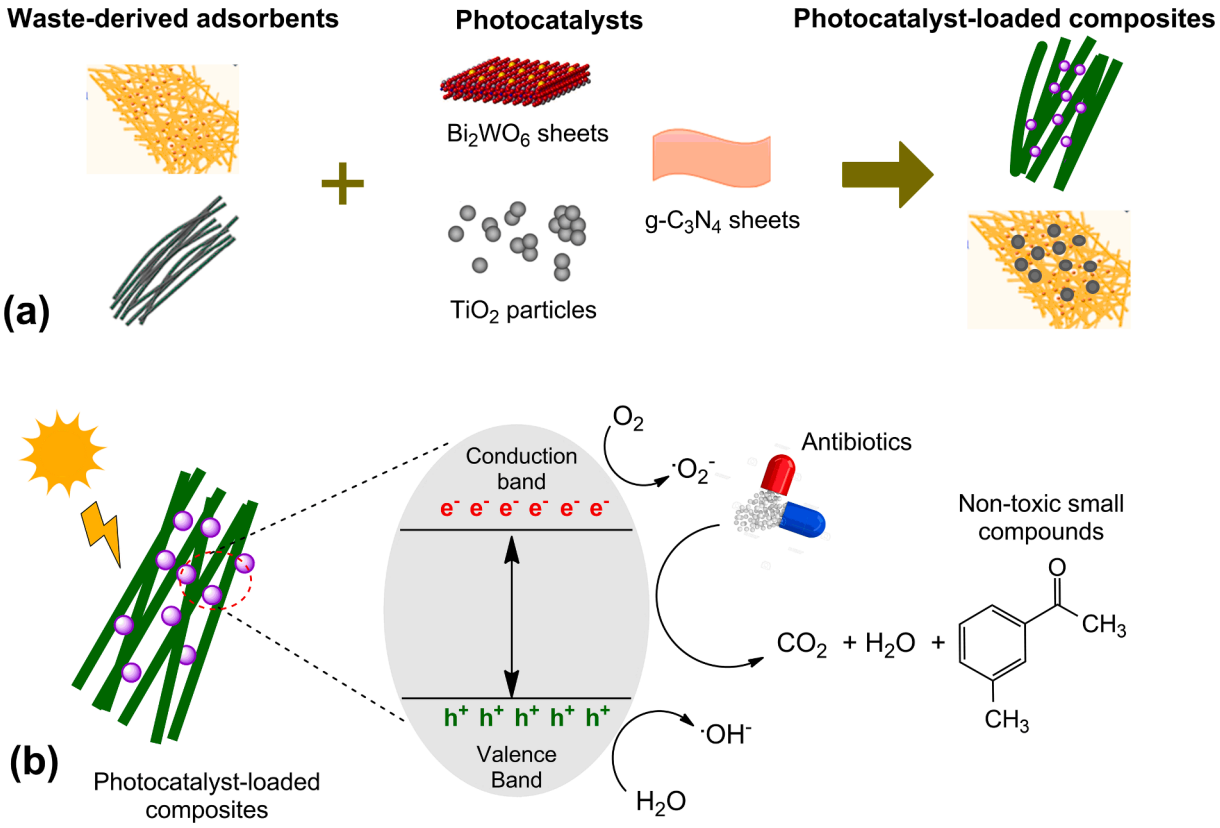


**Fig. 8.** (a) Formation of photocatalyst-loaded composites. (b) Degradation of antibiotics by UV radiation.

ability was enhanced by the $TiO_2$-gel layer with an adsorption capacity of 153 mg/g under ultraviolet, in comparison with 60 mg/g under darkness conditions. The $TiO_2$ photocatalyst was even effective under natural light (112 mg/g). The improvement was justified due to the oxidation of CIP (accumulated on the composite's surface) into small molecules and even $CO_2$ and $H_2O$, similar to a "capture & destroy" process. Similarly, Xiao and colleagues synthesized several g-$C_3N_4$/biochar composites with different g-$C_3N_4$-to-biochar mass ratios; the composite with 50% g-$C_3N_4$-to-biochar mass ratio had the highest enrofloxacin removal, removing 45.2% and 81.1% of ENR under darkness and visible conditions [254]. Besides, the introduction of biochar not only enhanced the absorption of light and excited more photons to generate $e^-$ and $h^+$, but also promoted the electron transfer efficiency to enhance the separation efficiency of electron-hole pairs [253,254]. Other photocatalytic-based adsorbents are detailed in Table 6.

## 9. Desorption and reusability

After the adsorption process, the antibiotic-saturated adsorbents need a proper management system. Typical waste management schemes include direct disposal in landfills, incineration, and regeneration and reusability; nonetheless, the first two frequently lead to the pollution of air, soil, and even surface and groundwater [262]. Hence, desorption and reusability might be the best strategy to manage spent adsorbents. Besides that, the regeneration capacity of an adsorbent is a relevant aspect to evaluate its viability in practical applications. To date, several methods have been employed in adsorbent regeneration; among them are thermal regeneration, solvent-assisted regeneration (chemical regeneration), microwave irradiation regeneration, and supercritical fluid regeneration [105]. Nevertheless, not all of them have been used for antibiotic-saturated adsorbents.

**Table 6**
Waste-derived adsorbents with a synergistic effect of adsorption and degradation.

| Composite | Photocatalyts | Antibiotic | $S_{BET}$ ($m^2$/g) | $q_e$ (mg/g)[a] | $q_e$ (mg/g)[b] | % R[a] | %R[b] | Ref. |
|---|---|---|---|---|---|---|---|---|
| $TiO_2$ hydrogel/Rice straw fiber | $TiO_2$ | CIP | 7.57 | 60 | 153 | – | – | [60] |
| N,S-$TiO_2$/Sugarcane bagasse | N,S-$TiO_2$ | CIP | – | – | – | 66 | ~90 | [255] |
| g-$C_3N_4$/Red mud | g-$C_3N_4$ | TET | 16.75 | – | – | 40 | 79 | [99] |
| | | OTC | | | | 35 | 60 | |
| | | CTC | | | | ~60 | 83.8 | |
| $TiO_2$/BC | $TiO_2$ | SMX | 102.16 | 6.59 | – | ~45 | 91.27 | [256] |
| $TiO_2$/BC | $TiO_2$ | SDZ | – | – | – | ~40 | 87 | [257] |
| | | ODX | | | | ~30 | 98 | |
| ZnO/BC | ZnO | SMX | 18.6 | – | – | ~15 | 99.3 | [258] |
| Zn-$TiO_2$/BC | Zn-$TiO_2$ | SMX | 169.16 | | | ~30 | 80.81 | [259] |
| g-$C_3N_4$/BC | g-$C_3N_4$ | ENR | 3.83 | 9.0 | 9.21 | 45.2 | 81.1 | [254] |
| $Bi_2WO_6$/$Fe_3O_4$/BC | $Bi_2WO_6$ | OFL | 35.89 | 11.5 | – | 55 | 99.85 | [260] |
| | | CIP | | 12.5 | – | 55 | 96.77 | |
| $Bi_2WO_6$/N,S co-doped BC | $Bi_2WO_6$ | CIP | 28.60 | – | – | ~20 | 90.33 | [261] |

[a] Adsorption capacity and removal percentage under darkness.
[b] Adsorption capacity and removal percentage under UV radiation.

For agricultural waste such as peanut shells, Li and colleagues conducted desorption experiments using deionized water, 10% HCl, and methanol. It was found that methanol had a higher desorption efficiency (>70%) to elute sulfonamides antibiotics from peanut shells. The primary justification was the similarity-intermiscibility theory, where antibiotics can dissolve more easily in organic solvents [55]. Likewise, Duan et al. [86] evaluated four desorbing agents to regenerate the *Calotropis gigantea* fiber saturated with CIP, NOR and ENR. The saturated adsorbent was immersed into 20 mL of 0.1 M HCl, 0.1 M NaCl, 0.1 M NaOH, and methanol for 3 h at 30 °C with constant stirring. It was found that NaOH gave the highest desorption percentage (95–100%), followed by HCl (70–85%) and NaCl (65–84%). Although NaOH was the best eluent, some authors stated that the alkali treatment might affect the strength of the fiber by changing the structure of plant fiber; hence alkali solutions are not highly recommended for lignocellulosic materials [263].

For carbon-based adsorbents, in general, thermal regeneration, solvent- and microwave-assisted generations have been evaluated. Zeng et al. [196] studied the effect of the temperature (373, 473, and 573 K) in the thermal regeneration of Fe-loaded BC saturated with SMX; it was observed that the regeneration efficiency increased along with the temperature, resulting in almost 100% regeneration efficiency at 573 K for 3 h in a furnace, as can be seen in Fig. 9a. Nonetheless, the regeneration efficiencies dropped from 100% to 46% after 4 cycles. This

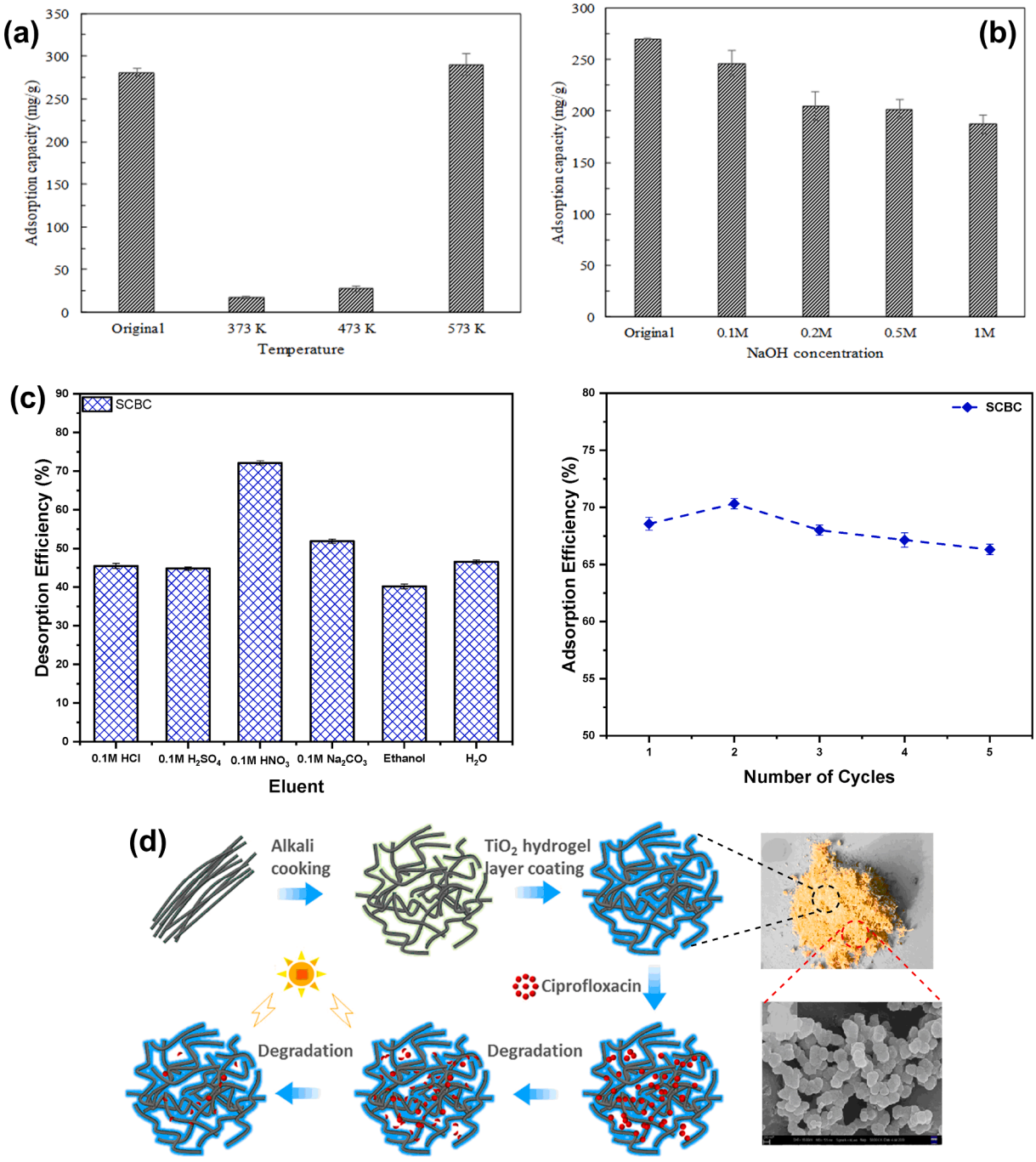


**Fig. 9.** (a) Desorption efficiency using different desorbing agents for $NaClO_2$-modified CGF. (b) Effect of the NaOH concentration in the desorption of Fe-loaded BC. Reproduced with permission from [196]. Copyright 2021 Elsevier B.V. (c) Effect of the eluent type on the BLX desorption from the $TiO_2$ NPs/BC composite [204]. (d) Adsorption and regeneration by UV irradiation. Reproduced with permission from [60]. Copyright 2021 Elsevier B.V.

dramatic decline has also been observed for other researchers [180]; this might be due to the decrease in hydrophobic interactions between antibiotic molecules and BC, alterations in surface chemistry, and reduction in surface area with damage to the pore structure after repeated thermal oxidation [180,196].

Regarding chemical regeneration, Zhang and colleagues tested five solvents (ultrapure water, methanol, ethanol, acetonitrile, and 0.1 M NaOH solution) for the desorption of SMX from saturated biochar. The less polar solvents (methanol, ethanol and acetonitrile) were good for the desorption of SMX with desorption rates ranging from 82% to 86%, compared to polar solvents like NaOH solution and ultrapure water (73% and 2.67%, respectively) [135]. Nonetheless, the recyclability of the biochar was not desirable as its adsorption capacity was reduced by 37.43% after two cycles and finally reduced from 205 to 34.85 mg/g after three cycles of regeneration with ethanol. In the same context, El-Azazy et al. [204] carried desorption studies using six eluents, namely 0.1 M aqueous solutions of HCl, $H_2SO_4$, $HNO_3$, $Na_2CO_3$, as well as ethanol and DI water for the desorption of balofloxacin (BLX) from the $TiO_2$/BC composite; the obtained data showed that the highest desorption efficiency was accomplished using 0.1 M $HNO_3$ with a desorption efficiency of 72.14% (Fig. 9c). The same eluent was studied for cyclic adsorption–desorption experiments; it was observed that after 5 cycles, the removal efficiency decreased to around 65 %. NaOH-driven desorption has also been extensively applied with several antibiotics (Table 7). Zeng et al. [196] studied the effect of NaOH concentration in the regeneration of Fe-loaded BC saturated with SMX; the authors found that the desorption efficiency improved as NaOH concentration increased, namely 90% with 0.1 M NaOH and 70% with 1 M NaOH (Fig. 9b). These findings establish that high pH with 0.1 M NaOH resulted in the effective desorption of antibiotics from BCs. However, after the 3rd-4th cycles, the NaOH-driven desorption led to a significant decrease in regeneration due to the deterioration of the biochar surface exposed to NaOH solution and possible accumulation of antibiotics on the BC surface [196].

These studies showed that solvents like methanol, ethanol and acetonitrile, $HNO_3$, and NaOH solution are suitable for regenerating carbon-based adsorbents. Nonetheless, their performance after several cycles is poor, limiting their application on real adsorption systems. A strategy to improve their regenerability for several cycles is to combine multiple regeneration methods in parallel. For instance, Ma and colleagues demonstrated that combining ultrasound and ethanol showed better regeneration capacities than sole NaOH and ethanol. By using this combined approach, the adsorption capacity only decreased by 10% after five cycles [197]. Ultrasound + NaOH has also shown good desorption capacities, reducing the adsorption performance by only 15% after 5 cycles indicating its excellent stability and potential as an adsorbent [189].

Despite the fact that solvents-assisted regeneration has proved excellent desorption capacities, the approach is questionable since the pollutant is passing from a solid phase to a new liquid phase, presenting an additional challenge to manage the new solution concentrated with antibiotics. Additionally, there is no universal eluent that can desorb all antibiotics from a given adsorbent; an eluent that works with a sulfonamide antibiotic may not be suitable with a quinolone antibiotic [55,86], which means that several chemicals must be used to desorb an adsorbent saturated with different types of antibiotics. Consequently, a new approach that includes the degradation of the pollutant has been studied in recent years. For this, catalysts and photocatalysts (such as $TiO_2$, $WO_3$, ZnO, $Fe_2O_3$, CuO, CoO) are loaded on the surface of adsorbents, and the degradation of the antibiotic occurs by catalytic oxidation. In this context, Nguyen et al. [205] deposited CoO nanoparticles on the surface of BC for the removal of TET and evaluated its reusability using only ultrapure water. It was observed that the extent of TET removal from synthetic solutions was greater than 93% during the first 8 cycles and decreased to 80% in the 10th cycle. Its reusability was also evaluated in real domestic wastewater, where the removal efficiency of

**Table 7**
Desorption and reusability studies of several adsorbents derived from agricultural and industrial waste.

| Adsorbent | Antibiotic | Regeneration agent | Adsorption capacity (mg/g) or % Removal[a] | | | | | Ref. |
|---|---|---|---|---|---|---|---|---|
| | | | 1st cycle | 2nd Cycle | 3th cycle | 4th Cycle | 5th Cycle | |
| NaOH and cellulase-modified maize stover | SMT | Acetone and methanol | 0.125 | ~0.12 | 0.117 | 0.11 | 0.105 | [38] |
| $NaClO_2$-modified CGF | ENR | 0.1 M HCl | 100% | 95% | 105% | 98% | 100% | [86] |
| | CIP | | 100% | 100% | 93% | 102% | 91% | |
| | NOR | | 100% | 100% | 100% | 101% | 98% | |
| Tb-Eu/$HNO_3$-modified garlic peels | ENR | UW with 5% ammonia | ~96% | ~91% | ~87% | 53% | 37% | [79] |
| NaY zeolite from wheat ash | DOX | 0.05 M NaOH | 65.75 | 58.59 | 57.48 | 52.71 | 50.17 | [243] |
| DES-modified rice husk ash | OFL | Hot air at 100 °C | ~72% | 70% | 61% | – | – | [66] |
| PmPD-grafted *Calotropis gigantea* fiber | CIP | 0.1 M HCl | ~42 | ~44 | ~44 | ~43 | ~42.5 | [77] |
| $HNO_3$-modifitied BC | SMT | 0.1 M HCl | 45 | 43 | 40.5 | 40 | – | [121] |
| | SCP | | 40 | 36 | 35.7 | 35 | – | |
| Sodalye and $HNO_3$-modified BC | TET | 0.2 M NaOH | 87 | 88 | 85 | 86 | 85.5 | [192] |
| HCl-modified BC | TET | 0.1 M NaOH | 142 | 138 | 134 | 132 | 130.5 | [189] |
| Fe-loaded BC | SMX | 0.1 M NaOH | 252.8 | ~250 | ~210 | ~180 | ~170 | [196] |
| Fe/Zn-loaded BC | TET | Ethanol + ultrasound | 98% | 95% | 91% | 88% | 85.2% | [197] |
| Mn/Fe loaded BC | LEV | 2 M NaOH | 170 | 110 | 85 | 80 | 50 | [199] |
| Attapulgite/BC composite | TET | Thermal generation at 300 °C | 300 | ~260 | ~245 | ~240 | ~230 | [180] |
| $TiO_2$ NPs/BC composite | BLX | 0.1 M $HNO_3$ | 68.56% | ~70% | ~68% | ~67% | 66.32% | [204] |
| $Ga_2S_3$/sulfur-BC composite | CIP | 0.2 M NaOH | 330.21 | 328.01 | 326.05 | 323.45 | 320.3 | [201] |
| CoO NPs/BC composite | TET | Ultrapure water | 100% | 98% | 97% | 96% | 96% | [205] |
| ZnO NPs/$Fe_3O_4$/BC composite | CIP | 0.1 M NaOH | 160 | 150 | 135 | 128 | – | [114] |
| $TiO_2$ NSs/HC composite | TET | 0.1 M NaOH | 8.86 | 7.92 | ~4.0 | – | – | [145] |
| $Fe_3O_4$/GO/HC composite | CIP | 0.1 NaOH | 250 | 248 | 246 | 235 | 230 | [216] |
| Mesoporous BC | TET | Thermal regeneration at 800 °C/2h | 98.8 | 98.1 | 100.0 | 99.0 | – | [151] |
| N-doped HPC | SMZ | 0.2 M NaOH | ~95% | ~90% | ~85% | – | – | [163] |
| | CAP | | ~95% | ~87% | ~80% | – | – | |
| Amine-modified bio graphene | MET | Acid water solution | 84% | 77% | 70% | 61% | 57% | [169] |
| Amine- functionalized bio graphene | CIP | 0.1 M HCl | 172.6 | 170.9 | 169.2 | 168.8 | 168.0 | [173] |

BC: biochar, HC: hydrochar, HPC: hierarchical porous carbon, DES: deep eutectic solvent, CGF: *Calotropis gigantea* fiber, PmPD: poly(m-phenylenediamine), NPs: nanoparticles, NSs: nanosheets.

[a] Data are reported as removal percentage when the % symbol is used; otherwise, it is adsorption capacity.

TET was around 78% in the 10th cycle, showing still great results and only slightly lower than the synthetic solution. This great regeneration capacity is thanks to CoO NPs that can degrade the TET molecule easing the regeneration of the composite. Similarly, Huang et al. [60] coated a $TiO_2$ hydrogel layer on the surface of alkali-modified rice straw, which enhanced the CIP removal ability by 63% under UV radiation. Besides, the photocatalyst $TiO_2$ allowed to regenerate the saturated adsorbent by exposing the adsorbent to UV radiation (Fig. 9d). These advances establish the great potential of adsorbents coated with catalysts and photocatalysts.

## 10. Conclusions and future prospects

In this review, adsorptive materials derived from agricultural and industrial waste and used for antibiotics removal were summarized. Adsorption properties of raw materials, modified materials, waste-based composites, carbon-based adsorbents, and other adsorbents were collected, analyzed, and discussed. Further, new strategies to create


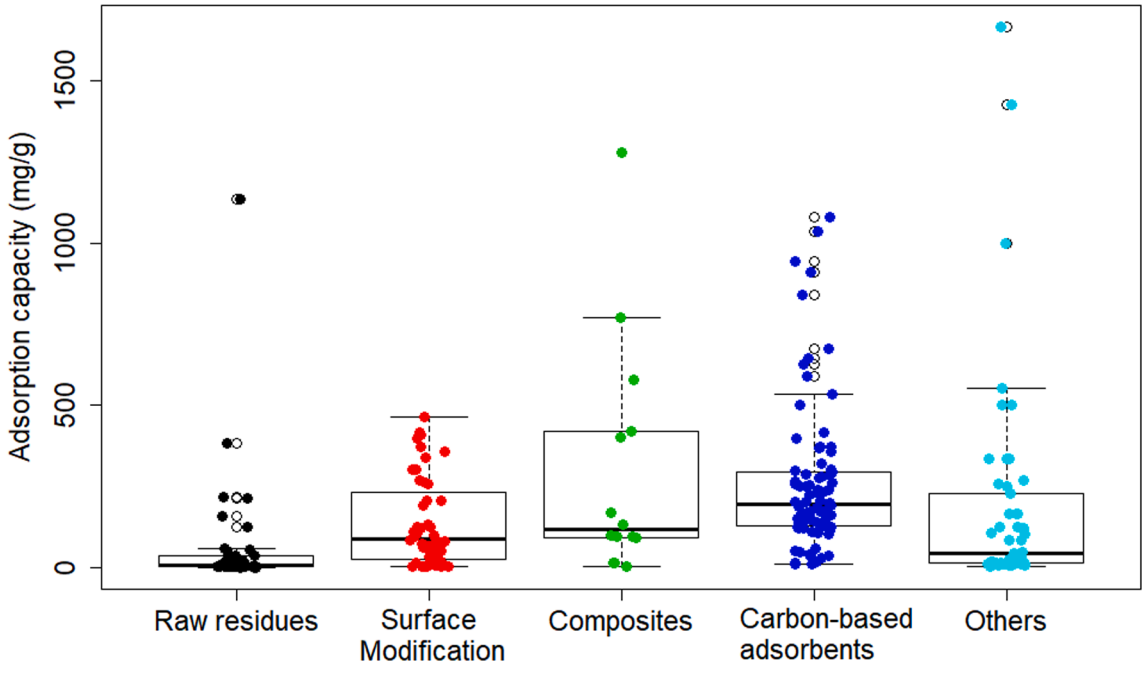


**Fig. 10.** Adsorbents derived from agricultural and industrial waste for the removal of antibiotics and adsorption performance. Data were taken from Tables 1–5.

these adsorbents from these residues were reported.

In Section 3, the use of pristine residues was assessed. On the whole, raw residues have poor adsorption performance with an adsorption uptake that ranges from 0.13 to 78.16 mg/g, as can be seen in the narrow distribution in Fig. 10, with few exceptions. This implies that large amounts of residues would be required to treat a significant volume of antibiotic-loaded effluents, which decreases their potential application in real wastewater plants. Therefore, modifying their porous structure, introducing new functional groups, and increasing their surface area through any approach detailed in the above sections is necessary. For future research works, it is encouraged the modification of the raw wastes, especially for those adsorbents with adsorption intakes lower than 50 mg/g, with the aim of seeing them as practical materials with properties similar to commercial adsorbents.

Several methodologies to modify the waste's surface were summarized in Section 4. In general, chemical modification methods can be classified according to the reagent used or the product formed. In this context, the use of acids, alkalines, oxidizing, surfactants, ionic liquids, and deep eutectic solvents falls into the first group. These agents not only introduce new functional groups onto the adsorbent's surface (especially oxygen-containing groups), but some also substantially enhance their physical properties. On the other hand, esterification, etherification, and grafting techniques focus on forming specific compounds on the adsorbent's surface, such as esters or ethers. Because of the aggregation phenomenon, their specific surface decline, but with an increase in the adsorption performance due to the introduction of new active sites. In any case, it was observed that by modifying their surface, their adsorption capacity improves significantly (2.16–462 mg/g). According to the literature, most studies used acid or alkaline solutions to modify these residues chemically. Although these solutions have shown satisfactory results, new and less toxic solvents should be tested, including ionic liquids and deep eutectic solvents. Additionally, a combination of different physical and chemical modification methods is encouraged, which according to several studies, can enhance further the adsorption properties compared to single treatments. Physical techniques like ball milling, microwave radiation, and ultrasonic can be applied in tandem with chemical agents to tailor the physicochemical properties of the waste-based adsorbents; these new combined-modification techniques might become an important research direction and hotspot for future research works.

The development of waste-based composites, reviewed in Section 5, also demonstrated being an efficient approach to boost the adsorption properties of poor resides; their adsorption capacity ranged between 3.45 and 900 mg/g (Fig. 10). Within this scheme, nanoparticles have been ordinarily deposited on the waste's surface in order to solve the easy aggregation of NPs and facilitate their recovery after adsorption tests. Other functional species also ought to be evaluated for future research, especially those with catalytic and photocatalytic properties to boost the antibiotic removal with a synergic effect of adsorption and degradation (Section 8). Besides, the leaching effect from the matrix should be studied to avoid secondary pollution of aqueous media, especially those composites prepared using the solution blending method.

Regarding carbon-based adsorbents (Section 6), this group of materials has been the most widely studied in the last decade. According to the reviewed literature, biochars, hydrochars, biochar- and hydrochar-based composites, mesoporous carbons, hierarchical porous carbons, heteroatoms-doped porous carbons, and bio-graphene can be prepared using agricultural and industrial wastes. The data collected shows that carbonaceous materials are an excellent choice to remove antibiotics from aquatic environments, with most adsorption capacities varying in the range of 9.68–541 mg/g. Nonetheless, it must be considered that these adsorbents require high-energy consumption procedures to obtain them in contrast with other materials, and at times more than one step (usually carbonization and activation) is required to acquire suitable adsorption capacities. For instance, the single pyrolysis produces biochar with poor adsorption performances ($q_e < 100$ mg/g); similar and even higher adsorption uptakes can be obtained with lower energy consuming procedures, like impregnation with chemical species or chemical modifications. On the other hand, mesoporous carbons, hierarchical porous carbons, and heteroatoms-doped porous carbons can be effective in removing antibiotics from aqueous media due to their outstanding physical properties and abundant functional groups that are bound with antibiotics, forming π-π EDA and hydrophobic interactions as predominant adsorption mechanisms. Since the production of these carbonaceous materials is a highly-demanding process in terms of energy. Therefore, further research needs to be conducted in order to optimize the carbonization process energetically. New alternatives, such as catalytic pyrolysis or microwave pyrolysis, should be studied in depth. Alternatively, the potential of uncommon physical and chemical modification methods, including ball milling, ultrasonic irradiation, deep eutectic solvents, ionic liquids, and anionic or cationic surfactants, need to be explored and analyzed.

In Section 7, other adsorptive materials were reviewed. In this section, the production of zeolites obtained from ash, hydroxyapatite from cement kiln dust or steel slag, some minerals like magnetite, maghemite, and jacobsite from water sludge, nanosilica from rice husk and straw, nanocellulose from grass, and $Fe_3O_4$ NPs from fruit peels and leaves, was emphasized. From this group, zeolite analcime obtained from electrolytic manganese residue through a hydrothermal method had the highest adsorption capacity reported in this review (1922 mg/g for ROX).

Desorption and reusability studies were summarized in Section 9. For the waste-derived adsorptive materials presented in this study, thermal and chemical-driven regenerations have been widely studied for the reusability of exhausted adsorbents. However, these methods still have limitations to overcome; specifically, the regeneration efficiencies drop significantly after several cycles. Besides, in the eluent-assisted regeneration method, a secondary concentrated solution is regenerated that requires another appropriate waste management. Alternatively, the degradation of antibiotics on the adsorbent thanks to catalysts and photocatalysts is a new promising approach that provides less decline in removal efficiency over multiple adsorption/desorption cycles and does not produce by-products. Therefore, studies with different catalytic and photocatalytic compounds should be studied. Notwithstanding, not all studies analyze this essential aspect; regeneration or appropriate waste management strategies need to be studied in tandem with adsorption tests in order to improve the economic feasibility of adsorbents as well as reduce their impact on the environment after saturation.

For the all types of adsorptive materials reviewed, their adsorption capacity data was plotted in a boxplot shown in Fig. 10. We observe a great variability in the adsorption capacity for the composites (scattered data), whereas $q_e$ varies less in surface modification, carbonaceous adsorbents, and other adsorbents. For CMs, their data points consistently hover around the center values, which shows its low variability. Besides, it is observed that CMs have the highest $q_e$ median value compared with other adsorbents. In particular, heteroatom-dopen carbons and hierarchical porous carbons exhibited the best adsorption performance, whose adsorption data was above other carbon-based adsorbents, as shown in Fig. 5b. Therefore, these materials are the most promising for their application in removing antibiotics from aqueous solutions.

Finally, adsorption tests should be performed with actual domestic wastewaters to estimate the real potential of these waste-derived adsorbents, or synthetic solutions with different organic pollutants such as analgesics, anti-inflammatories, endocrine disruptors, and other pharmaceuticals can also be explored.

## 11. Data availability statement

All the data used in this review has been detailed in Tables 1–6.

*CRediT authorship contribution statement*

**Diego M. Juela:** Conceptualization, Data curation, Formal analysis, Investigation, Methodology, Visualization, Writing – original draft, Writing – review & editing.

## Declaration of Competing Interest

The authors declare that they have no known competing financial interests or personal relationships that could have appeared to influence the work reported in this paper.

*Acknowledgement*

The author acknowledges all the researchers cited in this review for their valuable contribution to the adsorption field. Special thanks to Mateo Astudillo for providing support on the scientific databases.

*Funding*

This research did not receive any specific grant from funding agencies in the public, commercial, or not-for-profit sectors.

## References

[1] Y. Ben, M. Hu, X. Zhang, S. Wu, M.H. Wong, M. Wang, C.B. Andrews, C. Zheng, Efficient detection and assessment of human exposure to trace antibiotic residues in drinking water, Water Res. 175 (2020) 115699, https://doi.org/10.1016/j.watres.2020.115699.

[2] A.A. Inyinbor, A. Tsopmo, C.C. Udenigwe, Antibiotics threats on vegetables and the perils of low income nations practices, Sustainable Chem. Pharm. 21 (2021) 100448, https://doi.org/10.1016/j.scp.2021.100448.

[3] Z.E. Menkem, B.L. Ngangom, S.S.A. Tamunjoh, F.F. Boyom, Antibiotic residues in food animals: Public health concern, Acta Ecol. Sin. 39 (5) (2019) 411–415, https://doi.org/10.1016/j.chnaes.2018.10.004.

[4] M. Pan, L.M. Chu, Transfer of antibiotics from wastewater or animal manure to soil and edible crops, Environ. Pollut. 231 (2017) 829–836, https://doi.org/10.1016/j.envpol.2017.08.051.

[5] M. Bilal, S. Mehmood, T. Rasheed, H.M.N. Iqbal, Antibiotics traces in the aquatic environment: persistence and adverse environmental impact, Curr. Opin. Environ. Sci. Health 13 (2020) 68–74, https://doi.org/10.1016/j.coesh.2019.11.005.

[6] K. Chen, J.L. Zhou, Occurrence and behavior of antibiotics in water and sediments from the Huangpu River, Shanghai, China, Chemosphere 95 (2014) 604–612, https://doi.org/10.1016/j.chemosphere.2013.09.119.

[7] R. Kafaei, F. Papari, M. Seyedabadi, S. Sahebi, R. Tahmasebi, M. Ahmadi, G. A. Sorial, G. Asgari, B. Ramavandi, Occurrence, distribution, and potential sources of antibiotics pollution in the water-sediment of the northern coastline of the Persian Gulf, Iran, Sci. Total Environ. 627 (2018) 703–712, https://doi.org/10.1016/j.scitotenv.2018.01.305.

[8] A. Murata, H. Takada, K. Mutoh, H. Hosoda, A. Harada, N. Nakada, Nationwide monitoring of selected antibiotics: distribution and sources of sulfonamides, trimethoprim, and macrolides in Japanese rivers, Sci. Total Environ. 409 (24) (2011) 5305–5312, https://doi.org/10.1016/j.scitotenv.2011.09.014.

[9] M.B. Ahmed, J.L. Zhou, H.H. Ngo, W. Guo, Adsorptive removal of antibiotics from water and wastewater: Progress and challenges, Elsevier, 2015. https://doi.org/10.1016/j.scitotenv.2015.05.130.

[10] Z.Y. Lu, Y.L. Ma, J.T. Zhang, N.S. Fan, B.C. Huang, R.C. Jin, A critical review of antibiotic removal strategies: Performance and mechanisms, Elsevier Ltd, 2020. https://doi.org/10.1016/j.jwpe.2020.101681.

[11] R. Anjali, S. Shanthakumar, Insights on the current status of occurrence and removal of antibiotics in wastewater by advanced oxidation processes, Academic Press, 2019. https://doi.org/10.1016/j.jenvman.2019.05.090.

[12] R.K. Langbehn, C. Michels, H.M. Soares, Antibiotics in wastewater: From its occurrence to the biological removal by environmentally conscious technologies, Elsevier Ltd 275 (2021) 116603, https://doi.org/10.1016/j.envpol.2021.116603.

[13] L. Leng, L. Wei, Q. Xiong, S. Xu, W. Li, S. Lv, Q. Lu, L. Wan, Z. Wen, W. Zhou, Use of microalgae based technology for the removal of antibiotics from wastewater: A review, Elsevier Ltd 238 (2020) 124680, https://doi.org/10.1016/j.chemosphere.2019.124680.

[14] C. Du, Z. Zhang, G. Yu, H. Wu, H. Chen, L.u. Zhou, Y. Zhang, Y. Su, S. Tan, L. u. Yang, J. Song, S. Wang, A review of metal organic framework (MOFs)-based materials for antibiotics removal via adsorption and photocatalysis, Elsevier Ltd 272 (2021) 129501, https://doi.org/10.1016/j.chemosphere.2020.129501.

[15] N. Roy, S.A. Alex, N. Chandrasekaran, A. Mukherjee, K. Kannabiran, A comprehensive update on antibiotics as an emerging water pollutant and their removal using nano-structured photocatalysts, J. Environ. Chem. Eng. 9 (2) (2021) 104796, https://doi.org/10.1016/j.jece:2020.104796.

[16] S. Yu, H. Pang, S. Huang, H. Tang, S. Wang, M. Qiu, Z. Chen, H. Yang, G. Song, D. Fu, B. Hu, X. Wang, Recent advances in metal-organic framework membranes for water treatment: A review, Sci. Total Environ. 800 (2021) 149662, https://doi.org/10.1016/j.scitotenv.2021.149662.

[17] J. Dutta, A.A. Mala, Removal of antibiotic from the water environment by the adsorption technologies: A review, IWA Publishing (2020), https://doi.org/10.2166/wst.2020.335.

[18] A.F.d. Silva, J.L.d.S. Duarte, L. Meili, Different routes for MgFe/LDH synthesis and application to remove pollutants of emerging concern, Sep. Purif. Technol. 264 (2021) 118353, https://doi.org/10.1016/j.seppur.2021.118353.

[19] S. Zhuang, Y. Liu, J. Wang, Covalent organic frameworks as efficient adsorbent for sulfamerazine removal from aqueous solution, J. Hazard. Mater. 383 (2020) 121126, https://doi.org/10.1016/j.jhazmat.2019.121126.

[20] S. Zhang, J. Wang, Y. Zhang, J. Ma, L. Huang, S. Yu, L. Chen, G. Song, M. Qiu, X. Wang, Applications of water-stable metal-organic frameworks in the removal of water pollutants: A review, Environ. Pollut. 291 (2021) 118076, https://doi.org/10.1016/j.envpol.2021.118076.

[21] L. Zhang, L. Yao, L. Ye, B. Long, Y. Dai, Y. Ding, Benzimidazole-based hyper-cross-linked polymers for effective adsorption of chlortetracycline from aqueous solution, J. Environ. Chem. Eng. 8 (6) (2020) 104562, https://doi.org/10.1016/j.jece:2020.104562.

[22] B. Gulen, M. Bugdayci, A. Turan, P. Demircivi, Determination of adsorption characteristics of monolayer titanium carbide with fluoroquinolone pollutants in aqueous solution, J. Mol. Liq. 304 (2020) 112643, https://doi.org/10.1016/j.molliq.2020.112643.

[23] R. Romita, V. Rizzi, J. Gubitosa, J.A. Gabaldón, M.I. Fortea, T. Gómez-Morte, V. M. Gómez-López, P. Fini, P. Cosma, Cyclodextrin polymers and salts: An Eco-Friendly combination to modulate the removal of sulfamethoxazole from water and its release, Chemosphere 283 (2021) 131238, https://doi.org/10.1016/j.chemosphere.2021.131238.

[24] N. Khandelwal, G.K. Darbha, A decade of exploring MXenes as aquatic cleaners: Covering a broad range of contaminants, current challenges and future trends, Chemosphere 279 (2021) 130587, https://doi.org/10.1016/j.chemosphere.2021.130587.

[25] X. Ma, T.F. Scott, Approaches and challenges in the synthesis of three-dimensional covalent-organic frameworks, Commun Chem. 1 (2018) 1–15, https://doi.org/10.1038/s42004-018-0098-8.

[26] D. Juela, M. Vera, C. Cruzat, X. Alvarez, E. Vanegas, Mathematical modeling and numerical simulation of sulfamethoxazole adsorption onto sugarcane bagasse in a fixed-bed column, Chemosphere 280 (2021) 130687, https://doi.org/10.1016/j.chemosphere.2021.130687.

[27] M.E. Peñafiel, J.M. Matesanz, E. Vanegas, D. Bermejo, M.P. Ormad, Corncobs as a potentially low-cost biosorbent for sulfamethoxazole removal from aqueous solution, Sep. Sci. Technol. 55 (17) (2020) 3060–3071, https://doi.org/10.1080/01496395.2019.1673414.

[28] M.E. Peñafiel, E. Vanegas, D. Bermejo, J.M. Matesanz, M.P. Ormad, Organic residues as adsorbent for the removal of ciprofloxacin from aqueous solution, Hyperfine Interact. 240 (2019) 1–13, https://doi.org/10.1007/s10751-019-1612-9.

[29] M.E. Peñafiel, J.M. Matesanz, E. Vanegas, D. Bermejo, R. Mosteo, M.P. Ormad, Comparative adsorption of ciprofloxacin on sugarcane bagasse from Ecuador and on commercial powdered activated carbon, Sci. Total Environ. 750 (2021) 141498, https://doi.org/10.1016/j.scitotenv.2020.141498.

[30] S. Hu, Y. Zhang, G. Shen, H. Zhang, Z. Yuan, W. Zhang, Adsorption/desorption behavior and mechanisms of sulfadiazine and sulfamethoxazole in agricultural soil systems, Soil Tillage Res. 186 (2019) 233–241, https://doi.org/10.1016/j.still.2018.10.026.

[31] J. Mo, Q. Yang, N. Zhang, W. Zhang, Y. Zheng, Z. Zhang, A review on agro-industrial waste (AIW) derived adsorbents for water and wastewater treatment, J. Environ. Manage. 227 (2018) 395–405, https://doi.org/10.1016/j.jenvman.2018.08.069.

[32] M. Paredes-Laverde, J. Silva-Agredo, R.A. Torres-Palma, Removal of norfloxacin in deionized, municipal water and urine using rice (Oryza sativa) and coffee (Coffea arabica) husk wastes as natural adsorbents, J. Environ. Manage. 213 (2018) 98–108, https://doi.org/10.1016/j.jenvman.2018.02.047.

[33] B. Yan, C.H. Niu, Adsorption behavior of norfloxacin and site energy distribution based on the Dubinin-Astakhov isotherm, Sci. Total Environ. 631–632 (2018) 1525–1533, https://doi.org/10.1016/j.scitotenv.2018.03.119.

[34] N. Dhiman, N. Sharma, Batch adsorption studies on the removal of ciprofloxacin hydrochloride from aqueous solution using ZnO nanoparticles and groundnut (Arachis hypogaea) shell powder: a comparison, Indian Chem. Eng. 61 (1) (2019) 67–76, https://doi.org/10.1080/00194506.2018.1424044.

[35] D. Balarak, A. Joghatayi, F.K. Mostafapour, H. Azarpira, Biosorption of Amoxicillin form contaminated water onto palm bark biomass, International Journal of Life Science and Pharma, Research. 7 (2017) 1–8.

[36] A.D. Nieva, R.J.Q. Buenafe, L.M.S. Orense, J.M.R. Trinidad, Biosorption of doxycycline using Carica papaya L. peels, IOP Conf. Series: Earth Environ. Sci. 344 (1) (2019) 012010, https://doi.org/10.1088/1755-1315/344/1/012010.

[37] Y. Yin, X. Guo, D. Peng, Iron and manganese oxides modified maize straw to remove tylosin from aqueous solutions, Chemosphere 205 (2018) 156–165, https://doi.org/10.1016/j.chemosphere.2018.04.108.

[38] Y. Zhang, D. Peng, Y. Luo, D. Huang, X. Guo, L. Zhu, Cellulase modified waste biomass to remove sulfamethazine from aqueous solutions, Sci. Total Environ. 731 (2020) 138806, https://doi.org/10.1016/j.scitotenv.2020.138806.

[39] T.S. Khokhar, F.N. Memon, A.A. Memon, F. Durmaz, S. Memon, Q.K. Panhwar, S. Muneer, Removal of ciprofloxacin from aqueous solution using wheat bran as

adsorbent, Sep. Sci. Technol. 54 (8) (2019) 1278–1288, https://doi.org/10.1080/01496395.2018.1536150.
[40] W. Mekhamer, S. Al-Tamimi, Removal of ciprofloxacin from simulated wastewater by pomegranate peels, Environ. Sci. Pollut. Res. 26 (3) (2019) 2297–2304, https://doi.org/10.1007/s11356-018-3639-x.
[41] O.M. Ezekoye, K.G. Akpomie, S.I. Eze, C.N. Chukwujindu, J.U. Ani, O.T. Ujam, Biosorptive interaction of alkaline modified Dialium guineense seed powders with ciprofloxacin in contaminated solution: central composite, kinetics, isotherm, thermodynamics, and desorption, Int. J. Phytorem. 22 (10) (2020) 1028–1037, https://doi.org/10.1080/15226514.2020.1725869.
[42] V. Rizzi, D. Lacalamita, J. Gubitosa, P. Fini, A. Petrella, R. Romita, A. Agostiano, J.A. Gabaldón, M.I. Fortea Gorbe, T. Gómez-Morte, P. Cosma, Removal of tetracycline from polluted water by chitosan-olive pomace adsorbing films, Sci. Total Environ. 693 (2019) 133620, https://doi.org/10.1016/j.scitotenv.2019.133620.
[43] N. Fang, Q. He, L. Sheng, Y. Xi, L. Zhang, H. Liu, H. Cheng, Toward broader applications of iron ore waste in pollution control: Adsorption of norfloxacin, J. Hazard. Mater. 418 (2021) 126273, https://doi.org/10.1016/j.jhazmat.2021.126273.
[44] J. Chen, J. Zhang, W. Wang, X. Ma, Y. Guo, F. Sun, Y. Wang, Comparison of adsorption characteristics of acid-base modified fly ash to norfloxacin, Spectrosc. Lett. 53 (6) (2020) 416–429, https://doi.org/10.1080/00387010.2020.1766507.
[45] C. Dube, R. Tandlich, B. Wilhelmi, Adsorptive removal of ciprofloxacin and isoniazid from aqueous solution, Nova Biotechnol. Chi. 17 (2018) 16–28, https://doi.org/10.2478/nbec-2018-0002.
[46] Y. Wang, Q. Nie, B. Huang, H. Cheng, L. Wang, Q. He, Removal of ciprofloxacin as an emerging pollutant: A novel application for bauxite residue reuse, J. Cleaner Prod. 253 (2020) 120049, https://doi.org/10.1016/j.jclepro.2020.120049.
[47] J. Chang, Z. Shen, X. Hu, E. Schulman, C. Cui, Q. Guo, H. Tian, Adsorption of tetracycline by shrimp shell waste from aqueous solutions: adsorption isotherm, kinetics modeling, and mechanism, ACS Omega 5 (7) (2020) 3467–3477, https://doi.org/10.1021/acsomega.9b0378110.1021/acsomega.9b03781.s001.
[48] D.C. Henrique, D.U. Quintela, A.H. Ide, A. Erto, J.L.d.S. Duarte, L. Meili, Calcined Mytella falcata shells as alternative adsorbent for efficient removal of rifampicin antibiotic from aqueous solutions, J. Environ. Chem. Eng. 8 (3) (2020) 103782, https://doi.org/10.1016/j.jece:2020.103782.
[49] Y. Dai, K. Zhang, X. Meng, J. Li, X. Guan, Q. Sun, Y. Sun, W. Wang, M. Lin, M. Liu, S. Yang, Y. Chen, F. Gao, X. Zhang, Z. Liu, New use for spent coffee ground as an adsorbent for tetracycline removal in water, Chemosphere 215 (2019) 163–172, https://doi.org/10.1016/j.chemosphere.2018.09.150.
[50] M. El-Azazy, A.S. El-Shafie, A. Elgendy, A.A. Issa, S. Al-Meer, K.A. Al-Saad, A Comparison between Different Agro-wastes and Carbon Nanotubes for Removal of Sarafloxacin from Wastewater: Kinetics and Equilibrium Studies, Molecules 25 (2020) 5429, https://doi.org/10.3390/molecules25225429.
[51] K. Tolić, D. Mutavdžić Pavlović, N. Stankir, M. Runje, Biosorbents from tomato, tangerine, and maple leaves for the removal of ciprofloxacin from aqueous media, Water Air Soil Pollut. 232 (2021) 218. https://doi.org/10.1007/s11270-021-05153-9.
[52] D. Mutavdžić Pavlović, L. Ćurković, J. Macan, K. Žižek, Eggshell as a new biosorbent for the removal of pharmaceuticals from aqueous solutions, Clean - Soil, Air, Water 45 (12) (2017) 1700082, https://doi.org/10.1002/clen.v45.1210.1002/clen.201700082.
[53] M. Conde-Cid, G. Ferreira-Coelho, M. Arias-Estévez, C. Álvarez-Esmorís, J. C. Nóvoa-Muñoz, A. Núñez-Delgado, M.J. Fernández-Sanjurjo, E. Álvarez-Rodríguez, Competitive adsorption/desorption of tetracycline, oxytetracycline and chlortetracycline on pine bark, oak ash and mussel shell, J. Environ. Manage. 250 (2019) 109509, https://doi.org/10.1016/j.jenvman.2019.109509.
[54] A. Fernandez-Sanroman, V. Acevedo-García, M. Pazos, M.A. Sanromán, E. Rosales, Removal of sulfamethoxazole and methylparaben using hydrocolloid and fiber industry wastes: Comparison with biochar and laccase-biocomposite, J. Cleaner Prod. 271 (2020) 122436, https://doi.org/10.1016/j.jclepro.2020.122436.
[55] R. Li, Y. Zhang, W. Chu, Z. Chen, J. Wang, Adsorptive removal of antibiotics from water using peanut shells from agricultural waste, RSC Adv. 8 (24) (2018) 13546–13555, https://doi.org/10.1039/C7RA11796E.
[56] V.S. Tran, H.H. Ngo, W. Guo, C. Ton-That, J. Li, J. Li, Y. Liu, Removal of antibiotics (sulfamethazine, tetracycline and chloramphenicol) from aqueous solution by raw and nitrogen plasma modified steel shavings, Sci. Total Environ. 601–602 (2017) 845–856, https://doi.org/10.1016/j.scitotenv.2017.05.164.
[57] G. Kaur, N. Singh, A. Rajor, Ofloxacin adsorptive interaction with rice husk ash: Parametric and exhausted adsorbent disposability study, J. Contam. Hydrol. 236 (2021) 103737, https://doi.org/10.1016/j.jconhyd.2020.103737.
[58] M.J. Ahmed, B.H. Hameed, E.H. Hummadi, Insight into the chemically modified crop straw adsorbents for the enhanced removal of water contaminants: a review, J. Mol. Liq. 330 (2021) 115616, https://doi.org/10.1016/j.molliq.2021.115616.
[59] S.M. Abegunde, K.S. Idowu, O.M. Adejuwon, T. Adeyemi-Adejolu, A review on the influence of chemical modification on the performance of adsorbents, Resour., Environ. Sustain. 1 (2020) 100001, https://doi.org/10.1016/j.resenv.2020.100001.
[60] X. Huang, S. Wu, S. Tang, L.i. Huang, D. Zhu, Q.i. Hu, Photocatalytic hydrogel layer supported on alkali modified straw fibers for ciprofloxacin removal from water, J. Mol. Liq. 317 (2020) 113961, https://doi.org/10.1016/j.molliq.2020.113961.
[61] H. Fan, Y. Ma, J. Wan, Y. Wang, Z. Li, Y. Chen, Adsorption properties and mechanisms of novel biomaterials from banyan aerial roots via simple modification for ciprofloxacin removal, Sci. Total Environ. 708 (2020) 134630, https://doi.org/10.1016/j.scitotenv.2019.134630.
[62] M. Stjepanović, N. Velić, A. Lončarić, D. Gašo-Sokač, V. Bušić, M. Habuda-Stanić, Adsorptive removal of nitrate from wastewater using modified lignocellulosic waste material, J. Mol. Liq. 285 (2019) 535–544, https://doi.org/10.1016/j.molliq.2019.04.105.
[63] Z. Movasaghi, B. Yan, C. Niu, Adsorption of ciprofloxacin from water by pretreated oat hulls: Equilibrium, kinetic, and thermodynamic studies, Ind. Crops Prod. 127 (2019) 237–250, https://doi.org/10.1016/j.indcrop.2018.10.051.
[64] M.A. Ahsan, M.T. Islam, C. Hernandez, E. Castro, S.K. Katla, H. Kim, Y. Lin, M. L. Curry, J. Gardea-Torresdey, J.C. Noveron, Biomass conversion of saw dust to a functionalized carbonaceous materials for the removal of Tetracycline, Sulfamethoxazole and Bisphenol A from water, J. Environ. Chem. Eng. 6 (4) (2018) 4329–4338.
[65] M.A. Ahsan, M.T. Islam, M.A. Imam, A.H.M.G. Hyder, V. Jabbari, N. Dominguez, J.C. Noveron, Biosorption of bisphenol A and sulfamethoxazole from water using sulfonated coffee waste: Isotherm, kinetic and thermodynamic studies, J. Environ. Chem. Eng. 6 (5) (2018) 6602–6611.
[66] G. Kaur, N. Singh, A. Rajor, J.P. Kushwaha, Deep eutectic solvent functionalized rice husk ash for effective adsorption of ofloxacin from aqueous environment, J. Contam. Hydrol. 242 (2021) 103847, https://doi.org/10.1016/j.jconhyd.2021.103847.
[67] B. Yan, C.H. Niu, Modeling and site energy distribution analysis of levofloxacin sorption by biosorbents, Chem. Eng. J. 307 (2017) 631–642, https://doi.org/10.1016/j.cej.2016.08.065.
[68] M.T. Islam, A.G. Hyder, R. Saenz-Arana, C. Hernandez, T. Guinto, M.A. Ahsan, B. Alvarado-Tenorio, J.C. Noveron, Removal of methylene blue and tetracycline from water using peanut shell derived adsorbent prepared by sulfuric acid reflux, J. Environ. Chem. Eng. 7 (1) (2019) 102816, https://doi.org/10.1016/j.jece:2018.102816.
[69] M.T. Islam, R. Saenz-Arana, C. Hernandez, T. Guinto, M.A. Ahsan, H. Kim, Y. Lin, B. Alvarado-Tenorio, J.C. Noveron, Adsorption of methylene blue and tetracycline onto biomass-based material prepared by sulfuric acid reflux, RSC Adv. 8 (57) (2018) 32545–32557, https://doi.org/10.1039/C8RA05395B.
[70] M.A. Ahsan, S.K. Katla, M.T. Islam, J.A. Hernandez-Viezcas, L.M. Martinez, C. A. Díaz-Moreno, J. Lopez, S.R. Singamaneni, J. Banuelos, J. Gardea-Torresdey, J. C. Noveron, Adsorptive removal of methylene blue, tetracycline and Cr(VI) from water using sulfonated tea waste, Environ. Technol. Innovation 11 (2018) 23–40, https://doi.org/10.1016/j.eti.2018.04.003.
[71] I.A. Lawal, M. Klink, P. Ndungu, B. Moodley, Brief bibliometric analysis of “ionic liquid” applications and its review as a substitute for common adsorbent modifier for the adsorption of organic pollutants, Environ. Res. 175 (2019) 34–51, https://doi.org/10.1016/j.envres.2019.05.005.
[72] I.A. Lawal, B. Moodley, Sorption mechansim of pharmaceuticals from aqueous medium on ionic liquid modified biomass: sorption mechansim of pharmaceuticals from aqueous medium, J. Chem. Technol. Biotechnol. 92 (4) (2017) 808–818, https://doi.org/10.1002/jctb.5063.
[73] I.A. Lawal, D. Chetty, S.O. Akpotu, B. Moodley, Sorption of Congo red and reactive blue on biomass and activated carbon derived from biomass modified by ionic liquid, Environ. Nanotechnol. Monit. Manage. 8 (2017) 83–91, https://doi.org/10.1016/j.enmm.2017.05.003.
[74] J. Płotka-Wasylka, M. de la Guardia, V. Andruch, M. Vilková, Deep eutectic solvents vs ionic liquids: similarities and differences, Microchem. J. 159 (2020) 105539, https://doi.org/10.1016/j.microc.2020.105539.
[75] W. Duan, M. Li, W. Xiao, N. Wang, B. Niu, L. Zhou, Y. Zheng, Enhanced adsorption of three fluoroquinolone antibiotics using polypyrrole functionalized Calotropis gigantea fiber, Colloids Surf., A 574 (2019) 178–187, https://doi.org/10.1016/j.colsurfa.2019.04.068.
[76] D.F. Caicedo, G.S. dos Reis, E.C. Lima, I.A.S. De Brum, P.S. Thue, B.G. Cazacliu, D. R. Lima, A.H. dos Santos, G.L. Dotto, Efficient adsorbent based on construction and demolition wastes functionalized with 3-aminopropyltriethoxysilane (APTES) for the removal ciprofloxacin from hospital synthetic effluents, J. Environ. Chem. Eng. 8 (4) (2020) 103875, https://doi.org/10.1016/j.jece:2020.103875.
[77] E. Cao, W. Duan, A. Wang, Y. Zheng, Oriented growth of poly(m-phenylenediamine) on Calotropis gigantea fiber for rapid adsorption of ciprofloxacin, Chemosphere 171 (2017) 223–230, https://doi.org/10.1016/j.chemosphere.2016.12.087.
[78] L. Yi, G. Liang, W. Xiao, W. Duan, A. Wang, Y. Zheng, Rapid nitrogen-rich modification of Calotropis gigantea fiber for highly efficient removal of fluoroquinolone antibiotics, J. Mol. Liq. 256 (2018) 408–415, https://doi.org/10.1016/j.molliq.2018.02.060.
[79] Y. Zhao, W. Li, Z. Liu, J. Liu, L. Zhu, X. Liu, K. Huang, Renewable Tb/Eu-loaded garlic peels for enhanced adsorption of enrofloxacin: kinetics, isotherms, thermodynamics, and mechanism, ACS Sustainable Chem. Eng. 6 (11) (2018) 15264–15272, https://doi.org/10.1021/acssuschemeng.8b0373910.1021/acssuschemeng.8b03739.s001.
[80] O. Yaqubi, M.H. Tai, D. Mitra, C. Gerente, K.G. Neoh, C.-H. Wang, Y. Andres, Adsorptive removal of tetracycline and amoxicillin from aqueous solution by leached carbon black waste and chitosan-carbon composite beads, J. Environ. Chem. Eng. 9 (1) (2021) 104988, https://doi.org/10.1016/j.jece:2020.104988.
[81] D. Mitra, C. Zhou, M.H. Bin Hashim, T.M. Hang, K.-H. Gin, C.-H. Wang, K. G. Neoh, Emerging pharmaceutical and organic contaminants removal using carbonaceous waste from oil refineries, Chemosphere 271 (2021) 129542, https://doi.org/10.1016/j.chemosphere.2021.129542.

[82] T. Guérin, A. Ghinet, M. Hossart, C. Waterlot, Wheat and ryegrass biomass ashes as effective sorbents for metallic and organic pollutants from contaminated water in lab-engineered cartridge filtration system, Bioresour. Technol. 318 (2020) 124044, https://doi.org/10.1016/j.biortech.2020.124044.
[83] S.I. Eze, K.G. Akpomie, O.M. Ezekoye, C.N. Chukwujindu, F.K. Ojo, J.U. Ani, O. T. Ujam, Antibiotic adsorption by acid enhanced dialium guineense seed waste, Arab. J. Sci. Eng. 46 (1) (2021) 309–324, https://doi.org/10.1007/s13369-020-04771-5.
[84] Y. Fu, Z. Yang, Y. Xia, Y. Xing, X. Gui, Adsorption of ciprofloxacin pollutants in aqueous solution using modified waste grapefruit peel, Energy Sources Part A 43 (2) (2021) 225–234, https://doi.org/10.1080/15567036.2019.1624877.
[85] H. Alidadi, M. Dolatabadi, M. Davoudi, F. Barjasteh-Askari, F. Jamali-Behnam, A. Hosseinzadeh, Enhanced removal of tetracycline using modified sawdust: optimization, isotherm, kinetics, and regeneration studies, Process Saf. Environ. Prot. 117 (2018) 51–60, https://doi.org/10.1016/j.psep.2018.04.007.
[86] W. Duan, W. Xiao, N. Wang, B. Niu, Y. Zheng, Removal of three fluoroquinolone antibiotics by NaClO $_2$ -modified biosorbent from fruit fiber of C, Procera, J. Natural Fibers 17 (11) (2020) 1594–1604, https://doi.org/10.1080/15440478.2019.1584080.
[87] S. Sayen, M. Ortenbach-López, E. Guillon, Sorptive removal of enrofloxacin antibiotic from aqueous solution using a ligno-cellulosic substrate from wheat bran, J. Environ. Chem. Eng. 6 (5) (2018) 5820–5829.
[88] T. Chahm, L.F. de Souza, N.R. dos Santos, B.A. da Silva, C.A. Rodrigues, Use of chemically activated termite feces a low-cost adsorbent for the adsorption of norfloxacin from aqueous solution, Water Sci. Technol. 79 (2019) 291–301, https://doi.org/10.2166/wst.2019.052.
[89] M.T. Islam, R. Saenz-Arana, C. Hernandez, T. Guinto, M.A. Ahsan, D.T. Bragg, H. Wang, B. Alvarado-Tenorio, J.C. Noveron, Conversion of waste tire rubber into a high-capacity adsorbent for the removal of methylene blue, methyl orange, and tetracycline from water, J. Environ. Chem. Eng. 6 (2) (2018) 3070–3082.
[90] N. Imane, A. El Kassimi, Y. Achour, M. El Himri, S. Lazar, S. Rafqah, M. R. Laamari, M. El Haddad, Assessment of adsorptive competition of two antibiotics removal from aqueous media onto activated watermelon seeds: experimental and theoretical study using DFT method, Int. J. Environ. Anal. Chem. (2021) 1–19, https://doi.org/10.1080/03067319.2021.1928095.
[91] M.A. Ahsan, V. Jabbari, M.T. Islam, H. Kim, J.A. Hernandez-Viezcas, Y. Lin, C. A. Díaz-Moreno, J. Lopez, J. Gardea-Torresdey, J.C. Noveron, Green synthesis of a highly efficient biosorbent for organic, pharmaceutical, and heavy metal pollutants removal: engineering surface chemistry of polymeric biomass of spent coffee waste, J. Water Process Eng. 25 (2018) 309–319, https://doi.org/10.1016/j.jwpe.2018.08.005.
[92] M.A. Ahsan, M.T. Islam, C. Hernandez, H. Kim, Y. Lin, M.L. Curry, J. Gardea-Torresdey, J.C. Noveron, Adsorptive removal of sulfamethoxazole and bisphenol A from contaminated water using functionalized carbonaceous material derived from tea leaves, J. Environ. Chem. Eng. 6 (4) (2018) 4215–4225.
[93] A.A. Mohammed, T.J. Al-Musawi, S.L. Kareem, M. Zarrabi, A.M. Al-Ma'abreh, Simultaneous adsorption of tetracycline, amoxicillin, and ciprofloxacin by pistachio shell powder coated with zinc oxide nanoparticles, Arabian Journal of Chemistry. 13 (2020) 4629–4643. https://doi.org/10.1016/j.arabjc.2019.10.010.
[94] A.A. Mohammed, S.L. Kareem, Adsorption of tetracycline fom wastewater by using Pistachio shell coated with ZnO nanoparticles: equilibrium, kinetic and isotherm studies, Alexandria Eng. J. 58 (3) (2019) 917–928, https://doi.org/10.1016/j.aej.2019.08.006.
[95] S. Aydin, M.E. Aydin, F. Beduk, A. Ulvi, Removal of antibiotics from aqueous solution by using magnetic Fe3O4/red mud-nanoparticles, Sci. Total Environ. 670 (2019) 539–546, https://doi.org/10.1016/j.scitotenv.2019.03.205.
[96] Y. Shao, P. Zhao, Q. Yue, Y. Wu, B. Gao, W. Kong, Preparation of wheat straw-supported Nanoscale Zero-Valent Iron and its removal performance on ciprofloxacin, Ecotoxicol. Environ. Saf. 158 (2018) 100–107, https://doi.org/10.1016/j.ecoenv.2018.04.020.
[97] Q. Li, Z. Chen, H. Wang, H. Yang, T. Wen, S. Wang, B. Hu, X. Wang, Removal of organic compounds by nanoscale zero-valent iron and its composites, Sci. Total Environ. 792 (2021) 148546, https://doi.org/10.1016/j.scitotenv.2021.148546.
[98] Y. Shao, Y. Gao, Q. Yue, W. Kong, B. Gao, W. Wang, W. Jiang, Degradation of chlortetracycline with simultaneous removal of copper (II) from aqueous solution using wheat straw-supported nanoscale zero-valent iron, Chem. Eng. J. 379 (2020) 122384, https://doi.org/10.1016/j.cej.2019.122384.
[99] W. Shi, H. Ren, X. Huang, M. Li, Y. Tang, F. Guo, Low cost red mud modified graphitic carbon nitride for the removal of organic pollutants in wastewater by the synergistic effect of adsorption and photocatalysis, Sep. Purif. Technol. 237 (2020) 116477, https://doi.org/10.1016/j.seppur.2019.116477.
[100] Y. Li, M. Deng, X. Wang, Y. Wang, J. Li, S. Xia, J. Zhao, In-situ remediation of oxytetracycline and Cr(VI) co-contaminated soil and groundwater by using blast furnace slag-supported nanosized Fe0/FeSx, Chem. Eng. J. 412 (2021) 128706, https://doi.org/10.1016/j.cej.2021.128706.
[101] X. Guo, Y. Yin, C. Yang, Z. Dang, Maize straw decorated with sulfide for tylosin removal from the water, Ecotoxicol. Environ. Saf. 152 (2018) 16–23, https://doi.org/10.1016/j.ecoenv.2018.01.025.
[102] M.J. M-Ridha, Y.R. Hasan, M.A. Ibrahim, Adsorption kinetics and mechanisms for meropenem antibiotic removal in batch mode via rice husk functionalized with Mg/Fe-layered double hydroxides, Sep. Sci. Technol. 56 (16) (2021) 2721–2733, https://doi.org/10.1080/01496395.2020.1852258.
[103] Y. Zhang, X. Wang, J. Wang, S. Yen, Z. Deng, Y. Ding, T. Liu, X. Bai, J. Tai, The adsorption-degradation effect of peanut shells loaded with sulfonamide-degrading bacteria, DWT 196 (2020) 256–270, https://doi.org/10.5004/dwt.2020.26051.
[104] A. Ashiq, M. Vithanage, B. Sarkar, M. Kumar, A. Bhatnagar, E. Khan, Y. Xi, Y. S. Ok, Carbon-based adsorbents for fluoroquinolone removal from water and wastewater: a critical review, Environ. Res. 197 (2021) 111091, https://doi.org/10.1016/j.envres.2021.111091.
[105] P. Krasucka, B.o. Pan, Y. Sik Ok, D. Mohan, B. Sarkar, P. Oleszczuk, Engineered biochar – a sustainable solution for the removal of antibiotics from water, Chem. Eng. J. 405 (2021) 126926, https://doi.org/10.1016/j.cej.2020.126926.
[106] R. Janu, V. Mrlik, D. Ribitsch, J. Hofman, P. Sedláček, L. Bielská, G. Soja, Biochar surface functional groups as affected by biomass feedstock, biochar composition and pyrolysis temperature, Carbon Resour. Convers. 4 (2021) 36–46, https://doi.org/10.1016/j.crcon.2021.01.003.
[107] N. Cheng, B. Wang, P. Wu, X. Lee, Y. Xing, M. Chen, B. Gao, Adsorption of emerging contaminants from water and wastewater by modified biochar: a review, Environ. Pollut. 273 (2021) 116448, https://doi.org/10.1016/j.envpol.2021.116448.
[108] L. Liang, F. Xi, W. Tan, X.u. Meng, B. Hu, X. Wang, Review of organic and inorganic pollutants removal by biochar and biochar-based composites, Biochar 3 (3) (2021) 255–281, https://doi.org/10.1007/s42773-021-00101-6.
[109] M. Zhao, M. Shao, X. Ma, K.H.M. Mansur, Y. Fu, Adsorption of sulfamethoxazole by wheat straw-derived biochars in seawater, E3S Web Conf. 251 (2021) 02036, https://doi.org/10.1051/e3sconf/202125102036.
[110] J. Hoslett, H. Ghazal, E. Katsou, H. Jouhara, The removal of tetracycline from water using biochar produced from agricultural discarded material, Sci. Total Environ. 751 (2021) 141755, https://doi.org/10.1016/j.scitotenv.2020.141755.
[111] K. Velusamy, S. Periyasamy, P.S. Kumar, T. Jayaraj, R. Krishnasamy, J. Sindhu, D. Sneka, B. Subhashini, D.-V. Vo, Analysis on the removal of emerging contaminant from aqueous solution using biochar derived from soap nut seeds, Environ. Pollut. 287 (2021) 117632, https://doi.org/10.1016/j.envpol.2021.117632.
[112] N. Acelas, S.M. Lopera, J. Porras, R.A. Torres-Palma, Evaluating the Removal of the Antibiotic Cephalexin from Aqueous Solutions Using an Adsorbent Obtained from Palm Oil Fiber, Molecules 26 (2021) 3340, https://doi.org/10.3390/molecules26113340.
[113] D. Naghipour, L. Hoseinzadeh, K. Taghavi, J. Jaafari, A. Amouei, Effective removal of tetracycline from aqueous solution using biochar prepared from pine bark: isotherms, kinetics and thermodynamic analyses, Int. J. Environ. Anal. Chem. (2021) 1–14, https://doi.org/10.1080/03067319.2021.1942462.
[114] Y.i. Hu, Y. Zhu, Y.i. Zhang, T. Lin, G. Zeng, S. Zhang, Y. Wang, W. He, M. Zhang, H. Long, An efficient adsorbent: Simultaneous activated and magnetic ZnO doped biochar derived from camphor leaves for ciprofloxacin adsorption, Bioresour. Technol. 288 (2019) 121511, https://doi.org/10.1016/j.biortech.2019.121511.
[115] B. Li, Y. Zhang, J. Xu, Y. Mei, S. Fan, H. Xu, Effect of carbonization methods on the properties of tea waste biochars and their application in tetracycline removal from aqueous solutions, Chemosphere 267 (2021) 129283, https://doi.org/10.1016/j.chemosphere.2020.129283.
[116] J. Yang, G. Ji, Y. Gao, W. Fu, M. Irfan, L. Mu, Y. Zhang, A. Li, High-yield and high-performance porous biochar produced from pyrolysis of peanut shell with low-dose ammonium polyphosphate for chloramphenicol adsorption, J. Cleaner Prod. 264 (2020) 121516, https://doi.org/10.1016/j.jclepro.2020.121516.
[117] J. Huang, A.R. Zimmerman, H. Chen, B. Gao, Ball milled biochar effectively removes sulfamethoxazole and sulfapyridine antibiotics from water and wastewater, Environ. Pollut. 258 (2020) 113809, https://doi.org/10.1016/j.envpol.2019.113809.
[118] S.O. Amusat, T.G. Kebede, S. Dube, M.M. Nindi, Ball-milling synthesis of biochar and biochar–based nanocomposites and prospects for removal of emerging contaminants: a review, J. Water Process Eng. 41 (2021) 101993, https://doi.org/10.1016/j.jwpe.2021.101993.
[119] K. Ram, N. Sivarajasekar, S. Muthusaravanan, K. Kumaravel, R.S. Ganesh, An ensemble based model for the adsorptive removal of amoxicillin by microwave-biochar of waste cotton seeds, in: Seoul, South Korea, 2020, p. 020010. https://doi.org/10.1063/5.0019385.
[120] B. Sajjadi, J.W. Broome, W.Y. Chen, D.L. Mattern, N.O. Egiebor, N. Hammer, C. L. Smith, Urea functionalization of ultrasound-treated biochar: A feasible strategy for enhancing heavy metal adsorption capacity, Ultrason. Sonochem. 51 (2019) 20–30, https://doi.org/10.1016/j.ultsonch.2018.09.015.
[121] X. Geng, S. Lv, J. Yang, S. Cui, Z. Zhao, Carboxyl-functionalized biochar derived from walnut shells with enhanced aqueous adsorption of sulfonamide antibiotics, J. Environ. Manage. 280 (2021) 111749, https://doi.org/10.1016/j.jenvman.2020.111749.
[122] P. Qin, D. Huang, R. Tang, F. Gan, Y. Guan, X. Lv, Enhanced adsorption of sulfonamide antibiotics in water by modified biochar derived from bagasse, Open Chem. 17 (2019) 1309–1316, https://doi.org/10.1515/chem-2019-0141.
[123] Z. Yang, Z. Zhao, X. Yang, Z. Ren, Xanthate modified magnetic activated carbon for efficient removal of cationic dyes and tetracycline hydrochloride from aqueous solutions, Colloids Surf., A 615 (2021) 126273, https://doi.org/10.1016/j.colsurfa.2021.126273.
[124] G. Kaur, N. Singh, A. Rajor, Efficient adsorption of doxycycline hydrochloride using deep eutectic solvent functionalized activated carbon derived from pumpkin seed shell, ChemistrySelect. 6 (13) (2021) 3139–3150, https://doi.org/10.1002/slct.202100182.
[125] I.A. Lawal, M. Klink, P. Ndungu, Deep eutectic solvent as an efficient modifier of low-cost adsorbent for the removal of pharmaceuticals and dye, Environ. Res. 179 (2019) 108837, https://doi.org/10.1016/j.envres.2019.108837.

[126] D. Akhil, D. Lakshmi, A. Kartik, D.-V. Vo, J. Arun, K.P. Gopinath, Production, characterization, activation and environmental applications of engineered biochar: a review, Environ. Chem. Lett. 19 (3) (2021) 2261–2297, https://doi.org/10.1007/s10311-020-01167-7.
[127] X. Zhu, Y. Gao, Q. Yue, Y. Song, B. Gao, X. Xu, Facile synthesis of hierarchical porous carbon material by potassium tartrate activation for chloramphenicol removal, J. Taiwan Inst. Chem. Eng. 85 (2018) 141–148, https://doi.org/10.1016/j.jtice.2018.01.025.
[128] M. Yuan, C. Li, B. Zhang, J. Wang, J. Zhu, J. Ji, Y. Ma, A mild and one-pot method to activate lignin-derived biomass by using boric acid for aqueous tetracycline antibiotics removal in water, Chemosphere 280 (2021) 130877, https://doi.org/10.1016/j.chemosphere.2021.130877.
[129] T. Ai, X. Jiang, Q. Liu, L. Lv, S. Dai, Single-component and competitive adsorption of tetracycline and Zn(II) on an $NH_4$ Cl-induced magnetic ultra-fine buckwheat peel powder biochar from water: studies on the kinetics, isotherms, and mechanism, RSC Adv. 10 (2020) 20427–20437, https://doi.org/10.1039/D0RA02346A.
[130] A. Chowdhury, S. Kumari, A.A. Khan, M.R. Chandra, S. Hussain, Activated carbon loaded with Ni-Co-S nanoparticle for superior adsorption capacity of antibiotics and dye from wastewater: Kinetics and isotherms, Colloids Surf., A 611 (2021) 125868, https://doi.org/10.1016/j.colsurfa.2020.125868.
[131] Y. Xiang, X. Yang, Z. Xu, W. Hu, Y. Zhou, Z. Wan, Y. Yang, Y. Wei, J. Yang, D.C. W. Tsang, Fabrication of sustainable manganese ferrite modified biochar from vinasse for enhanced adsorption of fluoroquinolone antibiotics: effects and mechanisms, Sci. Total Environ. 709 (2020) 136079, https://doi.org/10.1016/j.scitotenv.2019.136079.
[132] H. Chakhtouna, H. Benzeid, N. Zari, A.e.K. Qaiss, R. Bouhfid, Functional CoFe2O4-modified biochar derived from banana pseudostem as an efficient adsorbent for the removal of amoxicillin from water, Sep. Purif. Technol. 266 (2021) 118592, https://doi.org/10.1016/j.seppur.2021.118592.
[133] J. Liang, Y. Fang, Y. Luo, G. Zeng, J. Deng, X. Tan, N. Tang, X. Li, X. He, C. Feng, S. Ye, Magnetic nanoferromanganese oxides modified biochar derived from pine sawdust for adsorption of tetracycline hydrochloride, Environ. Sci. Pollut. Res. 26 (6) (2019) 5892–5903, https://doi.org/10.1007/s11356-018-4033-4.
[134] Z. Xu, Y. Xiang, H. Zhou, J. Yang, Y. He, Z. Zhu, Y. Zhou, Manganese ferrite modified biochar from vinasse for enhanced adsorption of levofloxacin: effects and mechanisms, Environ. Pollut. 272 (2021) 115968, https://doi.org/10.1016/j.envpol.2020.115968.
[135] R. Zhang, X. Zheng, B. Chen, J. Ma, X. Niu, D. Zhang, Z. Lin, M. Fu, S. Zhou, Enhanced adsorption of sulfamethoxazole from aqueous solution by Fe-impregnated graphited biochar, J. Cleaner Prod. 256 (2020) 120662, https://doi.org/10.1016/j.jclepro.2020.120662.
[136] J. Liu, B. Zhou, H. Zhang, J. Ma, B. Mu, W. Zhang, A novel Biochar modified by Chitosan-Fe/S for tetracycline adsorption and studies on site energy distribution, Bioresour. Technol. 294 (2019) 122152, https://doi.org/10.1016/j.biortech.2019.122152.
[137] L. Capobianco, F. Di Caprio, P. Altimari, M.L. Astolfi, F. Pagnanelli, Production of an iron-coated adsorbent for arsenic removal by hydrothermal carbonization of olive pomace: effect of the feedwater pH, J. Environ. Manage. 273 (2020) 111164, https://doi.org/10.1016/j.jenvman.2020.111164.
[138] T. Wang, Y. Zhai, Y. Zhu, C. Li, G. Zeng, A review of the hydrothermal carbonization of biomass waste for hydrochar formation: process conditions, fundamentals, and physicochemical properties, Renew. Sustain. Energy Rev. 90 (2018) 223–247, https://doi.org/10.1016/j.rser.2018.03.071.
[139] X. Zhang, Y. Zhang, H.H. Ngo, W. Guo, H. Wen, D. Zhang, C. Li, L.i. Qi, Characterization and sulfonamide antibiotics adsorption capacity of spent coffee grounds based biochar and hydrochar, Sci. Total Environ. 716 (2020) 137015, https://doi.org/10.1016/j.scitotenv.2020.137015.
[140] L. Delgado-Moreno, S. Bazhari, G. Gasco, A. Méndez, M. El Azzouzi, E. Romero, New insights into the efficient removal of emerging contaminants by biochars and hydrochars derived from olive oil wastes, Sci. Total Environ. 752 (2021) 141838, https://doi.org/10.1016/j.scitotenv.2020.141838.
[141] J. Guan, Y. Liu, F. Jing, R. Ye, J. Chen, Contrasting impacts of chemical and physical ageing on hydrochar properties and sorption of norfloxacin with coexisting Cu2+, Sci. Total Environ. 772 (2021) 145502, https://doi.org/10.1016/j.scitotenv.2021.145502.
[142] L. Cheng, Y. Ji, Q. Shao, Facile modification of hydrochar derived from cotton straw with excellent sorption performance for antibiotics: coupling DFT simulations with experiments, Sci. Total Environ. 760 (2021) 144124, https://doi.org/10.1016/j.scitotenv.2020.144124.
[143] F.M. Jais, C.Y. Chee, Z. Ismail, S. Ibrahim, Experimental design via NaOH activation process and statistical analysis for activated sugarcane bagasse hydrochar for removal of dye and antibiotic, J. Environ. Chem. Eng. 9 (1) (2021) 104829, https://doi.org/10.1016/j.jece:2020.104829.
[144] H. Li, J. Hu, L. Yao, Q. Shen, L. An, X. Wang, Ultrahigh adsorbability towards different antibiotic residues on fore-modified self-functionalized biochar: competitive adsorption and mechanism studies, J. Hazard. Mater. 390 (2020) 122127, https://doi.org/10.1016/j.jhazmat.2020.122127.
[145] Z. Mengting, T.A. Kurniawan, R. Avtar, M.H.D. Othman, T. Ouyang, H. Yujia, Z. Xueting, T. Setiadi, I. Iswanto, Applicability of TiO2(B) nanosheets@hydrochar composites for adsorption of tetracycline (TC) from contaminated water, J. Hazard. Mater. 405 (2021) 123999, https://doi.org/10.1016/j.jhazmat.2020.123999.
[146] J. Deng, X. Li, X. Wei, Y. Liu, J. Liang, B. Song, Y. Shao, W. Huang, Hybrid silicate-hydrochar composite for highly efficient removal of heavy metal and antibiotics: Coadsorption and mechanism, Chem. Eng. J. 387 (2020) 124097, https://doi.org/10.1016/j.cej.2020.124097.
[147] H. Huang, Z. Niu, R. Shi, J. Tang, L. Lv, J. Wang, Y. Fan, Thermal oxidation activation of hydrochar for tetracycline adsorption: the role of oxygen concentration and temperature, Bioresour. Technol. 306 (2020) 123096, https://doi.org/10.1016/j.biortech.2020.123096.
[148] L. Leng, Q. Xiong, L. Yang, H. Li, Y. Zhou, W. Zhang, S. Jiang, H. Li, H. Huang, An overview on engineering the surface area and porosity of biochar, Sci. Total Environ. 763 (2021) 144204, https://doi.org/10.1016/j.scitotenv.2020.144204.
[149] J. Xi, H. Li, J. Xi, S. Tan, J. Zheng, Z. Tan, Preparation of high porosity biochar materials by template method: a review, Environ. Sci. Pollut. Res. 27 (17) (2020) 20675–20684, https://doi.org/10.1007/s11356-020-08593-8.
[150] R. Kueasook, N. Rattanachueskul, N. Chanlek, D. Dechtrirat, W. Watcharin, P. Amornpitoksuk, L. Chuenchom, Green and facile synthesis of hierarchically porous carbon monoliths via surface self-assembly on sugarcane bagasse scaffold: Influence of mesoporosity on efficiency of dye adsorption, Microporous Mesoporous Mater. 296 (2020) 110005, https://doi.org/10.1016/j.micromeso.2020.110005.
[151] Z. Zheng, B. Zhao, Y. Guo, Y. Guo, T. Pak, G. Li, Preparation of mesoporous batatas biochar via soft-template method for high efficiency removal of tetracycline, Sci. Total Environ. 787 (2021) 147397, https://doi.org/10.1016/j.scitotenv.2021.147397.
[152] Y. Wang, H. Zhang, G. Wang, L. Liu, Y. Yu, A. Chen, Preparation of mesoporous carbon from biomass for heavy metal ion adsorption, Fullerenes, Nanotubes, Carbon Nanostruct. 25 (2) (2017) 102–108, https://doi.org/10.1080/1536383X.2016.1262355.
[153] U.I. Nda-Umar, I. Ramli, E.N. Muhamad, N. Azri, Y.H. Taufiq-Yap, Optimization and characterization of mesoporous sulfonated carbon catalyst and its application in modeling and optimization of acetin production, Molecules 25 (2020) 5221, https://doi.org/10.3390/molecules25225221.
[154] L. Xu, M. Zhang, Y. Wang, F. Wei, Highly effective adsorption of antibiotics from water by hierarchically porous carbon: effect of nanoporous geometry, Environ. Pollut. 274 (2021) 116591, https://doi.org/10.1016/j.envpol.2021.116591.
[155] M. Zhang, A.D. Igalavithana, L. Xu, B. Sarkar, D. Hou, M. Zhang, A. Bhatnagar, W. C. Cho, Y.S. Ok, Engineered/designer hierarchical porous carbon materials for organic pollutant removal from water and wastewater: A critical review, Critical Rev. Environ. Sci. Technol. 51 (20) (2021) 2295–2328, https://doi.org/10.1080/10643389.2020.1780102.
[156] R. Zhang, Z. Zhou, A. Xie, J. Dai, J. Cui, J. Lang, M. Wei, X. Dai, C. Li, Y. Yan, Preparation of hierarchical porous carbons from sodium carboxymethyl cellulose via halloysite template strategy coupled with KOH-activation for efficient removal of chloramphenicol, J. Taiwan Inst. Chem. Eng. 80 (2017) 424–433, https://doi.org/10.1016/j.jtice.2017.07.032.
[157] X. Wei, Z. Zhang, L. Qin, J. Dai, Template-free preparation of yeast-derived three-dimensional hierarchical porous carbon for highly efficient sulfamethazine adsorption from water, J. Taiwan Inst. Chem. Eng. 95 (2019) 532–540, https://doi.org/10.1016/j.jtice.2018.09.009.
[158] H. Wang, L. Shan, Q. Lv, S. Cai, G. Quan, J. Yan, Production of hierarchically porous carbon from natural biomass waste for efficient organic contaminants adsorption, J. Cleaner Prod. 263 (2020) 121352, https://doi.org/10.1016/j.jclepro.2020.121352.
[159] J. Dai, L. Qin, R. Zhang, A. Xie, Z. Chang, S. Tian, C. Li, Y. Yan, Sustainable bovine bone-derived hierarchically porous carbons with excellent adsorption of antibiotics: equilibrium, kinetic and thermodynamic investigation, Powder Technol. 331 (2018) 162–170, https://doi.org/10.1016/j.powtec.2018.03.005.
[160] D. Yu, L. Wang, M. Wu, Simultaneous removal of dye and heavy metal by banana peels derived hierarchically porous carbons, J. Taiwan Inst. Chem. Eng. 93 (2018) 543–553, https://doi.org/10.1016/j.jtice.2018.08.038.
[161] Y. Shen, N. Zhang, Y. Fu, Synthesis of high-performance hierarchically porous carbons from rice husk for sorption of phenol in the gas phase, J. Environ. Manage. 241 (2019) 53–58, https://doi.org/10.1016/j.jenvman.2019.04.012.
[162] B.M. Matsagar, R.-X. Yang, S. Dutta, Y.S. Ok, K.-W. Wu, Recent progress in the development of biomass-derived nitrogen-doped porous carbon, J. Mater. Chem. A 9 (7) (2021) 3703–3728, https://doi.org/10.1039/D0TA09706C.
[163] L. Qin, Z. Zhou, J. Dai, P. Ma, H. Zhao, J. He, A. Xie, C. Li, Y. Yan, Novel N-doped hierarchically porous carbons derived from sustainable shrimp shell for high-performance removal of sulfamethazine and chloramphenicol, J. Taiwan Inst. Chem. Eng. 62 (2016) 228–238, https://doi.org/10.1016/j.jtice.2016.02.009.
[164] J. Sun, M. Li, Z. Zhang, J. Guo, Unravelling the adsorption disparity mechanism of heavy-metal ions on the biomass-derived hierarchically porous carbon, Appl. Surf. Sci. 471 (2019) 615–620, https://doi.org/10.1016/j.apsusc.2018.12.050.
[165] T. Wang, L.u. Xue, L. Zheng, S. Bao, Y. Liu, T. Fang, B. Xing, Biomass-derived N/S dual-doped hierarchically porous carbon material as effective adsorbent for the removal of bisphenol F and bisphenol S, J. Hazard. Mater. 416 (2021) 126126, https://doi.org/10.1016/j.jhazmat.2021.126126.
[166] L.u. Luo, L. Luo, J. Deng, T. Chen, G. Du, M. Fan, W. Zhao, High performance supercapacitor electrodes based on B/N Co-doped biomass porous carbon materials by KOH activation and hydrothermal treatment, Int. J. Hydrogen Energy 46 (63) (2021) 31927–31937, https://doi.org/10.1016/j.ijhydene.2021.06.211.
[167] H. Liu, C. Xu, Y. Ren, D. Tang, C. Zhang, F. Li, X. Wei, C. Huo, X. Li, R. Zhang, O-N–S self-doped hierarchical porous carbon synthesized from lotus leaves with high performance for dye adsorption, ACS Omega 5 (42) (2020) 27032–27042, https://doi.org/10.1021/acsomega.0c0202110.1021/acsomega.0c02021.s001.
[168] S. Xiaoqing, G. Jindiao, S. Jingchun, T. Gongsong, Z. Nan, W. Yifan, Z. Mei'e, [Green synthesis of N, P-codoped porous biomass carbon for high-performance Li-

S batteries][氮磷共掺杂生物质多孔碳的绿色合成及其在锂硫电池中的应用], Trans. Chinese Soc. Agric. Eng. 37 (2021) 231–237. https://doi.org/10.11975/j.issn.1002-6819.2021.03.028.
[169] Z. Bonyadi, FarzanehAkhound Noghani, A. Dehghan, J.P.V. der Hoek, D. A. Giannakoudakis, S.K. Ghadiri, I. Anastopoulos, M. Sarkhosh, J.C. Colmenares, M. Shams, Biomass-derived porous aminated graphitic nanosheets for removal of the pharmaceutical metronidazole: Optimization of physicochemical features and exploration of process mechanisms, Colloids Surf., A 611 (2021) 125791, https://doi.org/10.1016/j.colsurfa.2020.125791.
[170] S.K. Ghadiri, S. Nasseri, R. Nabizadeh, M. Khoobi, S. Nazmara, A.H. Mahvi, Adsorption of nitrate onto anionic bio-graphene nanosheet from aqueous solutions: Isotherm and kinetic study, J. Mol. Liq. 242 (2017) 1111–1117, https://doi.org/10.1016/j.molliq.2017.06.122.
[171] S. Sadeghi, H.R. Zakeri, M.H. Saghi, S.K. Ghadiri, S.S. Talebi, M. Shams, G. L. Dotto, Modified wheat straw–derived graphene for the removal of Eriochrome Black T: characterization, isotherm, and kinetic studies, Environ. Sci. Pollut. Res. 28 (3) (2021) 3556–3565, https://doi.org/10.1007/s11356-020-10647-w.
[172] F. Bahmei, N. Bahramifar, H. Younesi, V. Tolstoy, Synthesis of porous graphene nanocomposite and its excellent adsorption behavior for Erythromycin antibiotic, Nanosystems: Phys. Chem. Math. 11 (2) (2020) 214–222, https://doi.org/10.17586/2220-8054-2020-11-2-214-222.
[173] S.K. Ghadiri, H. Alidadi, N. Tavakkoli Nezhad, A. Javid, A. Roudbari, S.S. Talebi, A.A. Mohammadi, M. Shams, S. Rezania, M. Al-Ghouti, Valorization of biomass into amine- functionalized bio graphene for efficient ciprofloxacin adsorption in water-modeling and optimization study, PLoS ONE 15 (4) (2020) e0231045, https://doi.org/10.1371/journal.pone.023104510.1371/journal.pone.0231045.g00110.1371/journal.pone.0231045.g00210.1371/journal.pone.0231045.g00310.1371/journal.pone.0231045.g00410.1371/journal.pone.0231045.g00510.1371/journal.pone.0231045.g00610.1371/journal.pone.0231045.g00710.1371/journal.pone.0231045.g00810.1371/journal.pone.0231045.t00110.1371/journal.pone.0231045.t00210.1371/journal.pone.0231045.t00310.1371/journal.pone.0231045.t00410.1371/journal.pone.0231045.t00510.1371/journal.pone.0231045.t00610.1371/journal.pone.0231045.t00710.1371/journal.pone.0231045.t00810.1371/journal.pone.0231045.t00910.1371/journal.pone.0231045.t01010.1371/journal.pone.0231045.t01110.1371/journal.pone.0231045.s00110.1371/journal.pone.0231045.s00210.1371/journal.pone.0231045.s00310.1371/journal.pone.0231045.s00410.1371/journal.pone.0231045.r00110.1371/journal.pone.0231045.r00210.1371/journal.pone.0231045.r00310.1371/journal.pone.0231045.r004.
[174] F.E. Che Othman, M.S. Ismail, N. Yusof, S. Samitsu, M.Z. Yusop, N.F. Tajul Arifin, N.H. Alias, J. Jaafar, F. Aziz, W.N. Wan Salleh, A.F. Ismail, Methane adsorption by porous graphene derived from rice husk ashes under various stabilization temperatures, Carbon Lett. 30 (5) (2020) 535–543, https://doi.org/10.1007/s42823-020-00123-3.
[175] A. Javid, A. Roudbari, N. Yousefi, M.A. Fard, B. Barkdoll, S.S. Talebi, S. Nazemi, M. Ghanbarian, S.K. Ghadiri, Modeling of chromium (VI) removal from aqueous solution using modified green-Graphene: RSM-CCD approach, optimization, isotherm, and kinetic studies, J. Environ. Health Sci. Eng. 18 (2) (2020) 515–529, https://doi.org/10.1007/s40201-020-00479-8.
[176] S.S. Talebi, A.B. Javid, A.A. Roudbari, N. Yousefi, S.K. Ghadiri, M. Shams, A. Mousavi Khaneghah, Defluoridationof drinking water by metal impregnated multi-layer green graphene fabricated from trees pruning waste, Environ. Sci. Pollut. Res. 28 (2021) 18201–18215, https://doi.org/10.1007/s11356-020-11743-7.
[177] J. Kaushik, V. Kumar, A.K. Garg, P. Dubey, K.M. Tripathi, S.K. Sonkar, Bio-mass derived functionalized graphene aerogel: a sustainable approach for the removal of multiple organic dyes and their mixtures, New J. Chem. 45 (20) (2021) 9073–9083, https://doi.org/10.1039/D1NJ00470K.
[178] J.F. Saldarriaga, N.A. Montoya, I. Estiati, A.T. Aguayo, R. Aguado, M. Olazar, Unburned material from biomass combustion as low-cost adsorbent for amoxicillin removal from wastewater, J. Cleaner Prod. 284 (2021) 124732, https://doi.org/10.1016/j.jclepro.2020.124732.
[179] H.M. Jang, E. Kan, A novel hay-derived biochar for removal of tetracyclines in water, Bioresour. Technol. 274 (2019) 162–172, https://doi.org/10.1016/j.biortech.2018.11.081.
[180] J. Tang, L.i. Zong, B. Mu, Y. Kang, A. Wang, Attapulgite/carbon composites as a recyclable adsorbent for antibiotics removal, Korean J. Chem. Eng. 35 (8) (2018) 1650–1661, https://doi.org/10.1007/s11814-018-0066-0.
[181] J. Li, G. Yu, L. Pan, C. Li, F. You, S. Xie, Y. Wang, J. Ma, X. Shang, Study of ciprofloxacin removal by biochar obtained from used tea leaves, J. Environ. Sci. 73 (2018) 20–30, https://doi.org/10.1016/j.jes.2017.12.024.
[182] Z. Zeng, X. Tan, Y. Liu, S. Tian, G. Zeng, L. Jiang, S. Liu, J. Li, N. Liu, Z. Yin, Comprehensive adsorption studies of doxycycline and ciprofloxacin antibiotics by biochars prepared at different temperatures, Front. Chem. 6 (2018) 80, https://doi.org/10.3389/fchem.2018.00080.
[183] C. Li, X. Zhu, H. He, Y. Fang, H. Dong, J. Lü, J. Li, Y. Li, Adsorption of two antibiotics on biochar prepared in air-containing atmosphere: influence of biochar porosity and molecular size of antibiotics, J. Mol. Liq. 274 (2019) 353–361, https://doi.org/10.1016/j.molliq.2018.10.142.
[184] J. Hu, X. Zhou, Y. Shi, X. Wang, H. Li, Enhancing biochar sorption properties through self-templating strategy and ultrasonic fore-modified pre-treatment: characteristic, kinetic and mechanism studies, Sci. Total Environ. 769 (2021) 144574, https://doi.org/10.1016/j.scitotenv.2020.144574.
[185] C. Ma, H. Huang, X. Gao, T. Wang, Z. Zhu, P. Huo, Y. Liu, Y. Yan, Honeycomb tubular biochar from fargesia leaves as an effective adsorbent for tetracyclines pollutants, J. Taiwan Inst. Chem. Eng. 91 (2018) 299–308, https://doi.org/10.1016/j.jtice.2018.05.032.
[186] Y. Chen, J. Liu, Q. Zeng, Z. Liang, X. Ye, Y. Lv, M. Liu, Preparation of Eucommia ulmoides lignin-based high-performance biochar containing sulfonic group: synergistic pyrolysis mechanism and tetracycline hydrochloride adsorption, Bioresour. Technol. 329 (2021) 124856, https://doi.org/10.1016/j.biortech.2021.124856.
[187] H. Wang, X. Lou, Q.i. Hu, T. Sun, Adsorption of antibiotics from water by using Chinese herbal medicine residues derived biochar: preparation and properties studies, J. Mol. Liq. 325 (2021) 114967, https://doi.org/10.1016/j.molliq.2020.114967.
[188] T. Chen, L. Luo, S. Deng, G. Shi, S. Zhang, Y. Zhang, O. Deng, L. Wang, J. Zhang, L. Wei, Sorption of tetracycline on H3PO4 modified biochar derived from rice straw and swine manure, Bioresour. Technol. 267 (2018) 431–437, https://doi.org/10.1016/j.biortech.2018.07.074.
[189] H. Liu, G. Xu, G. Li, The characteristics of pharmaceutical sludge-derived biochar and its application for the adsorption of tetracycline, Sci. Total Environ. 747 (2020) 141492, https://doi.org/10.1016/j.scitotenv.2020.141492.
[190] A.O. Egbedina, K.O. Adebowale, B.I. Olu-Owolabi, E.I. Unuabonah, M.O. Adesina, Green synthesis of ZnO coated hybrid biochar for the synchronous removal of ciprofloxacin and tetracycline in wastewater, RSC Adv. 11 (30) (2021) 18483–18492, https://doi.org/10.1039/D1RA01130H.
[191] Y. Zhou, Y. He, Y. He, X. Liu, B. Xu, J. Yu, C. Dai, A. Huang, Y. Pang, L. Luo, Analyses of tetracycline adsorption on alkali-acid modified magnetic biochar: Site energy distribution consideration, Sci. Total Environ. 650 (2019) 2260–2266, https://doi.org/10.1016/j.scitotenv.2018.09.393.
[192] L. Tang, J. Yu, Y. Pang, G. Zeng, Y. Deng, J. Wang, X. Ren, S. Ye, B. Peng, H. Feng, Sustainable efficient adsorbent: alkali-acid modified magnetic biochar derived from sewage sludge for aqueous organic contaminant removal, Chem. Eng. J. 336 (2018) 160–169, https://doi.org/10.1016/j.cej.2017.11.048.
[193] B. Hu, Y. Tang, X. Wang, L. Wu, J. Nong, X. Yang, J. Guo, Cobalt-gadolinium modified biochar as an adsorbent for antibiotics in single and binary systems, Microchem. J. 166 (2021) 106235, https://doi.org/10.1016/j.microc.2021.106235.
[194] Y. Mei, J. Xu, Y. Zhang, B. Li, S. Fan, H. Xu, Effect of Fe–N modification on the properties of biochars and their adsorption behavior on tetracycline removal from aqueous solution, Bioresour. Technol. 325 (2021) 124732, https://doi.org/10.1016/j.biortech.2021.124732.
[195] X. Fan, Z. Qian, J. Liu, N. Geng, J. Hou, D. Li, Investigation on the adsorption of antibiotics from water by metal loaded sewage sludge biochar, Water Sci. Technol. 83 (2021) 739–750, https://doi.org/10.2166/wst.2020.578.
[196] S. Zeng, Y.-K. Choi, E. Kan, Iron-activated bermudagrass-derived biochar for adsorption of aqueous sulfamethoxazole: effects of iron impregnation ratio on biochar properties, adsorption, and regeneration, Sci. Total Environ. 750 (2021) 141691, https://doi.org/10.1016/j.scitotenv.2020.141691.
[197] Y. Ma, M. Li, P. Li, L. Yang, L.i. Wu, F. Gao, X. Qi, Z. Zhang, Hydrothermal synthesis of magnetic sludge biochar for tetracycline and ciprofloxacin adsorptive removal, Bioresour. Technol. 319 (2021) 124199, https://doi.org/10.1016/j.biortech.2020.124199.
[198] S. Liu, Y. Liu, X. Tan, S. Liu, M. Li, N. Liu, Z. Yin, S. Tian, Y. Zhou, Facile synthesis of $MnO_x$ -loaded biochar for the removal of doxycycline hydrochloride: effects of ambient conditions and co-existing heavy metals, J. Chem. Technol. Biotechnol. (2019) jctb.6000, https://doi.org/10.1002/jctb.6000.
[199] Y. Xiang, Z. Xu, Y. Zhou, Y. Wei, X. Long, Y. He, D. Zhi, J. Yang, L. Luo, A sustainable ferromanganese biochar adsorbent for effective levofloxacin removal from aqueous medium, Chemosphere 237 (2019) 124464, https://doi.org/10.1016/j.chemosphere.2019.124464.
[200] Y. Zhou, X. Liu, Y. Xiang, P. Wang, J. Zhang, F. Zhang, J. Wei, L. Luo, M. Lei, L. Tang, Modification of biochar derived from sawdust and its application in removal of tetracycline and copper from aqueous solution: Adsorption mechanism and modelling, Bioresour. Technol. 245 (2017) 266–273, https://doi.org/10.1016/j.biortech.2017.08.178.
[201] X. Zheng, X. He, H. Peng, J. Wen, S. Lv, Efficient adsorption of ciprofloxacin using Ga2S3/S-modified biochar via the high-temperature sulfurization, Bioresour. Technol. 334 (2021) 125238, https://doi.org/10.1016/j.biortech.2021.125238.
[202] Q. Shen, Z. Wang, Q. Yu, Y. Cheng, Z. Liu, T. Zhang, S. Zhou, Removal of tetracycline from an aqueous solution using manganese dioxide modified biochar derived from Chinese herbal medicine residues, Environ. Res. 183 (2020) 109195, https://doi.org/10.1016/j.envres.2020.109195.
[203] Z. Zeng, S. Ye, H. Wu, R. Xiao, G. Zeng, J. Liang, C. Zhang, J. Yu, Y. Fang, B. Song, Research on the sustainable efficacy of g-MoS2 decorated biochar nanocomposites for removing tetracycline hydrochloride from antibiotic-polluted aqueous solution, Sci. Total Environ. 648 (2019) 206–217, https://doi.org/10.1016/j.scitotenv.2018.08.108.
[204] M. El-Azazy, A.S. El-Shafie, H. Morsy, Biochar of Spent Coffee Grounds as Per Se and Impregnated with TiO2: Promising Waste-Derived Adsorbents for Balofloxacin, Molecules 26 (2021) 2295, https://doi.org/10.3390/molecules26082295.
[205] V.-T. Nguyen, T.-B. Nguyen, C.-W. Chen, C.-M. Hung, C.P. Huang, C.-D. Dong, Cobalt-impregnated biochar (Co-SCG) for heterogeneous activation of peroxymonosulfate for removal of tetracycline in water, Bioresour. Technol. 292 (2019) 121954, https://doi.org/10.1016/j.biortech.2019.121954.
[206] Z. Li, Z. Wang, X. Wu, M. Li, X. Liu, Competitive adsorption of tylosin, sulfamethoxazole and Cu(II) on nano-hydroxyapatitemodified biochar in water, Chemosphere 240 (2020) 124884, https://doi.org/10.1016/j.chemosphere.2019.124884.

[207] Z. Li, M. Li, Q.i. Che, Y. Li, X. Liu, Synergistic removal of tylosin/sulfamethoxazole and copper by nano-hydroxyapatite modified biochar, Bioresour. Technol. 294 (2019) 122163, https://doi.org/10.1016/j.biortech.2019.122163.
[208] A. Ashiq, B. Sarkar, N. Adassooriya, J. Walpita, A.U. Rajapaksha, Y.S. Ok, M. Vithanage, Sorption process of municipal solid waste biochar-montmorillonite composite for ciprofloxacin removal in aqueous media, Chemosphere 236 (2019) 124384, https://doi.org/10.1016/j.chemosphere.2019.124384.
[209] A. Ashiq, N.M. Adassooriya, B. Sarkar, A.U. Rajapaksha, Y.S. Ok, M. Vithanage, Municipal solid waste biochar-bentonite composite for the removal of antibiotic ciprofloxacin from aqueous media, J. Environ. Manage. 236 (2019) 428–435, https://doi.org/10.1016/j.jenvman.2019.02.006.
[210] C. Li, Y. Gao, A. Li, L. Zhang, G. Ji, K. Zhu, X. Wang, Y. Zhang, Synergistic effects of anionic surfactants on adsorption of norfloxacin by magnetic biochar derived from furfural residue, Environ. Pollut. 254 (2019) 113005, https://doi.org/10.1016/j.envpol.2019.113005.
[211] Y. Chen, J. Shi, Q. Du, H. Zhang, Y. Cui, Antibiotic removal by agricultural waste biochars with different forms of iron oxide, RSC Adv. 9 (25) (2019) 14143–14153, https://doi.org/10.1039/C9RA01271K.
[212] W. Chen, M. Shen, G. Li, Highly-Efficient Adsorptive Removal of Tetracycline Using Magnetic Sugarcane Bagasse Biochar Modified by Lanthanum, Nat. Environ. Pollut. Technol. 18 (2019) 5.
[213] M.Z. Afzal, R. Yue, X.-F. Sun, C. Song, S.-G. Wang, Enhanced removal of ciprofloxacin using humic acid modified hydrogel beads, J. Colloid Interface Sci. 543 (2019) 76–83, https://doi.org/10.1016/j.jcis.2019.01.083.
[214] Y.-P. Chen, C.-H. Zheng, Y.-Y. Huang, Y.-R. Chen, Removal of chlortetracycline from water using spent tea leaves-based biochar as adsorption-enhanced persulfate activator, Chemosphere 286 (2022) 131770, https://doi.org/10.1016/j.chemosphere.2021.131770.
[215] J. Wei, Y. Liu, J. Li, Y. Zhu, H. Yu, Y. Peng, Adsorption and co-adsorption of tetracycline and doxycycline by one-step synthesized iron loaded sludge biochar, Chemosphere 236 (2019) 124254, https://doi.org/10.1016/j.chemosphere.2019.06.224.
[216] Y. Zhou, S. Cao, C. Xi, X. Li, L. Zhang, G. Wang, Z. Chen, A novel Fe3O4/graphene oxide/citrus peel-derived bio-char based nanocomposite with enhanced adsorption affinity and sensitivity of ciprofloxacin and sparfloxacin, Bioresour. Technol. 292 (2019) 121951, https://doi.org/10.1016/j.biortech.2019.121951.
[217] J. Pan, W. Shen, Y. Zhao, H. Sun, T. Guo, Y. Cheng, N. Zhao, H. Tang, X. Yan, Difunctional hierarchical porous SiOC composites from silicone resin and rice husk for efficient adsorption and as a catalyst support, Colloids Surf., A 584 (2020) 124041, https://doi.org/10.1016/j.colsurfa.2019.124041.
[218] Y. Li, G. Liang, L. Chang, C. Zi, Y. Zhang, Z. Peng, W. Zhao, Conversion of biomass ash to different types of zeolites: a review, Null. 43 (14) (2021) 1745–1758, https://doi.org/10.1080/15567036.2019.1640316.
[219] D. Zide, O. Fatoki, O. Oputu, B. Opeolu, S. Nelana, O. Olatunji, Zeolite 'adsorption' capacities in aqueous acidic media; The role of acid choice and quantification method on ciprofloxacin removal, Micropor. Mesopor. Mater. 255 (2018) 226–241, https://doi.org/10.1016/j.micromeso.2017.07.033.
[220] X. Li, Y. Zeng, F. Chen, T. Wang, Y. Li, Y. Chen, H. Hou, M. Zhou, Synthesis of zeolite from carbothermal reduction electrolytic manganese residue for the removal of macrolide antibiotics from aqueous solution, Materials 11 (2018) 2133, https://doi.org/10.3390/ma11112133.
[221] M.M.M. Ali, M.J. Ahmed, B.H. Hameed, NaY zeolite from wheat (Triticum aestivum L.) straw ash used for the adsorption of tetracycline, J. Cleaner Prod. 172 (2018) 602–608, https://doi.org/10.1016/j.jclepro.2017.10.180.
[222] W.A. Khanday, B.H. Hameed, Zeolite-hydroxyapatite-activated oil palm ash composite for antibiotic tetracycline adsorption, Fuel 215 (2018) 499–505, https://doi.org/10.1016/j.fuel.2017.11.068.
[223] A.A.H. Faisal, D.N. Ahmed, M. Rezakazemi, N. Sivarajasekar, G. Sharma, Cost-effective composite prepared from sewage sludge waste and cement kiln dust as permeable reactive barrier to remediate simulated groundwater polluted with tetracycline, J. Environ. Chem. Eng. 9 (3) (2021) 105194, https://doi.org/10.1016/j.jece:2021.105194.
[224] Y.u. Chen, Z. Wang, D. Liang, Y. Liu, H. Yu, S. Zhu, L. Zhang, Conversion of Fe-rich sludge to KFeS2 cluster: spontaneous hydrolysis of KFeS2 for the effective adsorption of doxycycline, Arabian J. Chem. 14 (6) (2021) 103173, https://doi.org/10.1016/j.arabjc.2021.103173.
[225] Z. Qu, Y. Wu, S. Zhu, Y. Yu, M. Huo, L. Zhang, J. Yang, D. Bian, Y.i. Wang, Green synthesis of magnetic adsorbent using groundwater treatment sludge for tetracycline adsorption, Engineering. 5 (5) (2019) 880–887, https://doi.org/10.1016/j.eng.2019.06.001.
[226] T. Hu, H. Wang, R. Ning, X. Qiao, Y. Liu, W. Dong, S. Zhu, Upcycling of Fe-bearing sludge: preparation of erdite-bearing particles for treating pharmaceutical manufacture wastewater, Sci Rep. 10 (2020) 12999, https://doi.org/10.1038/s41598-020-70080-4.
[227] Z. Qu, G.e. Dong, S. Zhu, Y. Yu, M. Huo, K.e. Xu, M. Liu, Recycling of groundwater treatment sludge to prepare nano-rod erdite particles for tetracycline adsorption, J. Cleaner Prod. 257 (2020) 120462, https://doi.org/10.1016/j.jclepro.2020.120462.
[228] R. Bian, J. Zhu, Y.u. Chen, Y. Yu, S. Zhu, L. Zhang, M. Huo, Resource recovery of wastewater treatment sludge: synthesis of a magnetic cancrinite adsorbent, RSC Adv. 9 (62) (2019) 36248–36255, https://doi.org/10.1039/C9RA06940B.
[229] S. Zhu, Y. Wu, Z. Qu, L. Zhang, Y. Yu, X. Xie, M. Huo, J. Yang, D. Bian, H. Zhang, L. Zhang, Green synthesis of magnetic sodalite sphere by using groundwater treatment sludge for tetracycline adsorption, J. Cleaner Prod. 247 (2020) 119140, https://doi.org/10.1016/j.jclepro.2019.119140.
[230] A. Khan, Y. Huo, Z. Qu, Y. Liu, Z. Wang, Y. Chen, M. Huo, A facile calcination conversion of groundwater treatment sludge (GTS) as magnetic adsorbent for oxytetracycline adsorption, Sci. Rep. 11 (2021) 5276, https://doi.org/10.1038/s41598-021-84231-8.
[231] S.-J. Chao, K.-H. Chung, Y.-F. Lai, Y.-K. Lai, S.-H. Chang, Keratin particles generated from rapid hydrolysis of waste feathers with green DES/KOH: efficient adsorption of fluoroquinolone antibiotic and its reuse, Int. J. Biol. Macromol. 173 (2021) 211–218, https://doi.org/10.1016/j.ijbiomac.2021.01.126.
[232] E. Vismara, G. Bertolini, C. Bongio, N. Massironi, M. Zarattini, D. Nanni, C. Cosentino, G. Torri, Nanocellulose from cotton waste and its glycidyl methacrylate grafting and allylation: synthesis, characterization and adsorption properties, Nanomaterials 11 (2021) 476, https://doi.org/10.3390/nano11020476.
[233] T.T.T. Truong, T.N. Vu, T.D. Dinh, T.T. Pham, T.A.H. Nguyen, M.H. Nguyen, T. D. Nguyen, S.-I. Yusa, T.D. Pham, Adsorptive removal of cefixime using a novel adsorbent based on synthesized polycation coated nanosilica rice husk, Prog. Org. Coat. 158 (2021) 106361, https://doi.org/10.1016/j.porgcoat.2021.106361.
[234] W. Cai, X. Weng, Z. Chen, Highly efficient removal of antibiotic rifampicin from aqueous solution using green synthesis of recyclable nano-Fe3O4, Environ. Pollut. 247 (2019) 839–846, https://doi.org/10.1016/j.envpol.2019.01.108.
[235] M. Conde-Cid, P. Paíga, M.M. Moreira, J.T. Albergaria, E. Álvarez-Rodríguez, M. Arias-Estévez, C. Delerue-Matos, Sulfadiazine removal using green zero-valent iron nanoparticles: A low-cost and eco-friendly alternative technology for water remediation, Environ. Res. 198 (2021) 110451, https://doi.org/10.1016/j.envres.2020.110451.
[236] H.T. Nguyen, V.N. Phuong, T.N. Van, P.N. Thi, P. Dinh Thi Lan, H.T. Pham, H. T. Cao, Low-cost hydrogel derived from agro-waste for veterinary antibiotic removal: Optimization, kinetics, and toxicity evaluation, Environ. Technol. Innovation 20 (2020) 101098, https://doi.org/10.1016/j.eti.2020.101098.
[237] M. Stan, I. Lung, M.-L. Soran, C. Leostean, A. Popa, M. Stefan, M.D. Lazar, O. Opris, T.-D. Silipas, A.S. Porav, Removal of antibiotics from aqueous solutions by green synthesized magnetite nanoparticles with selected agro-waste extracts, Process Saf. Environ. Prot. 107 (2017) 357–372, https://doi.org/10.1016/j.psep.2017.03.003.
[238] F. He, W. Cai, J. Lin, B. Yu, G. Owens, Z. Chen, Reducing the impact of antibiotics in wastewaters: Increased removal of mitoxantrone from wastewater by biosynthesized manganese nanoparticles, J. Cleaner Prod. 293 (2021) 126207, https://doi.org/10.1016/j.jclepro.2021.126207.
[239] M. Leili, M. Fazlzadeh, A. Bhatnagar, Green synthesis of nano-zero-valent iron from Nettle and Thyme leaf extracts and their application for the removal of cephalexin antibiotic from aqueous solutions, Environ. Technol. 39 (9) (2018) 1158–1172, https://doi.org/10.1080/09593330.2017.1323956.
[240] T.G. Kebede, S. Dube, M.M. Nindi, Application of mesoporous nanofibers as sorbent for removal of veterinary drugs from water systems, Sci. Total Environ. 738 (2020) 140282, https://doi.org/10.1016/j.scitotenv.2020.140282.
[241] J. Tang, B. Mu, L. Zong, A. Wang, From waste hot-pot oil as carbon precursor to development of recyclable attapulgite/carbon composites for wastewater treatment, J. Environ. Sci. 75 (2019) 346–358, https://doi.org/10.1016/j.jes.2018.05.014.
[242] A.A. Kadam, B. Sharma, G.D. Saratale, R.G. Saratale, G.S. Ghodake, B.M. Mistry, S.K. Shinde, S.C. Jee, J.-S. Sung, Super-magnetization of pectin from orange-peel biomass for sulfamethoxazole adsorption, Cellulose 27 (6) (2020) 3301–3318, https://doi.org/10.1007/s10570-020-02988-z.
[243] M.M.M. Ali, M.J. Ahmed, Adsorption behavior of doxycycline antibiotic on NaY zeolite from wheat (Triticum aestivum) straws ash, J. Taiwan Inst. Chem. Eng. 81 (2017) 218–224, https://doi.org/10.1016/j.jtice.2017.10.026.
[244] T. Shahnaz, V. Vishnu Priyan, S. Pandian, S. Narayanasamy, Use of Nanocellulose extracted from grass for adsorption abatement of Ciprofloxacin and Diclofenac removal with phyto, and fish toxicity studies, Environ. Pollut. 268 (2021) 115494, https://doi.org/10.1016/j.envpol.2020.115494.
[245] J. Sun, L. Cui, Y. Gao, Y. He, H. Liu, Z. Huang, Environmental application of magnetic cellulose derived from Pennisetum sinese Roxb for efficient tetracycline removal, Carbohydr. Polym. 251 (2021) 117004, https://doi.org/10.1016/j.carbpol.2020.117004.
[246] T. Pham, T. Bui, V. Nguyen, T. Bui, T. Tran, Q. Phan, T. Pham, T. Hoang, Adsorption of polyelectrolyte onto nanosilica synthesized from rice husk: characteristics, mechanisms, and application for antibiotic removal, Polymers 10 (2018) 220, https://doi.org/10.3390/polym10020220.
[247] T.D. Pham, T.T. Bui, T.T. Trang Truong, T.H. Hoang, T.S. Le, V.D. Duong, A. Yamaguchi, M. Kobayashi, Y. Adachi, Adsorption characteristics of beta-lactam cefixime onto nanosilica fabricated from rice HUSK with surface modification by polyelectrolyte, J. Mol. Liq. 298 (2020) 111981, https://doi.org/10.1016/j.molliq.2019.111981.
[248] T.D. Pham, T.N. Vu, H.L. Nguyen, P.H.P. Le, T.S. Hoang, Adsorptive removal of antibiotic ciprofloxacin from aqueous solution using protein-modified nanosilica, Polymers 12 (2020) 57, https://doi.org/10.3390/polym12010057.
[249] S. Fakhrian, H. Baseri, Production of a magnetic biosorbent for removing pharmaceutical impurities, Korean J. Chem. Eng. 37 (9) (2020) 1541–1551, https://doi.org/10.1007/s11814-020-0523-4.
[250] J.-Y. Jo, J.-G. Kim, Y.F. Tsang, K. Baek, Removal of ammonium, phosphate, and sulfonamide antibiotics using alum sludge and low-grade charcoal pellets, Chemosphere 281 (2021) 130960, https://doi.org/10.1016/j.chemosphere.2021.130960.
[251] W. Liu, T. He, Y. Wang, G. Ning, Z. Xu, X. Chen, X. Hu, Y. Wu, Y. Zhao, Synergistic adsorption-photocatalytic degradation effect and norfloxacin mechanism of ZnO/

ZnS@BC under UV-light irradiation, Sci. Rep. 10 (2020) 11903, https://doi.org/10.1038/s41598-020-68517-x.
[252] Y. Wan, J. Wang, F. Huang, Y. Xue, N. Cai, J. Liu, W. Chen, F. Yu, Synergistic effect of adsorption coupled with catalysis based on graphene-supported MOF hybrid aerogel for promoted removal of dyes, RSC Adv. 8 (60) (2018) 34552–34559, https://doi.org/10.1039/C8RA05873C.
[253] M. Qiu, B. Hu, Z. Chen, H. Yang, L.i. Zhuang, X. Wang, Challenges of organic pollutant photocatalysis by biochar-based catalysts, Biochar. 3 (2) (2021) 117–123, https://doi.org/10.1007/s42773-021-00098-y.
[254] Y. Xiao, H. Lyu, C. Yang, B. Zhao, L. Wang, J. Tang, Graphitic carbon nitride/biochar composite synthesized by a facile ball-milling method for the adsorption and photocatalytic degradation of enrofloxacin, J. Environ. Sci. 103 (2021) 93–107, https://doi.org/10.1016/j.jes.2020.10.006.
[255] L.T. Nguyen, H.T. Nguyen, K.M. Nguyen, T.T. Pham, B.V. der Bruggen, Combined adsorption and photocatalytic degradation for ciprofloxacin removal using sugarcane bagasse/N, S-TiO2 powder composite, Water 13 (2021) 2300, https://doi.org/10.3390/w13162300.
[256] H. Zhang, Z. Wang, R. Li, J. Guo, Y. Li, J. Zhu, X. Xie, TiO2 supported on reed straw biochar as an adsorptive and photocatalytic composite for the efficient degradation of sulfamethoxazole in aqueous matrices, Chemosphere 185 (2017) 351–360, https://doi.org/10.1016/j.chemosphere.2017.07.025.
[257] C.P. Silva, D. Pereira, V. Calisto, M.A. Martins, M. Otero, V.I. Esteves, D.L.D. Lima, Biochar-TiO2 magnetic nanocomposites for photocatalytic solar-driven removal of antibiotics from aquaculture effluents, J. Environ. Manage. 294 (2021) 112937, https://doi.org/10.1016/j.jenvman.2021.112937.
[258] M.G. Gonçalves, P.A. da Silva Veiga, M.R. Fornari, P. Peralta-Zamora, A. S. Mangrich, S. Silvestri, Relationship of the physicochemical properties of novel ZnO/biochar composites to their efficiencies in the degradation of sulfamethoxazole and methyl orange, Sci. Total Environ. 748 (2020) 141381, https://doi.org/10.1016/j.scitotenv.2020.141381.
[259] X. Xie, S. Li, H. Zhang, Z. Wang, H. Huang, Promoting charge separation of biochar-based Zn-TiO2/pBC in the presence of ZnO for efficient sulfamethoxazole photodegradation under visible light irradiation, Sci. Total Environ. 659 (2019) 529–539, https://doi.org/10.1016/j.scitotenv.2018.12.401.
[260] Z. Wang, X. Cai, X. Xie, S. Li, X. Zhang, Z. Wang, Visible-LED-light-driven photocatalytic degradation of ofloxacin and ciprofloxacin by magnetic biochar modified flower-like Bi2WO6: The synergistic effects, mechanism insights and degradation pathways, Sci. Total Environ. 764 (2021) 142879, https://doi.org/10.1016/j.scitotenv.2020.142879.
[261] W. Mao, L. Zhang, Y. Liu, T. Wang, Y. Bai, Y. Guan, Facile assembled N, S-codoped corn straw biochar loaded Bi2WO6 with the enhanced electron-rich feature for the efficient photocatalytic removal of ciprofloxacin and Cr(VI), Chemosphere 263 (2021) 127988, https://doi.org/10.1016/j.chemosphere.2020.127988.
[262] D. Harikishore Kumar Reddy, K. Vijayaraghavan, J.A. Kim, Y.-S. Yun, Valorisation of post-sorption materials: Opportunities, strategies, and challenges, Adv. Colloid Interface Sci. 242 (2017) 35–58, https://doi.org/10.1016/j.cis.2016.12.002.
[263] P. Valášek, M. Müller, V. Šleger, V. Kolář, M. Hromasová, R. D'Amato, A. Ruggiero, Influence of alkali treatment on the microstructure and mechanical properties of coir and abaca fibers, Materials. 14 (2021) 2636, https://doi.org/10.3390/ma14102636.